DESIGN OF A 120 MWt REACTOR FOR A SURFACE WARSHIP

By

Lt. ARUN J. RAO, IN

CLEAR ENGINEERING AND TECHNOLOGY PROGRAMME

AN INSTITUTE OF TECHNOLOGY KANPUR

AUGUST, 1984

DESIGN OF A 120 MWt REACTOR FOR A SURFACE WARSHIP

A Thesis Submitted
in Partial Fulfilment of the Requirements
for the Degree of

MASTER OF TECHNOLOGY
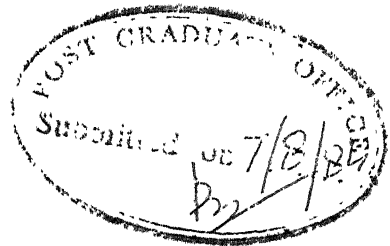
ɔɘ0ʃ੨

By

Lt. ARUN J. RAO, IN

to the

NUCLEAR ENGINEERING AND TECHNOLOGY PROGRAMME

INDIAN INSTITUTE OF TECHNOLOGY KANPUR

AUGUST, 1984

NETP - 1984 - M - RAO - DES

To

My dear Father and Mother,

My best teachers

C E R T I F I C A T E

This is to certify that the work "DESIGN OF A 120 MWt REACTOR FOR A SURFACE WARSHIP", has been carried out by Lt. Arun J Rao, IN under our supervision and that it has not been submitted elsewhere for a degree.

(P. Munshi)
Lecturer
Department of Nuclear Engineering
and Technology Programme,
Indian Institute of Technology,
Kanpur, INDIA.

(K. Sri Ram)
Professor
Department of Nuclear
Engineering and
Technology Programme,
Indian Institute of
Technology, Kanpur,
INDIA.
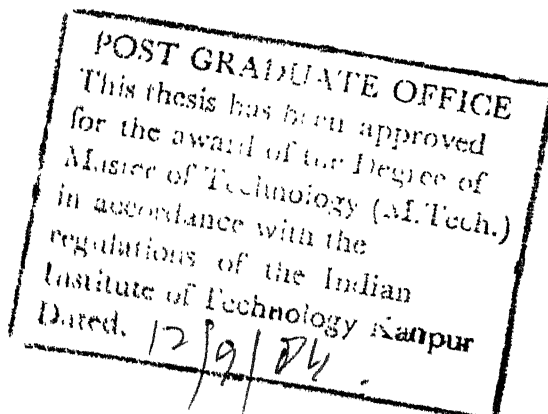
SYNOPSIS

'DESIGN OF A 120 MWt REACTOR FOR A SURFACE WARSHIP'

by

LT. ARUN J. RAO, IN

Never before has the strategy of maritime warfare diversified so much as with the ingress of the nuclear reactor onto warships. Subsurface or surface, the nuclear propelled warships are far superior both tactically and in performance over their conventional counterparts. With the fast dwindling number of warships due to their esclating costs, the possession of nuclear-powered warships for maintaining the same effectiveness and punch is becoming increasingly inescapable.

Reactor design is a multi-dimensional complex problem embracing many fields of engineering. The warship reactor design is more intricate than the land-based ones at it involves certain additional specialized problems like ship-motion effects, manoeuvring, vibrations, etc. The physical parameters of the core is restricted mostly by thermal considerations. Hence the Thermal hydraulic design requires careful attention to prevent core melt-down or coolant bulk-boiling. The Reactor physics design involves evolution of core enrichment and certain

other parameters to result in optimal design. Knowledge of
the neutron flux distribution is also required. Here, two-group
theory for heterogeneous core lattices has been used. The
Shielding design involves meticulous calculations to produce
the smallest possible reactor shield, both in size and weight
which is of paramount concern in a warship design.

Control of a marine reactor is different from
the land-based ones. Due to stringent manoeuvring requirements,
Power excursions from 20% to full-load require automatic
control with a high power increment/decrement rate of $3\%/s$.
The system has to be prompt acting, stable at all times
of operation with no unallowable overshoots. Finally, when
the reactor goes on the ship, certain other problems like
ship-motion effects, vibrations, etc., come in.

Due to the immense calculations involved, any
modern reactor design process is impossible without the aid
of a digital computer. Here, 3 computer CODES have been
developed, one each for thermal hydraulic, Reactor physics
and Shielding designs. The CODES & their results have been
presented separately.

The different design processes discussed till
now are inherently interactive among themselves and cannot
be considered isolatedly. This has been highlighted in the early
part of the thesis. It has, however, been the earnest endeavour
of the author to ensure an overall non-conflicting design.

*   *   *   *   *   *   *

ACKNOWLEDGEMENTS

CONTENTS

LIST OF TABLES

LIST OF FIGURES

NOMENCLATURE

MAIN SCRIPTS :-

A   -   Area; Mass number of elements

B   -   Buckling

C   -   Specific heat of material

D   -   Diffusion constant

E   -   Neutron Energy

F   -   Hot channel Factor

f   -   Friction factor; Thermal utilization factor

g   -   Non-1/v factor for Maxwellian Distribution; Acceleration due to gravity.

H   -   Height (of fuel rod)

h   -   Heat Transfer Coefficient

I   -   Resonance Integral; I^{135} concentration

K   -   Thermal Conductivity

k   -   Multiplication constant

L   -   Diffusion Length; Non-leakage Probability

l^{*} -   Neutron life-time (Thermal)

$\dot{m}$ -   Coolant mass flow rate

N   -   Number density of perticles

Nu   -   Nusselt's number

P   -   Pressure; Promethium concentration

p — Resonance escape probability

Pr — Prandtl number

q — Heat flux/intensity

R — Core radius

Re — Renault's number

S — Coupling coefficient; Source Strength; Samarium concentration

s — Fuel-rod pitch

T — Temperature

V — Volume

v — Coolant velocity through core

X — Xenon concentration

Y — Fission Yield

β — One group neutron percursor fraction

ε — Surface roughness factor; Fast fission factor

η — η of the fuel

λ — Decay constant

μ — Viscosity of coolant

ν — Neutrons released per fission

ξ — Logorithmic Energy decrement of neutrons

ρ — Density

Σ — Macroscopic neutron cross-section

σ — Microscopic neutron cross-section

τ — Neutron age; Time constant

φ — Neutron flux

SUBSCRIPTS:-

1	–	Core parameter
2	–	Reflector parameter
25,28	–	U^{235} , U^{238}
a	–	Absorption
av	–	Average
ac	–	Average coolant
B	–	Bulk coolant
circ	–	For smooth circular tubes
cl	–	Cladding
e	–	Extrapolotion distance
eff	–	Effective
F	–	Fuel-rod parameter; Fast neutron
fp	–	Fission product
fu	–	Fuel rod parameter
f	–	Fission
inf	–	Infinity
M,m	–	Moderator
o	–	Initial value ; at core centre
P	–	Poison; Promethium
r	–	Removal
S	–	Samarium
s	–	Scattering ; cladding parameter
Sat	–	At Saturation level
ss	–	Stainless steel
T	–	Thermal
t	–	Total
Tr	–	Transport
X	–	Xenon

****

C H A P T E R — I

INTRODUCTION

R E S U M E

1.1   SCOPE   OF   THE   THESIS

1.2   LITERATURE   REVIEW

1.3   THESIS   ABSTRACT

INTRODUCTION

In the modern era of fast depleting oil, coal and other forms of fossil fuels, nuclear energy takes a leading seat as the future global energy source. The nuclear reactor is virtually an interminable source of energy. Tapping of this energy is an engineering feat by itself. Though marginally more expensive, it is only a matter of time in this energy-crisised world before the reactor establishes itself as an inevitable source of energy. All this, and it is a mere 42 years old !

Today the cost of a nuclear reactor is prohibitive. Why then nuclear propulsion? The answer is straightforward - No repeated refuelling for the ship; which opens an entirely new era at sea! Where economic consideration is counterbalanced by military requirement, nuclear propulsion for Naval ships become essential. For the merchant ships, however, this is not so, as money is the key factor for trade. Consequently, we have only a handful of Nuclear merchant ships whereas the number of naval ships in the world (with nuclear propulsion) exceed three hundred.

SCOPE OF THE THESIS

A compact low weight system is of paramount importance in plants designed for ship propulsion. Marine

reactor design by itself, is a very vast topic merging land-based reactor design with certain specialized aspects like marine environment, light weight, limited space, etc. Our goal is to design a reactor system for a frigate/destroyer class warship. A drawing board design involves a vast amount of data, time and generation of numerous highly essential computer codes. This is definitely not being attempted. In the following pages, certain basic aspects of marine reactors have been discussed and a skeletal design attempted to highlight the varied & complex problem of marine reactor design. It is beyond the scope of this thesis to cover all topics envolving the design, be the skeletal stage itself. All important aspects have, however, been covered.

LITERATURE REVIEW

Most of the information regarding Naval reactors is classified. Though information on reactors of merchant ships are easily available, they don't satisfy the stringent measures of manoeuvrability, high power-to-weight ratio. and the limited space available in a warship where economic considerations fall into the background. Yet, a fair idea on problems encountered in marine reactor design, is available from them. International symposiums on Nuclear ships have been held in   (1960), Hamburg (1971) and Madrid (1972).

A subcommittee on military applications of the U.S. has presented the tactical and effective use of Nuclear Propulsion for Naval Warships[4]. It argues that though economically dear, when faced with the threat of submarines armed with either torpedoes or cruise missiles, or bombers or surface ships armed with cruise missles, the all-nuclear task force (consisting of an aircraft carrier and a few destroyers/frigates, all nuclear-powered) is less vulnerable to attack than a task force of conventional ships. The committee concludes, nuclear frigates for independent missions are far superior in performance than their conventional counterparts. John R Lamarsh[16] states that submarine reactors, being very small and compact, use fuel enriched in U^{235} to over 90 w% A.M. Petrosy.'ants[3] elucidating problems of nuclear science & technology, discusses Russian ships with nuclear engines - 'Lenin' & 'Arktika' (both ice-breakers) & their vastly superior performances over diesel icebreakers.

Extensive study & analysis of the world's first nuclear-propelled merchant ship 'Savannah'[5], in its sea environment, has thrown light over the problems faced by Marine reactors. Analysis of its core performance has been done by WJ Gallagher and Kaiz[1]. The Japanese Nuclear ship 'Mutsu' has also been discussed in detail by S. Sasaki[6]. Off-late, L. Chinaglia[2] of Fiat, Italy has presented a new design of

a PWR for ship propulsion. The inherent design interactions among various design aspects like thermal hydraulic design, nuclear design, shielding design, etc. has been well illustrated by RA Knief[13].

El-Vakil[17] deals with PWR thermal hydraulic design. Weisman[26] describes at length the various hot-spot factors concerning the thermal design. Regarding reactor physics analysis, Meem[22], with his 2-gp theory, gives sample calculations for reactor designers, that has been extensively referred. The Nuclear Engineering handbook[21] by Etherington has been used for related figures & references as and when mentioned. IAEA reports, Vienna, 1964[27], highlight the reactor shielding design and problem. B. Chinaglia[28] of Fiat, Italy, has also worked on shielding studies & control of ship-based gaseous activity release. J. Brown & A. Jackson[29] have carried out a study on shielding of Marine reactor installations. S.J. Thunell[30] has presented a comparative study on neutron fluxes in a metal-water shield in merchant ship reactors.

A Marine Reactor control & in-core instrumentation system design has been done by F. Basile, R.Merino & G. Selvada[32] wherein they have pointed out the differences between land-based reactor & marine reactor control. The control scheme used in the thesis is one evolved by Chinaglia[2] of Italy.

A detailed treatment of controllers has been illustrated
by MA Schultz [33], this has been used, however,
after a study of non-linear control system. References for
other aspects on reactor control have been Lewins[34] and
Glasstone & Sesonoke[12] and D.L. Hetrick[36].

Specialized marine problems like ship-motion
effects on steam-generator performance, collision barrier,
& grounding protection barrier for ships-reactors, and
safety of crew have been studied, respectively, by V. Jecob
and G. Selveggi[37], W. Jager & H. Lettnin [38] and L. Chinaglia
& P. Rucci[32].

1.3 THESIS ABSTRACT

The thesis starts with a brief history of marine
reactors. The tactical aspect of nuclear-powered vessels
over their conventional counterparts is discussed- this may
make the difference between winning or losing a battle which
is vital for any fighting force. The salient features of
ship-board reactors over the land-based ones are discussed.
The modern trends of marine reactors are also elucidated.

Chapter 3 highlights the design process. The
different aspects of reactor design like thermal hydraulic
design, nuclear design, shielding design, etc. are inherently
interactive among themselves and hence cannot be independently
considered; this is highlighted. A reactor core configuration

is then evolved and the systems used mentioned.

Core thermal hydraulic design is developed in chapter 4. A linear power rating of 11.0 KW/m is used. Since the power generated by a reactor is essentially restricted by the effective heat removal, this portion of the design is carefully considered as we desire the most compact and light-weight reactor for ship-board installation. A computer CODE, so vital for any thermal analysis, has been developed and used to arrive at optimum reactor Parameters. With this knowledge, we next move over to the reactor physics design (chapter 5). Two-group theory is used and the core studied for criticality using 2 regions (water as reflector). A computer CODE has been evolved which computes the effective multiplication constant (K_{eff}), the fast and thermal fluxes in both the regions, as well as the various 'poison' (unwanted neutron absorbants) activities in the core. The amount of control poison required for reactor control is also evolved. The control design hence would chiefly depend on the parameters obtained in this chapter. Care has been taken in the CODE that temperature and pressure dependencies of all parameters are considered.

We are aware that the overall reactor weight and size has to be the minimum possible for a marine reactor.

Bulk of this weight, however, is taken up by the biological shields. Consequently, reactor shielding assumes considerable importance and is analyzed at length in chapter-6. Biological shielding is mainly required for the fast neutron and gamma fluxes emerging from the shield materials due to thermal neutron capture. The biological dose rate from the secondary shielding is to be restricted to 0.75 mrem/hr. This has been achieved after the formulation of a shielding CODE. In addition an approximate weight calculation of the reactor (with shield materials) is demonstrated.

The control of a marine reactor is greatly different from a land-based one. This is because of high manoeuvring demands and a requirement of controlling the reactor automatically from full-load to part-load (20%). Chapter-7 elaborates these aspects and evolves a reactor control system. Careful stability analysis is also done from full-load to part-load using a two temperature feedback for the reactor. Certain other aspects of stability are also attempted after the calculation of the temperature coefficients of reactivity as applicable. A reactivity balance of the core using the CODE of chapter 5 is displayed. The control policy used is elucidated subsequently.

The integrated aspect of the reactor with the ship increases the design complexity further. Its effects are of practical significance to the operator on-board. Chapter-8 embellishes this integrated view. The ships three dimensional motion at sea has its effects on the steam generator performance. Collision barrier and grounding protection structure is required for the reactor compartment.

Chapter-9 concludes the present work illustrating the design that is ultimately arrived at. Other aspects of marine reactor design beyond the scope of this thesis are mentioned and suggestions for further study given. All references made in the current task are listed in the bibliography.

* * * * *

C H A P T E R - II

M A R I N E   A S P E C T S

OF

N U C L E A R   R E A C T O R S

Resume

2.1 History of the nuclear reactor at sea in :-

    2.1.1 Merchant Ships

    2.1.2 Warships

    2.1.3 Future trends of marine reactors

2.2 Tactical aspects of nuclear warships :-

    2.2.1 Drawbacks of conventional ships

    2.2.2 Nuclear submarines

    2.2.3 Nuclear surface ships- the importance of all
         nuclear task force

    2.2.4 Nuclear Propulsion for frigates

    2.2.5 Nuclear fleet strength of the world Navies

2.3 Salient Features of Marine Reactors:-

    2.3.1 Comparison with land-based reactors

    2.3.2 Basic design & safety criteria for warships

In 1942, Fermi & his co-workers made the world's first reactor critical at the University of Chicago. However, not until 1957 was a propulsion unit designed to operate on nuclear fuel. It was a small highly-enriched Pressurized Water Reactor (PWR), installed on board the Submarine USS NAUTILUS. As of today, there are over 300 ships propelled by nuclear energy. Most of these, however, are warships where economy is not the deciding factor in the choice of propulsion system.

2.1 BRIEF HISTORY

2.1.1 NUCLEAR MERCHANT SHIPS

The history of nuclear merchant vessels have never been bright. Nuclear power in merchant ships was used for the first time on a 16,000 ton Russian ice-breaker 'LENIN' in 1960. The decision was based not on economy but efficiency over the prevailing diesel electric system. In Arctic areas of heavy ice, nuclear ice-breakers with a 50% higher specific capacity*, can operate most of the year; but the conventional ones can make way only for 3-summer months due to danger of running out of fuel. The second ship was 'SAVANNAH', a U.S. Cargo-liner commissioned in dec '62 (no longer in active service). It's purpose was to test safety of nuclear plant aboardship & entrance of nuclear

---

*Specific capacity - power-to-displacement ratio.

vessels to civilian ports.

The 'OTTOHAHN' of FRG is a small scale experimental ship not planned for profitable operation (1968 vintage). Her purpose is to furnish all types of information theoritical, practical, economic & scientific with regards to nuclear propelled merchant ships at sea & refute arguments about their safety. The Japanese, on similar lines as FRG, launched a 10,400 ton specialized nuclear cargo ship in 1970 (MUTSU). Russia, finding the need for a second nuclear ice-breaker commissioned 'ARKTIKA' (displacement 23,460 tons) in 1975.

The reason for this bleak growth of nuclear ships are plain:-

(i) Cost economy - Capital cost of nuclear ships are 60% higher than conventional. The fuel cost is also higher. Till such time fossil fuel becomes prohibitive enough to counter-balance the above two reasons, nuclear ships will not be easily accepted.

(ii) Uncertainties-of investment cost; the future development in this area is hardly predictable.

(iii) Safety problems- Nuclear ships are not easily accepted by most of the civilian ports; psychological fear of public is mainly responsible for this.

2.1.2 NUCLEAR WARSHIPS

Nuclear Energy took birth in warships in the form of a submarine reactor for 'NAUTILUS', a U.S. Submarine, on 17 Jan '55. She generated 15,000 SHP, having 2 shafts and displacing 4040 tons. Initially she steamed submerged from Key West, Florida, to New London, a distance of 1397 sea miles*. She was refuelled after 2 years and 62,562 miles of steaming. Her success gave rise to a 'gold rush' and the US Navy ordered a pack of submarine reactors from Westinghouse Corporation. In 1960, Russia started her submarine fleet.

'ENTERPRISE', a 89,600 tons US Attack carrier, was the first surface ship to have nuclear propulsion (in 1961). She has 8 PWRs on 4 shafts, giving her a power of 280,000 SHP and a maximum speed of 35 knots**. She has had her core changed thrice, with the present feed giving her a sustainence of 10 to 13 years. In 1962, 'BAINBRIDGE', a U.S. Nuclear-Powered Guided Missile cruiser was the first cruiser to be nuclear-propelled (displacement 8580 tons).

Changes in ship reactor technology have also been incorporated to make ships more versatile and independent. The newer US aircraft carrier 'NIMITZ' (launched in 1975) has only 2 reactors contrary to her predecessor, 'ENTERPRISE' with 8; this generates a power of 260,000 SHP or 4 shafts, giving her 93,400 tons a maximum speed of 35 knot. She is the largest warship ever...

* 1 sea mile (or nautical mile) = 1.83 kms (2000 yards).
** 1 know = 1 nautical mile/hour.

built. She can steam an estimated 800,000 to 1 million miles
before refuelling. Interestingly, the energy equivalent of
her cores is 462 mega gallons (1.60 million tons) of fuel
oil- this is where nuclear energy scores over the conventional
form.

The largest submarine ever built, however, is
a Russian one, a 'typhoon' class Ballastic Missile submarine
(SSBN), launched in 1980. She displaces 30,000 tons dived
with speed exceeding 24 knots and having 2 nuclear reactors,
one per shaft, supplying a total of 120,000 SHP; she carries
20 SLBMs (Submarine Launched Ballistic Missiles). Presently,
nuclear submarines far outnumber nuclear surface ships.
However, many surface ships both cruisers and destroyers
are increasingly becoming nuclear-propelled, mainly due to
tactical reasons.

Due to the prohibitive cost & superior technology
for marine reactors, nuclear warships are expensive toys
handled only by a few economically advanced countries. However
with the Indian Ocean swarming with subsurface & surface,
nuclear & conventional warships, possession of nuclear warships
to effectively safeguard our exclusive economic zone . &
sea-frontiers, is becoming increasingly inescapable.

2.1.3 FUTURE TRENDS

For merchant ships greater than 70,000 tons displacement, preliminary studies indicate nuclear Power[23] to score over conventional power when operated for long durations. This might be used for constructing huge nuclear container ships in future when nuclear energy gets accepted in the merchant marine field. The smallest nuclear ship ever built is a US nuclear -powered ocean engineering & research vehicle 'NR-1' (1969), a submersible, built by USAEC', Knolls' Atomic Power laboratory. The vessel displaces only 400 tons, having dimensions of 136.4' x 12.4' x 14.6' with 2 propellors & carrying 5 crew members and 2 scientists. Such vessels are very useful for conducting detailed undisturbed experimentation on the continental shelf over long durations.

Now we hear the concept of NUFIS – Nuclear Floating Island, brought forward by Japanese scientists. Because of small area & dense population, the siting of Nuclear Power Plants in Japan is limited. Hence, the feasibility of NUFIS[9] has been studied and the project is about to commence. It is to be located 20 kms offshore at a sea-depth of 150 m. It is to have a 1200 MW_e PWR Plant on a 140 m x 140 m floating platform with a displacement of 298,000 tons. The power plant &. the associated facilities are to be situated

on it. Hence, the marine reactor technology will have to be applied to it. The technological feasibility of a floating centre for fuel fabrication, reprocessing, etc., is also being thought of.

2.2 TACTICAL ASPECTS OF NUCLEAR WARSHIPS

It was stated that the elimination of repeated refuelling opens an entirely new era at sea. Let us explore the tactical boost this gives.

Nuclear propulsion enables warships to traverse across seas at high speeds without pausing to refuel and without replenishment. With the escalating cost of warships, many many times that of equivalent merchant ships, the number of warships in the fleet is bound to dwindle. Hence, nuclear propulsion becomes prominent to maintain the same effectiveness with lesser warships. With the fast depleting oil sources in future, nuclear propulsion is going to become a necessity. It gives an additional tactical flexibility and opens new courses of action to the operators of the Naval Forces which would otherwise be unavailable. A nuclear powered naval force will be able to achieve many more productive results in any operation; such a force would be, in addition, less vulnerable to the action of the enemy.

2.2.1 DRAWBACKS OF CONVENTIONAL SHIPS

Here, mobility is limited by the need for refuelling at sea. Enemy action, bad weather & other uncontrollable forces directly impact upon refuelling ability which is not only time consuming but also requires the services of a considerable oil tanker fleet/train. The Fuel oil carried by ships being inflammable, in addition, poses a fire hazard onboard. A nuclear fleet, contrarily, is freed from the constraints of tankers & base support; hence it has increased speed, reliability, range, less fuel requirements & more payload.

2.2.2 NUCLEAR SUBMARINES

In the modern warfield, no other weapon has proved to be such an imminent threat as the nuclear submarine. As we see from Table 2.1, the super powers have maintained a parity on the number of nuclear submarines. Admiral Moorer of US Navy has stated[4] that he would rather have one nuclear powered, tactical cruise missile submarine (SSBN) than 5 of its conventional counterparts. Submarines are a particular threat because of their potential for approaching to within weapon ranges without being detected.

When their batteries run down, diesel submarines have to periodically 'snort*'. The quantity of fuel they carry

---

*'Snort'- come up to near sea-surface level to to run diesel engines for charging batteries that are used for propulsion underwater.

limit their edurance. The nuclear submarines, ostensibly,
never require to surface and can continuously move at high
speeds of 20 - 30 knots (almost double of diesel submarines).
The modern nuclear submarine being more quieter*, have a
high probability of going undetected by enemy sonars. Hence,
they are much more effective in penetrating anti-submarine
defences than diesel submarines.

2.2.3 SURFACE SHIPS - THE ALL NUCLEAR TASK FORCE

A naval task force consists of an aircraft
carrier with her modern air-wing, and her escorts of 3 to 4
destroyers/frigates to provide additional protection against
surface, sub-surface and air threats. The capability and
punch of the force is restricted by the endurance of each
of its ships. Hence, for maximum effectiveness, all ships
in it have to be nuclear-propelled. When faced with the
threat of submarines either armed with torpedoes or cruise
missiles, or bombers, or surface ships armed with cruise
missiles, the all-nuclear task force is less vulnerable to
attack than a task force of conventional ships which must
slow down to refuel in an extended encounter. It is therefore
much more difficult for the submarine to get in a favourable
position to attack the all-nuclear force. Further, the
logistic support forces upon which the conventional striking
forces are more dependent, are even more vulnerable to attack tha

---

* 'quieter' - Vibrations of hull due to inner machinery is
of lesser magnitude, making passive underwater
detection more difficult.

warships.

The tactical advantages of nuclear propulsion for ships of a nuclear task force can hence be summed up as follows:-

_____ They can move where required at top speeds without establishing logistic support before departure.

_____ Their virtually unlimited range enables them to use their superior speed to arrive at crisised situation much earlier than their conventional counterparts.

_____ When they do get there in a less vulnerable condition, they have far greater staying power, not only in terms of their ability to stick on without fuel, but also, significantly, in terms of aviation fuel & aviation ordanance for their airwing. For example, the USS 'NIMITZ' has 50% more aviation ordinance & twice as much jet fuel than equivalent conventional carriers.

_____ It can continue combat operation without support until aircraft fuel, ammunition, food or other supplies are exhausted.

_____ It can disengage if required to retire at top speed to less vulnerable sources of aircraft fuel & ammunition replenishment.

2.2.4 NUCLEAR PROPULSION FOR FRIGATES

By virtue of possesing their capability for high
sustained speeds and uninhibited endurance, nuclear frigates
are uniquely suited for assignment to independent tasks with
an effectiveness no non-nuclear ship can match. This can mean
difference between winning or losing engagements. In independent
operations, it matches the endurance of any nuclear submarine.
Since the aim of the thesis is design of a reactor for frigate /
destroyer, let us explore its tactical aspects a bit deeper.

Nuclear frigates combine the essentially unlimited
endurance of nuclear propulsion with the capabilities of the
most modern anti-air and anti-submarine weapon systems. Their
nuclear propulsion results in major improvements in offensive
& defensive capabilities :-

---- greater attack effectiveness due to increased mobility
& freedom of independent action; ability to transit at
high-speeds and thus arrive in attack position earlier
& ready to conduct operations immediately without pausing
to refuel; ability to be on attack station a higher
percentage of time; the freedom to extend attack to
larger areas,

--- reduce vulnerability due to freedom from dependence upon
replenishment in combat areas; and ability to avoid
submarine attack by transiting at high speed & using
evasive transit **routes.**

--- significantly reduced need for sea-based & land-based
logistic support forces.

----increased propulsion plant reliability due to the higher standards required in the design & construction of nuclear propulsion plants.

----increased overall effectiveness of the entire fleet by reducing the total number of combatant ships required to protect oilers.

2.2.5 WORLD'S NUCLEAR FLEET STRENGTH

Table 2.1 lists the nuclear strength of the world navies as of today. Though nuclear submarines for outnumber nuclear surface ships, we can see that the numbers of the latter has more than tripled in the last 10 years and many are being built.

T A B L E 2.1

WORLD'S NUCLEAR FLEET

S.No.	TYPE OF WARSHIP	U.S.S.R.		U.S.A.		U.K.		FRANCE		CHINA	
		1972	1982	1972	1982	1972	1982	1972	1982	1972	1982
	A. SUBMARINES										
1.	SSBN (Nuclear Powered tactical Ballastic Missile Submarine)	35	69	41	37+7*+2	4	4+4*	1	6	-	-
2.	SSGN (Nuclear powered tactical guided Missile Submarine)	40	49+1*	-	-	-	-	-	-	-	-
3.	SSN (Nuclear powered attack submarine)	25	58+3*+8	56	85+18*+3+5	4	11	-	-	-	2
	TOTAL	100	188	97	157	8	19	1	6	-	2
	Total of Non-nuclear Submarines:	243	293	41	47	26	16	19	19	-	20
	B. SURFACE WARSHIPS										
1.	CVN (Nuclear Powered Aircraft Carrier)	-	1	1	3+2*	-	-	-	-	-	-
2.	CGN (Nuclear Powered Missile Cruisers)	-	1+1*	3	9	-	-	-	-	-	-
	TOTAL	-	3	4	14	-	-	-	-	-	-

*(Active) + (Building)+ (Converting)+ (Reserve).

S.No.	MARINE REACTORS	LAND BASED REACTORS
5.	The crew (& passengers) constitute a 'captive' audience; they have no place of shelter in case of accidents.	In such an event, people could be evacuated to safer areas.
6.	Most likely place of accident is in the least favourable location - the port areas.	This problem is non-existent.
	(ii) DESIGN	
7.	There are many more start-up and shutdowns as well as widely varying needs for power in manoeuvering. This results on a greater stress & strain on the nuclear machinery (to be taken care of in design.)	The design need not be that stringent.
8.	Due to space limitations, the machinery of working plants is much more crowded than in stationary plants.	No such limitations.
9.	Due to weight & space limitations, the shops, spare-parts and maintenance facilities are kept to a minimum.	- do -
10.	Design has to cater for specialist aspects on ships like vibrations (of propeller & machinery), sea conditions (roll, pitch, yaw) and limited space and weight.	Earthquake protection is required for reactors.

S.No.	MARINE REACTORS	LAND-BASED REACTORS
11.	Irrespective of economic considerations, only the best materials are to be chosen such as to achieve highest possible specific capacity.	Materials chosen should be such as to minimize capital & maintenance cost while still being effective.
12.	Reactor control should be such as to make it inherently safe, in the event of a tsunami or sinking of the ship.	No such restriction
13.	Propulsion system design should cater for an emergency conventionally powered propulsion system compatable with the main machinery, in the event of a complete breakdown.	No such condition.
14.	In warships, adequate shock protection for reactors is required against firing of onboard guns and missiles; also required is (i) protection against shelling (ii) grounding & collision protection against external accidents.	No such condition required to be catered for.
15.	Only PWR's are used as marine reactors.	All types of reactors are possible on land.

2.3.2 BASIC DESIGN CRITERIA FOR NUCLEAR WARSHIPS

Threats to crew health & safety do not arise out of normal operation of nuclear ships but rather due to the possibility of internally and externally caused accidents to them. To minimize these, a variety of special safeguards in design, construction & operation are required. These will be briefly elucidated. There are also, a variety of recommendations applicable to nuclear ships; these, however, won't be discussed here but can be found in references (7) & (10).

Considerations such as the following lead to certain basic objectives that must be achieved in the design of a nuclear warship :-

- There must be continual knowledge of the level of radio-activity in all normal effluent streams, & of the levels at various locations around the ship.

- There must be complete control of all normal effluent streams, with storage capacity sufficient to permit detailed release of effluents under unfavourable circumstances.

- There must be an extraordinary degree of conservatism/ redundancy & dependability in the design of the reactor so that the likelihood of accidents will be reduced to the lowest practicable level. Following aspects are important:-

Marine environment like roll, pitch, yaw,

- ✓ Propeller & machinery vibrations of the reactor compartment.

- ✓ Proper reactor containment design for safety.

- ✓ Collision & grounding barrier protection for reactor compartment.

- ✓ Protection of reactor against shocks impressed by weapons firing onboard.

- ✓ The ship should have highest possible specific capacity.

- There must be devices & safeguards to minimize the hazardous consequences in case serious accidents should occur.

- There must be an adequate conventional emergency propulsion system in case of complete main-engine breakdown.

Thus the importance of nuclear propulsion for warships as a means towards strategic mobility is obvious to all who pause to consider the matter. It will remain as until a superior form of ocean propulsion for the weapon systems is produced.

****

C H A P T E R - 3

REACTOR DESIGN PROCESS

RESUME

It is well known that only PWRs are used as mobile reactors. In this chapter, this has been justified. In addition, the design methodology, the fuel assembly design and the steam-cycle used has also been elaborated.

3.1 CHOICE OF REACTOR

"SEAWOLF", the second nuclear-powered U.S. Submarine was fitted with a liquid metal (Nak) reactor called the Submarine Intermediate Reactor (SIR) in 1956. During dockside trials, steam-leaks deveoped due to Nak alloy coolant entering the superheater steam-piping. After repairs she was put to sea. However, due to recurrence of the above leaks in Dec '58, the reactor had to be replaced with a PWR.

The above experience was an eye-opener for the choice of mobile reactors. Alternately, if BWRs were used, they would give inherent system instability due to the reactor water level constantly varying with the ship-motion effects; in addition, for direct cycle the turbines require shielding, hiking up the gross machinery weight which is a very undesirable phenomenon.

Here, it is not possible to compare the various types of reactors due to space limitations. However, the salient features of a PWR over other reactors have been listed below:-

Advantages

- Moderator and coolant same.

- Water easily available and cheap.

- Water poses no serious long-term radioactive hazard.

- A primary heat exchanger leak is not hazardous to personnel as primary loop is shielded.

- Reactor has a high negative temperature coefficient making it safe & stable to operate.

- For moderate enrichment and closely-packed lattices, burnup is the highest.

- Being pressurised, the reactor is compact and size a minimum due to high power densities.

- PWR technology is very well known as it is the most common type of naval reactor today.

Disadvantages

- High primary loop pressure required due to the low boiling point of water; so pressure vessel should be very strong.

- Poor thermodynamic efficiency-20-25% for mobile reactors.

- As ordinary (light) water has a large neutron absorption cross-section neutron economy is poor.

- Reactor should be shut-down for reloading; (i.e. reloading not possible at sea).

Despite its moderate disadvantages, the power-to-weight ratio of a PWR is the highest; this is a highly desirable factor where compactness and light-weight is a chief requirement. All marine reactors operating today are hence only PWRs.

3.2 THE DESIGN SCHME

3.2.1 THE PROCESS

This may be divided into the following categories:-

(i) Core thermal hydraulics design

(ii) Core Nuclear design

(iii) Shielding Design

(iv) Reactor control and safety

(v) Materials Design

Since each of the categories is complex by itself, it is being treated separately in chapters that follow. The last topic (v), however, has not been included separately, but sketchily covered throughout. Being a reactor for defence purpose, no study on cost-economics has been done.

3.2.2. INTERACTIONS

The integrated reactor design requires substantial interaction among often conflicting design principles of (i) to (iv) above; safety considerations like biological dose

Fig. 3.1

REACTOR DESIGN INTERACTIONS.

~DESIGN SPECIFICATIONS~

SHIELDING DESIGN

DATA phy.prop. c sec.

NUCLEAR DESIGN

FLUX

DATA phy.prop. c sec.

CONTROL DESIGN

CORE POWER DIS-TRIBUTION

Axial
Radial } distrbn
Linr powrtg

GEOMETRY

THERMAL HYDRAULIC DESIGN

DATA Reac.coeffs. Time consts.

ENGINEERING SAFETY SYSTEMS

DATA phy. prop.

TEMPERATURE AND FLOW PATTERNS

MATERIALS DESIGN

MATERIAL SPECIFICATIONS

DATA phy pro

limitation, prevention of core melt-down, etc, provide very stringent constraints.

Fig 3.1 gives a pictorial view of these interactions in the present design. Nuclear, thermal-hydraulic and material design components result in composition, geometry and operational specifications that characterize the marine reactor system. Nuclear design begins with preliminary cross-sections data. For the calculational modules, flux-averaged cross-sections with appropriate modifications to the working conditions have been used. The flux, power distribution and burnup contribute to a final specification of enrichment. The thermal hydraulic design interacts with power distribution to develop a geometry and its related temperature and flow distributions, limited by material specifications. The nuclear design also yields the reactivity requirements required for the control design.

The control system design for marine reactors is intricate. Whereas a power variation of only 10% is allowed in land-based PWR's, variation from 100% down to 20% is required to be automatically controlled that too in much shorter times for marine reactors. This calls for a non-conventional control system design with careful stability analysis. This is dealt with in chapter-7.

3.3 FUEL ASSEMBLY DESIGN : The first step in core design is to evolve the type of fuel assembly required

Fig.3.2

The fuel assembly

K E Y

CONTROL ROD BANKS
A – HIGHEST WORTH
B – MODERATE WORTH
C – LOWEST WORTH

CORE BAFFLE
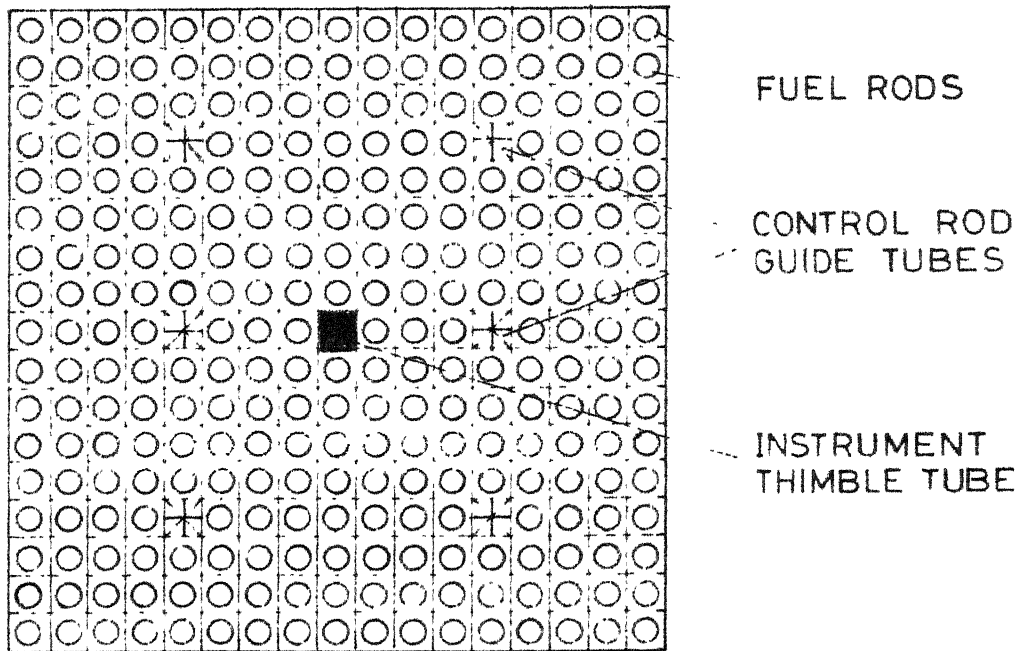
FUEL ASSEMBLIES
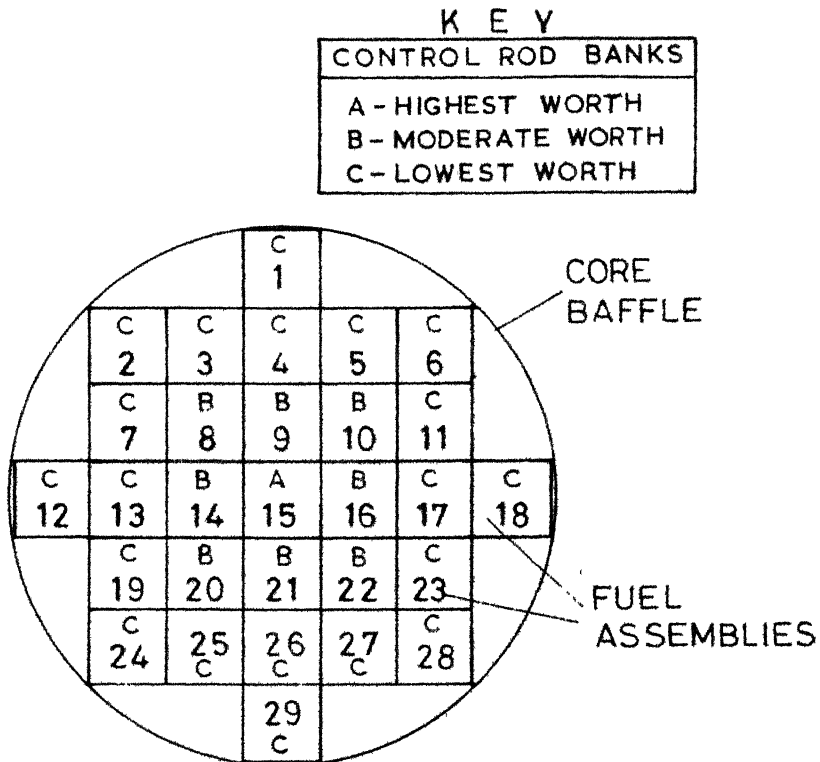
Fig.3.3

The core configuration

The basic features of the assembly selected is shown in Fig 3.2 (Ref.(7)). A 17 x 17 square pitch layout has been chosen with 282 cylinderical fuel rods per assembly. This configuration represents recent designs that enhance linear heat-rate limits (Ref.(13)). The taxonomy of the fuel assemblies is as shown in Fig. 3.3 . This symmetrical arrangement employs an open lattice that permits some flow mixing between adjucent units which is a desirable phenomenon. The diameter of the core baffle is 7.071 times the width of a fuel assembly.

A constant fuel enrichment has been chosen throughout the core. For a linear power rating chosen as 11.00 KW/m (see chapter 4) and 120 MWt power output, the number of fuel assemblies required are 29 (8178 rods). This gives a core height of 133.39 cms. The core-radius is dependent on the fuel rod-pitch (which will be determined later).

There are 6 control-rod poison fingers per assembly-each finger being of the same length as the core. It contains B_4C (Boron carbide) enclosed in stainless steel tubes. Their concentration and size are to be determined. The reactivity control is provided by 29 Rod Cluster Control (RCC) assemblies (1 rod-cluster per assembly). They have been constituted in 3 banks A, B and C as shown in Fig. 3.3. No burnable poison

GEAR BOX

TO PROPELLER

L P TURBINE

SHAFT

H.P TURBINE

MOISTURE SEPTR & REHEATER

EXTRACTION STEAM

FEED PUMP

FEED WATER HEATERS

CONDENSER

CONDENSATE PUMP

STEAM GENERATOR

PRESSURIZER

REACTOR

SECONDARY SHIELDING

KEY

— STEAM LINE
— PRIMARY COOLANT
— FEED WATER
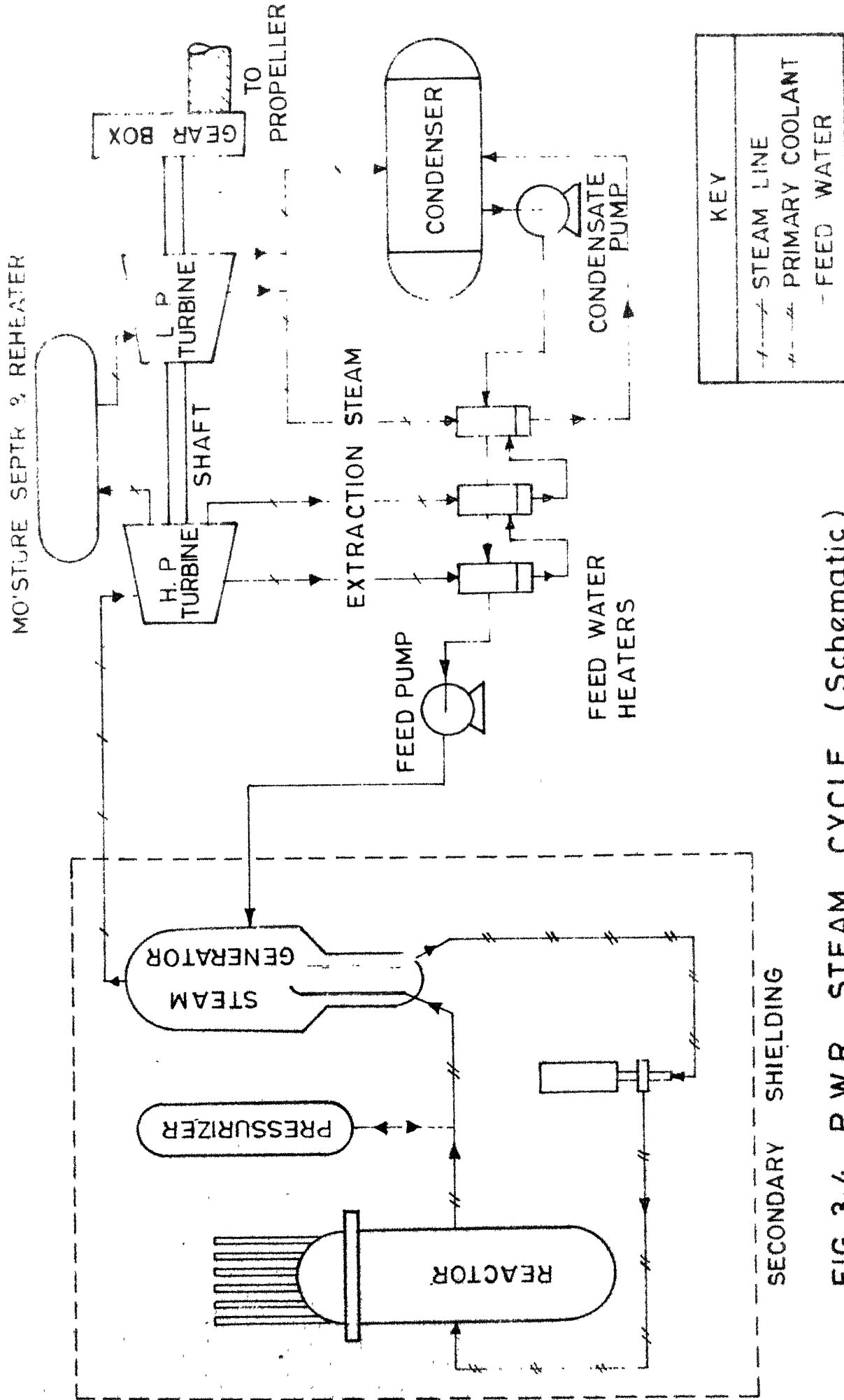
FIG. 3·4. P W R STEAM CYCLE (Schematic)

or soluble poison scheme has been included. Each assembly,
in addition, has been provided with a central instrument thimble
space meant for a movable in core flux measurement detector
tube.

3.4 STEAM CYCLE

The steam cycle used is illustrated in Fig.3.4.
The 2-loop system is in vogue in almost all working PWR's.
The primary system contains water at 2000 psi (14 MPa).
Coolant pump regulates flow in the loop and pressure vessel.
The presurizer maintains the system pressure within a specified
range. 2 primary coolant loops supplying to 2 U-tube steam
generators of 60 MWt capacity each are chosen.

The secondary loop generates steam at 500 psi
(3.5 MPa) at 100% load at a quality of 0.9975. Regenerative
cycles for the turbines have/used to improve efficiency.
been
Further details about the steam cycle have not been attempted.

3.5 INFERENCE

We have now determined few of the reactor core
parameters and the system we have to work on in the succeeding
chapters. We also know about system interactions. While
considering the various design processes in the subsequent
chapters, these interactions have to be borne in mind for
an overall non-conflicting design. This has been the earnest
endeavour of the author.

****

C H A P T E R - 4

CORE   THERMAL   DESIGN

R E S U M E

4.1 INTRODUCTION

A nuclear reactor is capable of operating at very high power densities. However, the core must be operated at such a power level that with the best available heat removal systems, the cladding and fuel temperatures anywhere in the core do not exceed safe limits. A fuel element damage, otherwise, will result either in the transfusion of the highly radio-active fission-products into the coolant, or in core-fuel meltdown. Both these effects are highly undesirable . Hence, the core design is dictated more by the thermal limitations rather than any nuclear consideration.

GOVERNING EQUATION

The rate of heat removal, (Q) is given by the simple relation (p:369,(17))

$$Q = h * A * \Delta t$$

overall ht. transfer coefficient.
Area of heat transfer
Tempr.diff.between fuel & coolant.

'h' is governed by conductive heat transfer through fuel elements and cladding, and convictive heat transfer through coolant. As the fuel is UO_2 , its thermal conductivity is fixed. So fuel-cladding should have least resistance to heat conduction, in addition to low neutron absorption cross-section, workability,

ability to withstand high temperatures and withstand the corrosive
action of the coolant fluid; some of these considerations are
conflicting; hence a compromise between high thermal conductivity
and high temperature operation necessitated the use of stainless
steel (SS-347) as the cladding material. Resistance to heat
conduction is reduced by keeping the cladding thickness to the
minimum. Heat transfer by convection to water depends on the
properties of water at the operating conditions, and coolant
velocity.

"A" is maximized by having as many fuel rods
as possible. Since a large quantity of heat is generated in the
compact core, the maximum possible heat transfer area should
be squeezed into it.

"$\triangle t$", finally, should be high; high rates of heat
release requires low coolant temperatures; this conflicts with
basic thermodynamic considerations as a good thermal efficiency
requires high coolant temperatures. Hence, to keep coolant
temperatures as high as possible and yet retain a high $\triangle t$ in the
core, fuel elements have to operate at the highest possible
temperatures which are limited only by metallurgical & burn-up
considerations.

Hence, it is seen that reactor core design necessitates
a compromise between often conflicting nuclear, metallurgical,

structural, thermodynamic and heat-transfer requirements. To ensure that the core is safe under all operating conditions and transients in our main motto.

4.2 DESIGN CHARACTERISTICS

4.2.1 SALIENT FEATURES

The main problems encountered in thermal hydraulic design are :-

(i) assure inlet & outlet core flow distribution compatable with power distribution foreseen during the core lifetime.

(ii) assure cooling of the control rod pins and hydraulic dashpot action (for slowing down control rod velocity at the end of its insertion) during all operating and accident conditions.

(iii) DNB (Departure from Nucleate Boiling) should not occur under all operating conditions & transients (i.e. Heat flux anywhere, to be kept below CHF (Gritifal Heat Flux))

(iv) Bulk boiling of the coolant should hot be allowed to occur in any channel.

(v) The fuel centre-line temperature should not exceed 2500°C under any circumstance (fuel m.p. 2850 °C)

(vi) Hot-channel factors should be judiciously chosen; with the heat-flux increased by these factors, points (iii),(iv) and (v) above should be satisfied.

TOP

(C)
$(\pi-z)*\sin(\pi-z)$
(towards end of life)

(B)
$\sin(Z)$

CORE

(A)
$Z*\sin(Z)$
(at beginning of life)

COOLANT FLOW

H

BOTTOM
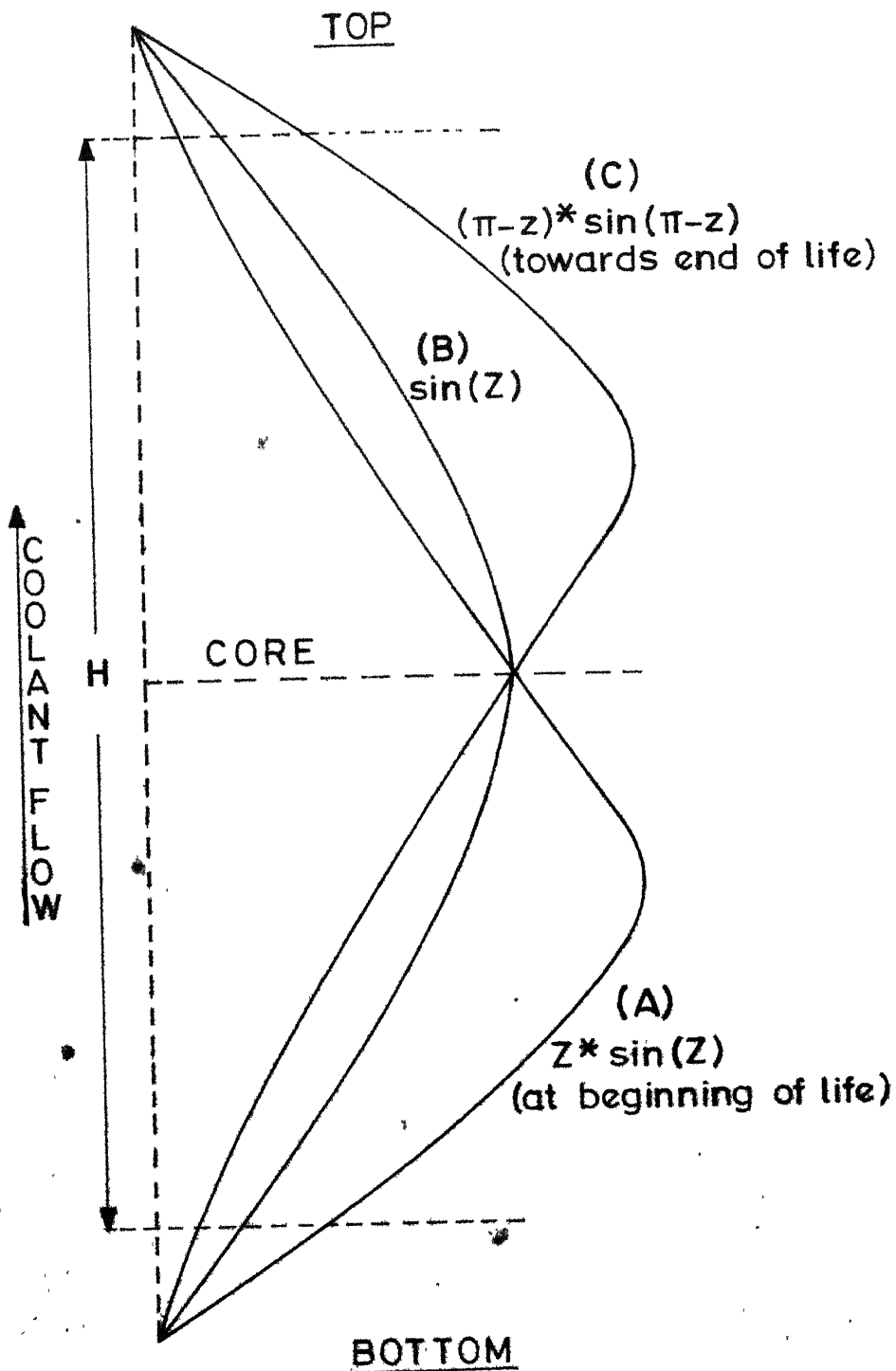
FIG. 4.1 FLUX FUNCTIONS USED
(also refer P. 27 of computer print-outs

4.2.2 CORE FLUX DISTRIBUTION

The basic core flux distribution has been taken from the "Reactor Physics Design" section (Ch.5). Radial flux distribution has been assumed as a truncated Bessel's function; the axial distribution, truncated cosine. Due to the high inbuilt reactivity of the core, control rods remain partially inserted in the core. At the BOC (Beginning of Life, of Core) the flux peaks as shown in Fig.(4.1), (A). As the rods are gradually retracted due to burnup, the flux assumes a more sinussidal distribution. Finally at the EOL (End of Life), the distribution assumes profile (C). For calculational purposes, (B) is assumed as $Sin(Z)$ and (A) and (C) as $Z-Sin(Z)$ and $(\pi-Z).Sin(.\pi-Z)$ respectively. For comparitive purposes, the normalized flux distributions have been shown as a computer printout. (See p.27 of computer printouts)

4.2.3 HOT CHANNEL FACTORS

In the thermal design of a marine reactor core one is concerned with the most severe conditions in the core. If the design is adequate for these conditions, it is certain to be satisfactory elsewhere. Hence the 'hot-channel' is that coolant channel where heat-flux and enthalpy rise are at a maximum.

(a) Nuclear hot channel factor (F_Q^N)

or Nuclear heat flux factor is defined as:

$$F_Q^N = \frac{\text{Estimated maximum heat flux in core(based on nominal fuel enrichment \& dimensions).}}{\text{Mean Heat flux in core}}$$

$F_Q^N = F_Z^N * F_R^N$ where, subscripts 'Z' & 'R' stand for axial & radial flux factors. This is the peaking of the flux in the axial & radial directions given as "Peaking Factors" in the CODE.

$F_R^N \leqslant 2.32$; $F_Z^N \leqslant 1.57$ for $\sin(Z)$ flux to $F_Z^N \leqslant 1.82$

for $Z-\sin(Z)$ and $(\pi-Z)\sin(\pi-Z)$ fluxes. This causes $F_Q^N \leqslant 4.2224$ (We have obtained $F_Q^N = 3.4411$ for $Z \cdot \sin(Z)$ flux.) This factor has already been included in the CODE.

(b) Engineering hot-channel factor (F_Q^E).

The maximum heat flux may increase under the following engineering uncertainties:-

(i) Local fuel density being greater than nominal (factor concerned - F_3^E).

(ii) Fuel dimensions being in excess of nominal (F_d^E)

(iii) Local fuel enrichments being greater than nominal (F_e^E).

$$F_Q^E = F_3^E * F_d^E * F_e^E$$

For a PWR this gives a value of 1.08 to 1.10 (Ref(26), pp.170-177). But this approach is unnecessarily conservative and the effect of fabrication tolerances is evaluated statistically giving

$$F_Q^E = 1.04 \quad . \text{ (Ref.(20))}$$

(c) Engineering hot-channel factor for enthalpy rise :- ($F_{\Delta h}^{E}$).

This accounts for engineering uncertainties in the maximum enthalpy rise in the concerned hot-channel. $F_{\Delta h}^{E}$ depends on the following factors:-

(i) Fabrication tolerance subfactor, $F_{\Delta h,Fab}^{E}$, accounts for fuel enrichment variation, fuel weight variation & coolant flow variation; it is evaluated statistically.

(ii) Core Flow Sub-factor ($F_{\Delta h,Flow}^{E}$). accounts for the hot-channel receiving less than its expected share of coolant flow.

(iii) Core mixing sub-factor ($F_{\Delta h,mix}^{E}$) , accounts for flow from surrounding cooler channels mixing with flow in the hottest channel. This is favourable countering the deleterious effect of the other subfactors.

Typical values of above for a PWR are:-

$$F_{\Delta h}^{E} = F_{\Delta h,Fab}^{E} * F_{\Delta h,Flow}^{E} * F_{\Delta h,mix}^{E} \cong 1.08$$

(d) Overall hot-channel Factor(F)

The engineering (F^{E}) uncertainty factor would be

$$F^{E} = F_{Q}^{E} * F_{\Delta h}^{E} (1.167 \text{ for PWR })$$

However, in the Italian ship Design (Ref(2),p.598) $F_{\Delta h}^{E} = 1.22$ has been used instead of the above figure, giving $F^{E} = 1.269$; this has been used in this analysis. This means if the heat flux is increased by this amount in the CODE, the core design ~~should~~

should sustain itself. (F_Q^N has, as stated earlier, already been included in the CODE).

The overall factor F, would hence be:

$$F = F_Q^N * F^E = 4.367 ;$$

This implies the core should sustain a heat flux over its average value, of 4.367 times everywhere in the core.

4.2.4 THE THERMAL HYDRAULIC CODE

The thermal design of a core is virtually impossible without the aid of a computer. In the computer CODE, care has been exercised to entertain all thermal effects and variation of material properties with temperature. It lists output in a 3-dimensional manner giving axial variations of temperatures & pressure for the rods at the core centre, and then at discrete steps upto the core periphere. The analysis of the rod is for:-

(i) Coolant integrity
(ii) Cladding integrity.
(iii) Coolant exit conditions and pressure drop.

In addition for:-

(iv) Radial flux variation in the core

(v) Pumping requirements for primary system.

(vi) Determination of core diameter (for 120 MWth power), and total number of rods.

(vii) Temperature feedback for reactor neutronics calculations.

The importance of the CODE is felt when one has to do repeated analysis of a core with small variations in input, to arrive at an optimum solution. In addition, cores of different reactors can easily be analysed since material properties are fixed. The CODE developed is versatile enough to be used either for stainless steel or Zirconium cladding, and either a square-arrayed core or a hexagonal arrayed core.

4.3 THERMAL AND HYDRAULIC DESIGN

The fuel rod has been axially divided into 50 equal segments. The properties of materials in one segment are considered constant and so also temperatures, axially. The basic theory governing the temperature distribution, heat transfer rates, pressure drops & energy balance is presented below, and done for each of the 50 segments, successively. Temperature distribution. in fuel & cladding are calculated using one-dimensional radial heat conduction. The pressure drops & heat transfer coefficients are calculated using empirical relations for flow channels.

4.3.1 FLOW CHANNEL
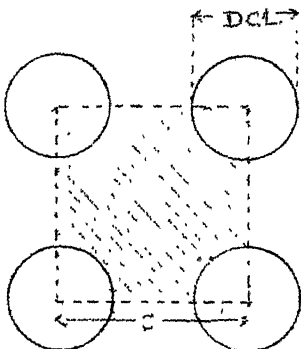
In this core design, the square arrary has been used. For the fuel rods of diameter DCL and pitch s , the flow area (A) per rod is given by

$$A = s^2 - \frac{\pi * DCL^2}{4} \quad \text{(shaded portion)}$$

$$\ldots\text{Eqn}\ldots(4.1)$$

4.3.2 HEAT GENERATION

Fission heat generated is directly proportional to thermal flux (taking cross-sections as constant). The volumetric source strength q''' is :-

$$q''' = 3.204 * 10^{-11} * \Sigma_f * \emptyset (r,z) \ . \ J/cm^3-s$$

Thus, q'' varies axially & radially as:

$$q'''(z,r) = q_o''' * Cos(\frac{\pi}{H}z) * J_o(\frac{2.405}{R+d}.r) \ .... Eqn (4.2)$$

for $z=0$ to H

$r=0$ to R where q_o''' is the peak flux at centre of core.

R= Core Radius

d= distance from core face where flux = 0.

An important quantity required to be known beforehand is heat-flux generated per unit length of rod (kw/m) q_{av}' . This is an average quantity for all rods. After a review of the reactors of the world (Ref.(14)), a figure of 11.0   KW/m was arrived at. This factor is related to the average volumetric heat flux thus-

$$q_{av}''' = q_{av}' \ /\pi \ r_{fu}^2 \quad where, \quad r_{fu} = fuel \ pellet \ radius$$

The volumetric power density at the core centre   is:

$$q_o''' = F_R^N * F_Z^N *. \ q_{av}'''$$

where F_R^N & F_Z^N are hot-channel factors as explained before.

since by virtue of definition

$$q_{av}''' = \frac{1}{V} \iint_{\substack{\text{all} \\ \text{core}}} q_0''' \cdot \text{Cos}\left(\frac{\pi}{He}z\right) \cdot \left(\frac{2.405}{R+\bar{u}}r\right) \cdot 2 \cdot r \, dr \, d\theta$$

where V= core volume

we arrive at the following relations :-

$$F_R^N = \cfrac{1}{2\cfrac{J_1(LR)}{LR} + 2\left(\cfrac{C}{A}\right)\cfrac{I_1(mR)}{mR}} \quad , \quad \text{for a truncated Bessel's function flux-distribution,}$$

$$F_Z^N = \frac{\pi}{2} * \frac{H}{He} \Big/ \text{Sin}\left(\frac{\pi}{2H_e}H\right) \; , \; \text{for truncated cosine}$$

$$= \frac{1.8197 * \pi * H}{He\left(-A\text{Cos}(A) + B\,\text{Cos}(B) + \text{Sin}(A) - \text{Sin}(B)\right)} \; , \; \text{for}$$

truncated $(\pi - z) \cdot \text{Sin}(\pi - z)$ function

where, $A = \dfrac{H\pi}{He}$ and $B = \left(\dfrac{He-H}{2He}\pi\right)$.

Refer Appendix A3-1 for the above inferences.

4.3.3 TEMPERATURE DISTRIBUTIONS

(1) In fuel rod -

The basic heat conduction equation with heat generation is (in cylinderical coordinates)

$$\frac{d^2 T}{dr^2} + \frac{1}{r}\frac{dT}{dr} + \frac{q'''}{K_{Fu}} = 0$$

with boundary conditions as

$$T = To \text{ at } r = o \text{ (fuel centre-line temperature)}$$

$$\frac{dT}{dr} = 0 \text{ at } r = 0$$

the solution of the above equation is

$$T = To - \frac{q'''}{4 K_{Fu}} r^2 ,$$

showing a parabolic temperature distribution with the maximum at the fuel rod centre. Hence, at the fuel outer radius (r_{Fu}) ,

$$T_F = To - \frac{q'''}{4 K_{Fu}} r_{Fu}^2 \quad \dots \text{ (Eqn 4.3)}$$

During the steady state condition, all of the energy generated must be transferred out to the cladding – since K_{Fu} changes with temperature, an iterative technique has been used to obtain the cladding thermal conductivity to within 1%.

If $K_{Fu}(T) = a + bT$ where a and b are constants,

then we find that the value of K_{Fu} to be used is precisely equal to K_{Fu} evaluated at the mean temperature $\frac{To + T_F}{2}$.

i.e. in Eqn. 4.3, $K_{Fu}(T) = K_{Fu}(\frac{To + T_F}{2})$

(Refer Appendix A4-2)

(2) In gas gap

The temperature drop across the gas gap is taken as

$$T_f - T_g = \frac{q''' \, r_{Fu}}{2 \, h_{gap}} \quad \dots \dots \text{ (Eqn 4.4)}$$

where h_{gap} = gap conductance = 0.6 W/cm^2-K

(p.356, ref (12))

h_{gap} is taken as constant throughout the core.

(3) In the cladding

Technique used here is similar to that in the fuel rod. The governing equation is :-

$$\frac{1}{r} \cdot \frac{d}{dr} \left(r \frac{dt}{dr} \right) = 0 \quad \dots \text{Eqn.}(4.4b)$$

with initial conditions as

$$T = T_g \text{ at } r = r_\varepsilon \text{ (outer radius of gap)}$$

$$\frac{dT}{dr} = \mp \frac{r_{Fu}}{2K_{cl}} q''' \quad \text{at} \quad r = r_g$$

where, K_{cl} = thermal conductivity of cladding.

Eqn. 4.4b gives a simple logarithmic solution :

$$T = T_g - \frac{q''' r_{Fu}^2}{2 K_{cl}} + \ln\left(\frac{r_{cl}}{r_{Fu}} \right) \dots\dots(\text{Eqn} 4.5)$$

where r_{cl} = outer cladding radius.

Here again, K_{cl} is a linear function of temperature and hence an iterative technique has been used to obtain K_{cl} to within 1% occuracy,

$$K_{cl}(T) = K_{cl}\left(\frac{T_F + T_S}{2} \right)$$

(4) In the coolant

All heat energy generated by the fuel must be ultimately transferred to the coolant through the fluid layers near the cladding outer surface. Newton's law of cooling has been used

for this purpose:-

$$q_s = h \, A_s \, (T_s - T_B)$$

heat transfer   heat transfer   heat transfer
rate.   coefficient   area

T_B is a mass-weighted average temperature of the water in the flow channel.

$$\text{As,} \quad q_s = q''' \, \pi \, (r_{Fu})^2 \, \triangle l$$

$$A_s = 2 \, \pi \, r_{cl} \, \triangle l$$

thus,

$$T_s - T_B = \frac{q''' \, r_{Fu}^2}{2 \cdot h \cdot r_{c.l}} \quad \ldots\ldots\ldots \text{(Eqn 4.6)}$$

The method of determining (h) is elucidated later in this section (4.3.5).

$$T_B \text{ is to be known}$$

before we start temperature calculations. After that, T_s, T_g, T_f and To are determined using equations 4.6, 4.5, 4.4 and 4.3 successively. Method of calculating T_B has been stated later (4.3.6).

4.3.4 <u>COOLANT PRESSURE DROP</u>

We shall determine only the pressure drop in the core here. There are 2 types of losses occuring.

(i) Frictional pressure drop along the channel, $\triangle P_F$

(ii) entrance and exit permanent pressure losses, $\triangle P_E$.

(i) ΔP_F occurs due to the shear stress on the flowing fluid by the walls of the flow channel. This is given by the relation:-

$$\Delta P_F = f \cdot \frac{\Delta l}{D_e} \times \frac{\rho v_B}{2g} \quad \ldots\ldots \quad (\text{Eqn } 4.7)$$

where, f = friction factor

Δl = segment axial length

ρ = water density at T_B

v_B = average channel coolant velocity

D_e = Equivalent channel diamter, and

g = gravitational accleration constant, $9.81 \ m/s^2$

Here, $D_e = \dfrac{\text{flow area}}{\text{wetted Perimeter}} = \dfrac{A}{2\pi r_{cd}}$, 'A' defined by

(Eqn. 4.1).

The value of f depends on flow and surface conditions in channel. The flow conditions are characterized by Reynold's number, Re.

$$Re = \frac{\rho v_B D_e}{\mu} \quad \ldots\ldots\ldots \quad (\text{Eqn. } 4.8)$$

where, μ = Coefficient of viscosity of water.

Re should be greater than 2000 for turbulent flow that is desirable due to the higher heat transport rates. In our case, $R_e = 237842.1.$ (see p. 28 of computer printouts).

The second condition, the surface condition is characterized by ratio of surface roughness (ε) height, to the equivalent diameter ε/D_e. The flow channel exhibits smooth tube behaviour if $\varepsilon < t$, the laminar sublayer thickness. Hence the cladding outer surface

smoothness should be so controlled that this criterion is met.

The smooth circular tube friction factor (F_{cire}) is got by using this coorelation widely accepted in reactor work:

$$f_{cire} = 0.184 * R_e^{-0.20} \quad \ldots\ldots\ldots \text{(Eqn 4.9)}$$

The Deissler & Taylor correlation for the correction of circular tube data to the rod-bundle geometry has been used:-

$$\frac{f}{f_{circ}} = -3.475 + 8.053 \left(\frac{s}{D_e}\right) - 4.705 \left(\frac{s}{D_e}\right)^2 + 0.9162\left(\frac{s}{De}\right)^3$$

$$\ldots\ldots \text{(Eqn. 4.10)}$$

This value of 'f' has been used in Equation 4.7.

(ii) $\triangle P_E$ losses are the result of increased viscous energy

dissipation resulting from increased turbulent activity

at inlet and outlet.

$$P_E = K \frac{\rho V_B^2}{2g}$$

where K = resistance coefficent for sudden contraction

from large to small flow diameter; K=0.5 at core inlet,

K=1.0 at outlet.

4.3.5 HEAT TRANSFER COEFFICIENT (h)

A two-step procedure has been obtained to calculate 'h'

(i) 'h' for flow in circular tubes in found first.

(ii) A correlation correction is applied then to obtain 'h'

for actual reactor coolant flow geometry. No direct analytical

methods for predicting 'h' for turbulent flow ...

exist. However, by use of an analogy between heat & momentum
transport, dependence of 'h' on Re can be predicted. Then,
by applying the results of a heat transfer analysis for laminar
flow over a flat plate, an estimate of the prandtl number, P_r,
dependence on heat transfer is obtained. In this analysis, the
Dittus-Boelter correlation has been used :-

$$Nu_{circ} = 0.023 * R_e^{0.8} * P_r^{0.4} \quad \cdots \quad (Eqn.4.11)$$

where Nu_{circ} = Nusselt number for circular tube

$\qquad R_e$ = Renault's number (given by Eqn.4.8)

$\qquad P_r = \dfrac{C_p \mu}{K}$

Now, Deissler & Taylor correlation for the actual coolant
channel is done, like in Eqn.4.10

$$\frac{Nu}{Nu_{circ}} = -3.475 + 8.053 \left(\frac{S}{D_e}\right) - 4.705 \left(\frac{S}{D_e}\right) + 0.9162 \left(\frac{S}{D_e}\right)^3$$

$$(Eqn. 4.12)$$

since $\quad Nu = \dfrac{h \, D_e}{K}$

$\qquad h = \dfrac{Nu * K}{D_e} \quad \cdots\cdots\cdots (Eqn. 4.13)$

4.3.6 TEMPERATURE INCREASE BY THE FLOWING COOLANT

Coolant temperature varies from a minimum at the
inlet to a maximum at the core exit. The temperature in our
analysis is assumed to very discretely from one segment to
another. The bulk temperature T_B at any point (required in

Section (4.3.3) is determined from an energy balance between the total energy added by heat transfer, and the energy rise of the coolant; i.e.

$$\dot{m} \cdot C_p \Delta T = \ddot{q}' \pi r_{fu}^2 \Delta l \quad ,$$

where, $\dot{m}$ = mass flow rate of coolant

Δl = length of the segment

ΔT = increase in Bulk temperature from one segment to another, $(T_{B2} - T_{B1})$

Thus, $T_{B2} = T_{B1} + \dfrac{\pi r_{fu}^2 \Delta l}{\dot{m} C_p}$ .... (Eqn 4.14)

for the first segment T_{B1} = inlet temperature and thus T_{B2} is evaluated. For successive segments T_{B2} becomes T_{B1} and the calculation proceeds.

4.3.7 SPECIAL CONSIDERATIONS

Two important checks are required to ensure proper coolant conditions:-

(1) No Bulk-Boiling occurs anywhere in the core;

To ensure this $T_B < T_{SAT}$, the coolant saturation temperature at the local pressure. The critical location is, of course the core exit for the central rod where bulk temperature is maximum and pressure the minimum.

(2) No local boiling or sub-cooled boiling occurs near the surface of the fuel rod. Whenever $T_s > T_{SAT}$ at a local point, this phenomenon may occur like during peak loads. This may result in Boiling burnout of the surface. To assess this, the local heat flux , is compared with the CHF, Critical Heat Flux (or DNB) at which state blanketing of the heat transfer surface by coalesced vapour bubbles is just imminent. Any further flux increase requires heat transfer through this blanket. Due to the low conductivity of the vapour blanket, a catastrophic increase in surface temperature would result, leading to melting of the cladding.

Determination of the CHF has been done using the widely accepted Jens and Lottes correlation:

$$CHF = C \left(\frac{\dot{m}}{10^6}\right)^M (T_{SAT} - T_B)^{0.22} \quad \ldots (Eqn\ 4.15)$$

where, C, M = pressure dependent constants (see sec.4.3.8)

Whenever sub-cooled flow boiling exists to any extent, Newton's law of cooling for determining T_c is invalid (as 'h' in it does not reflect the increased agitation in the boiling film due to the vapour bubbles). Jens & Lottes correlation for sub-cooled boiling gives (in f.p.s. system)

$$T_s = 1.9\ (q'')^{0.25}\ exp\ (-P/900) + T_{SAT}$$

where, P = local coolant pressure

$$q'' = q''' \frac{r_{fu}^2}{2\ r_{cl}}$$

The CHFR (CHF ratio)defined as ratio of CHF and q'', should hence be greater than 1 to satisfy condition (2) above.

4.3.8 OTHER EMPIRICAL CORRELATIONS

The thermal conductivities, viscosity, density and specific heat at constant pressure are all functions of temperature. As temperature in the coolant channel continually varies, correlations for them would be required .

They are (in c.g.s. system)

$$K_{fu}(T) = 0.10308 - 0.14186 \text{ E-3} * T + 0.73263\text{E-7} * T^2,$$

$$K_{cl}(T) = 0.14194 + 0.6924\text{E-4} * T,$$

for the coolant:-

$$K(T) = 0.27656\text{E-2} + 0.39731\text{E-4} * T - 0.10152 \text{ E-6} * T^2.$$

$$\mu(T) = 0.329\text{E-2} - 0.12479\text{E-4} *T + 0.15296\text{E-7} * T^2;$$

$$\mathcal{S}(T) = 0.738 + 0.6445 \text{ E-3} *T - 0.45827\text{E-5} * T^2;$$

$$C_p(T) = 17.677 - 0.1104 * T + 0.2338 \text{ E-3} * T^2;$$

certain other phenomena depend on local pressures. They are correlated as under (P in p.s.i.)

$$T_{SAT}(P) = 0.23357\text{E3} + 0.6129\text{E-1} * P - 0.5666\text{E-5} * P^2,$$

$$C(P) = 0.11312\text{E1} - 0.78\text{E-3} * P + 0.3312\text{E-6} *P^2 - 0.56355 \text{ E-10} * P^3,$$

$$M(P) = 0.48141\text{E-1} + 0.22471 \text{ E-3} * P + 0.8302\text{E-9} *P^2,$$

(C & M as in eqn 4.15)

Finally, a series expansion has been used to evaluate Bessel's

functions $J_o(x)$ & $J_1(x)$ and modified Bessel's functions $I_o(x)$ &

$I_1(x)$ (from ref (40)).

4.4 RESULTS AND COMMENTS

Analysis of core performance of merchant ships

SAVANNAH, MUTSU and LENIN was done using the Thermal Hydraulic

CODE & results obtained were within 1°C accuracy. A pellet

diameter and clad thickness of respectively 0.858 cm & 0.66 mm

was chosen after an optimization study using ref(14). Results

for various combinations of pellet dia. and clad thickness for

a constant volume ratio of fuel & water (for satisfying Reactor

Physics considerations) are given below; the design chosen

(case 1) can hence be justified as being optimum:-

Parameter	Case 1	Case 2	Case 3	Case 4
Pellet size	0.858	1.000	1.000	0.700
Clad thickness	0.066	0.066	0.100	0.066
Pitch	1.30	1.766	1.810	1.262
Core dia (for 120 MWt)	134.29	182.41	186.99	130.34
Core Power Den.	63.51	34.42	32.76	67.41
Max fuel Centre-line Tempr.	1696.8	1678.6	1688.4	1725.3
Min. CHFR obtained	2.701	3.334	3.530	2.313
Max. burnout flux	1.615	2.946	3.000	1.809
Burnup	1469 8	16982	16530	10685

The thermal Hydraulic CODE can be used for various flux functions Sin(z) , z .Sin(z) & (π -z).Sin(π -z) by feeding an input 'flux code' 000,111 or 222 respectively. Some results obtained by this exercise ensue as follows:-

Parameter	Sin(z)	z.Sin(z)	(π - z).Sin(π
Minimum CHFR	3.248	2.701	2.797
Total F_Q^N	3.705	4.367	4.367
Max. fuel C-Line tempr. (°C)	1541.4	1696.8	1696.8
Max. cladding tempr.(°C)	335.86	335.87	335.88
Flux beyond which bulk boiling/burnout occurs (times of average flux)	1.615	1.586	1.586
Coolant exit tempr. from bottest channel(°C)	316.33	316.92	316.91

Results obtained from the CODE are given in pages 28 to 36 of computer print-outs; flux distribution illustrated is   Sin(z). For comperitive purposes, fuel-rod conditions for the hottest channel for Sin(z) & (π -z).Sin(π distribution are tabulated in pages 46 to 48 of printouts.

****

C H A P T E R - 5
REACTOR PHYSICS DESIGN

RESUME

5.1 INTRODUCTION

A nuclear reactor is an assembly of a proper size of fissionable material and other associated materials essential to sustain a chain reaction. The power generated is directly dependent on the neutron flux. It is of prominence to understand the behaviour of these neutrons in the reactor.

In this chapter, we consider those reactor-core calculations that provide k_{eff}, effective multiplication factor. and the stationary neutron-flux distribution at Steady-state operation. k_{eff} is required to establish nuclear composition and configuration, which satisfies criticality and control requirements. The steady-state flux distribution must be known to calculate reaction rates and power distributions that are needed for the thermal & shielding design of the reactor.

Evaluation of k_{eff} necessitates the determination of the 4 factors η, ε, p, f and non-leakage probabilities L_T and L_F . For sketching the flux distributions, 2-group 2-region theory has been used with water as the reflector. Heterogeneous effects have been considered at all stages of calculation.

5.1.1 Neutron Cycle :

A typical history of 100 fast fission neutrons and how they sustain a chain reaction is illustrated in Fig(5.1). All important neutron interactions are indicated in it; the parameters used are applicable to the present design.
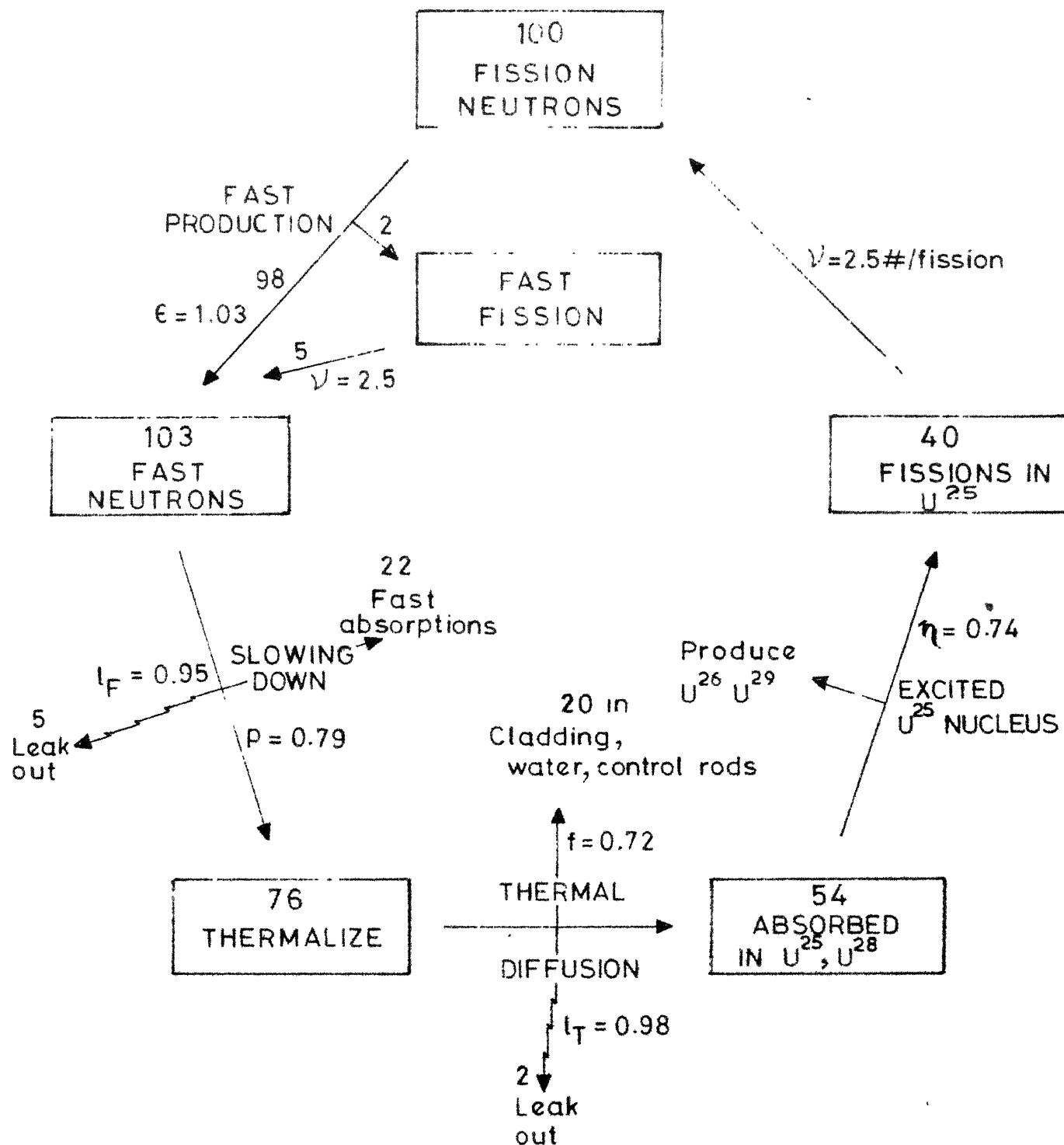
FIG. 5·1 CORE NEUTRON CYCLE

5.1.2 Reactor Physics Computer CODE

A computer CODE has been generated for determining k_{eff} and the flux distributions. The amount of 'poison' required in control rods has also been estimated. All parameters used have been corrected for the operating temperature and pressure. The inputs like core dimensions and temperatures of fuel & moderator have been taken from Chapter 4 . An enrichment of 5.0% has been chosen (chapter 3). The scheme of fuel loading in reactor is as per chapter 3 .

The scheme of computations is as follows. Input data are enrichment, fuel-rod & reactor dimensions, reflector thickness & average fuel & moderator temperatures. The only variable parameter fed in is the volume fraction (of moderator) of Poison, P_{frac}. P_{frac} is changed by interpolation till the critical determinent = 0; this will denote a steady-state reactor operation with the nett control poison of P_{frac}. The flux in both core and reflector are sketched for the above.

5.2 CRITICALITY OF THE REACTOR

5.2.1 Evaluation of k_{inf}:

Considering the reactor core as homogeneous will be erroneous as neutrons may undergo several collisions within a fuel rod before encountering the moderator. Calculation of $k_{inf} = \eta \, \epsilon \cdot pf$ still holds; but differences with respect to

homogeneous considerations should be noted.

ETA (η_T) :-

      This gives the ratio of neutrons produced to that absorbed in the fuel rod. Since absorption cross-section of Oxygen is essentially zero,

$$\eta_T = \frac{\nu_{25} \, \Sigma_{f25}}{\Sigma_{a25} + \Sigma_{a28}} \qquad \dots\dots\dots \qquad \text{(Eqn 1)}$$

where, $\nu_{25} = 2.47$ and Σ_{a25}, Σ_{f25} is dependent on fuel enrichment (hereafter) and cross-sections corrected for average fuel temperature obtained from chapter 4.

THERMAL UTILIZATION (f)

      This gives the probability that a thermal neutron is absorbed in the fuel itself with respect to the whole core i.e. ratio of neutrons absorbed in fuel only, to that absorbed in fuel, moderator & other structural materials.

$$f = \frac{\Sigma_{afu} \cdot \phi_{Tfu} \cdot V_{fu}}{\Sigma_{afu} \cdot \phi_{Tfu} \cdot V_{fu} + \Sigma_{am} \cdot \phi_{Tm} \cdot V_m + \Sigma_{ass} \cdot \phi_{Tss} \cdot V_{ss}}$$

where, all fluxes and cross-sections are average values. Since $\phi_{Tss} \cong \phi_{Tm}$,

$$f = \frac{\Sigma_{afu} \cdot V_{fu}}{\Sigma_{afu} \, V_{fu} + (\Sigma_{am} \cdot V_m + \Sigma_{ass} \cdot V_{ss}) \, \xi_T} \qquad \dots \text{Eqn(2)}$$

where $\xi_T = \dfrac{\phi_{Tm}}{\phi_{Tfu}}$ is called thermal Disadvantage factor(TDF).

                       (ranges from 1.00 to 1.05).

This factor is peculiar of heterogeneous reactors, taking

into consideration reduction of thermal flux in fuel rod
due to self-absorption. As f is unknown,
f is evolved through lattice functions for cylinderical fuel

rods:-

$$\frac{1}{f} = \frac{\Sigma_{am} \cdot V_m + \Sigma_{ass} \cdot V_{ss}}{\Sigma_{afu} \cdot V_{fu}} * F(x) + E(y,z)$$

....Eqn(3)

where $F(x)$ and $E(y,z)$ evolved from diffusion theory, are

lattice functions defined by :-

$$F(x) = \frac{x * I_0(x)}{2 I_1(x)}$$

$$E(y,z) = \frac{z^2 - y^2}{2y} \cdot \left(\frac{I_0(y)K_1(z) + K_0(y) I_1(z)}{I_1(z) K_1(y) - K_1(z) I_1(y)} \right)$$

where, $x = \frac{a}{L_{fu}}$, $y = \frac{a}{L_m}$ $z = \frac{b}{L_m}$

a = fuel rod radius

b = radius of equivalent fuel cell = $\frac{Pitch}{\sqrt{\pi}}$

L = thermal diffusion lengths.

The above equations, however, are valid for $a \ll b$ and hence

inaccurate for closely packed lattices. For x, y, z,

individually being < 0.75, the following series expansions

are quite accurate :-

$$F(x) = 1 + \sum_{i=1}^{\infty} \frac{1}{2 * i} \left(\frac{x}{2}\right)^{2i} \qquad \cdots\cdots Eqn (4)$$

$$E(y,z) = 1 + \frac{z^2}{2} \left\{ \frac{z^2}{z^2 - y^2} \cdot \ln\left(\frac{z}{y}\right) + \sum_{i=2}^{\infty} \frac{(-1)^{i+1} * 3}{2 * i} \left(\frac{y}{z}\right)^{2(i-2)} \right\}$$

....Eqn.(5)

'f' is the most important factor that controls k_{eff}. Control rod positions greatly alter it. The above treatment does not include control poison. In Eqn.(3), the value of Σ_{am} has to be modified to include the effect of Boron Poison. This is done by considering the poison as being equally dispersed in moderator and a term ($P_{frac} * \Sigma_{ap}$) now gets added, where Σ_{ap} = macroscopic absorption (thermal) of poison & P_{frac} is the volume fraction of moderator the poison occupies. P_{frac} varies linearly with control-rod position.

RESONANCE ESCAPE PROBABILITY (p)

This is the probability that a fission neutron will escape capture in resonances in U^{28} as it slows down to thermal energies. It is given by

$$p = \exp \left(- \frac{N_{fu} \cdot V_{fu} \cdot I \cdot \phi_{fu}}{\xi_m \cdot \Sigma_{sm} \cdot V_m \cdot \phi_m} \right) \quad \ldots \ldots \text{Eqn.(6)}$$

$$\text{where } \phi_{\mathfrak{z}} = \text{fast fluxes}$$

Here we are neglecting fast absorptions in cladding material and Poison which are negligibly small. $\dfrac{\phi_m}{\phi_{fu}}$, above, called the disadvantage factor for resonance neutrons is unknown. So p can't be evaluated through Eqn.(6). In a similar manner to f, p is evaluated through lattice functions.

Defining 'f_r' , resonance utilization factor

$$f_r = \frac{\text{Fast absorptions in fuel resonance}}{\text{Total fast absorptions}} \quad ;$$

$$= \frac{N_{fu} \cdot I_{eff} \cdot V_{fu} \cdot \varnothing_{fu}}{I_{eff} \cdot N_{fu} \cdot V_{fu} \cdot \varnothing_{fu} + \sum_{i} \Sigma_{sm} \cdot V_m \cdot \varnothing_m}$$

(or) $1/f_r = 1 + \dfrac{\sum_{i} \Sigma_{sm} \cdot V_m}{N_{fu} \cdot I_{eff} \cdot V_{fu}} \left(\dfrac{\varnothing_m}{\varnothing_{fu}}\right)$ .... Eqn.(7)

and from Eqn.(7) $p = \exp\left(-\dfrac{1}{\dfrac{1}{f_r} - 1}\right)$ .... Eqn (8)

As $\left(\dfrac{\varnothing_m}{\varnothing_{fu}}\right)$ is unknown, f_r can't be evaluated. We hence use

the following lattice functions (for cylinderical rods):-

$$\frac{1}{f_r} = \frac{\sum_{i} \Sigma_{sm} \cdot V_m}{N_{fu} \cdot I_{eff} \cdot V_{fu}} \ast F(x) + E(y,z) \quad ..... \text{ Eqn.(9)}$$

where, F(x) and E(y,z) have same meaning as Eqns.(4) & (5)
with x,y,z being functions of fast diffusion lengths here.
Knowing f_r, p is calculated using Eqn(8). In eqn.(10) $\sum_{i}\Sigma_{sm}$
is taken directly from tabulated experimental values – for
water 1.46 cm^{-1} (P.232 Ref. (23)) and I_{eff} the effective
resonance integral, is well represented for cylinderical fuel
rods as :-

$$I_{eff} = A + \frac{C}{\sqrt{a \cdot \mathcal{S}}} .... \text{ Eqn. (10)}$$

where A,C are constants (Ref.ibid)

$\quad$ a = fuel rod radius

$\quad \mathcal{S}$ = fuel density.

Eqn. (10) evaluates itself to 21.254 barns.

<u>Note</u>: Though listed values are for pure $U^{28}O_2$ they are valid

for slight fuel enrichments (upto 5%) as it does not

significantly after the extent of resonance absorption

in U^{28}.

In Eqn.(9) the effect of Poison on $\zeta^{\ell} \Sigma_{sm}$ should be

considered. The effective values of $(\zeta^{\ell}_{eff} * \Sigma_{smeff})$ should

be taken.

$$\zeta^{\ell}_{eff} = \frac{(\zeta^{\ell} \Sigma_{sm})_m + (\zeta^{\ell} \Sigma_{sp})_p}{\Sigma_{sm} + \Sigma_{sp}} \qquad \ldots. \text{Eqn (11)}$$

and $\Sigma_{smeff} = (\Sigma_{sm} + \Sigma_{sp})$

FAST FISSION FACTOR $(\varepsilon \cdot)$:-

All neutrons don't succeed in escaping from fuel

and subsequently slowing down in moderator. Some are absorbed

in resonances above fission threshold as well as upto the

lower threshold of inelastic scattering in fuel, giving

rise to fast fissions, a favourable phenomenon. ε is the ratio

of number of neutrons having first collision in moderator

to the total produced in thermal fission. For determination

of ε , the method of Spinard, Fleishman & Soodak (SFS)

modified for closely-packed lattices has been used. The

neutrons are classified into 3 energy-groups in fuel with

corresponding neutron escape probabilities without having a

collision in fuel as P_1, P_2 & P_3 defined by Wigner's approximate

$$P_i = \frac{1}{\bar{r} \sum_{it} + 1} \quad \text{for } i = 1 \text{ to } 3 \quad \ldots\ldots \text{ Eqn (12)}$$

where, $\bar{r} = \frac{4 \ast \text{Volume}}{\text{Surface area}}$ of fuel rod

$= 2 \ast r_{fu}$ for cylinderical rods.

$\sum_{it}$ = Total Group i cross-section.

The 2 fractions of fission neutrons in the 2 energy groups, with the first above and the second below the fission threshold of 1 MeV, are given as $\psi_1 = 0.561$ and $\psi_2 = 0.439$. The third group contains neutrons scattered from the first group into energies below fission threshold given by fractions:-

$$\beta_1 = \frac{\psi_1 \nu_1 \sigma_{1f} + \sigma_{11}}{\sigma_{1t}} \quad \ldots\ldots\ldots \text{ Eqn (13)}$$

$$\beta_2 = \frac{\sigma_{22}}{\sigma_{2t}} \quad ; \quad \beta_3 = \frac{\sigma_{33}}{\sigma_{3t}}$$

Now, ε is defined as the sum of 3 probability terms as :-

$$\varepsilon = \frac{\psi_1 P_1}{1-(1-P_1)\beta_1} + \left\{ \psi_2 + \frac{\psi_2 \psi_1 \nu_1 (1-P_1)\sigma_{1f}}{\sigma_{1t}(1-(1-P_1)\beta_1)} \right\} \ast$$

$$\ast \left\{ \frac{P_2}{1-(1-P_2)\beta_2} \right\} + \left\{ \frac{\psi_1 (1-P_1) \cdot \sigma_{13}}{\sigma_{1t}(1-(1-P_1)\beta_1)} \right\} \ast$$

$$\ast \left\{ \frac{P_3}{1-(1-P_3)\beta_3} \right\} \quad \ldots\ldots\ldots \text{ Eqn (14)}$$

The cross-section used in Eqn.13 and Eqn. 14 are taken directly from p.402-406, Ref(23).

k_{inf} :-

Having evaluated the above k_{inf} is given by

$$k_{inf} = \eta_T * \varepsilon * p * f$$

5.2.2 LEAKAGE AND k_{eff} :-

Since the material & geometric buckling have to be equal for a critical system $B_g^2 = \dfrac{k_{inf} - 1}{L_{th}^2}$

taking fast leakage into consideration:-

$$k_{eff} = \frac{k_{inf} * \exp(-B\tau)}{1 + L_{th}^2 \cdot B^2} \qquad \ldots\ldots\ldots\ldots \text{Eqn (15)}$$

In steady-state reactor operation, $k_{eff} = 1.00$

5.2.3 CONTROL REQUIREMENT:-

The amount of Poison required is determined from the CODE by trial and error method for varying values of P_{frac} such that the critical determinent(refer Eqn.63) is a minimum. This will be the steady-state value of Poison required to maintain criticality. The inbuilt reactivity of the core is determined by putting $P_{frac} = 0.0$ and setting the core at room temperatures. The boron Poison required is evaluated by choosing a slightly higher value so that the reactor remains subcritical even in the cold condition.

5.2.4 TEMPERATURE AND PRESSURE EFFECTS:-

(i) Thermal group constants:-

(a) The averaged thermal absorption and fission cross-sections are strong functions of temperature. Taking the Maxwellian distribution, they vary as

$$\sigma_a(T) = \frac{\sqrt{\pi}}{2} g_a^{(T)} \left(\frac{T_0}{T}\right)^{0.5} * \sigma_{a\,2200} \qquad \ldots\ldots\ldots \text{Eqn.(16)}$$

$$\sigma_f(T) = \frac{\sqrt{\pi}}{2} g_f^{(T)} \left(\frac{T_0}{T}\right)^{0.5} * \sigma_{f\,2200} \qquad \ldots\ldots\ldots \text{Eqn (17)}$$

where, $T_0 = 295.1$ K   T = average fuel temperature

$g_a(T)$, $g_f(T)$ are non-$\frac{1}{v}$ absorption and fission factors, respectively for deviation from Maxwellian distribution.

For materials other than fuel, $g_a(T) = 1.0 \,\forall\, T$

The cross-sections for all materials have been corrected as above using following average temperatures :-

Moderator (in core) .... From Chapter-4 CODE.

Water (in reflector) .... 280°C

Fuel temperature   .... From Chapter-4 CODE

Other materials in core ......Average Coolant temperature

(b) The diffusion length for water is a strong function of temperature and pressure. An experimental value for L_{th} given by Deutsch (p.92, Ref(22)) has been used:

$$\bar{L}_{th}(T,pr) = \frac{2.719}{\rho(T)} * (\frac{T+273.1}{295.1})^{0.5}$$

$$\frac{1.0614}{1+0.0614 \ (\frac{T+273.1}{295.1})^{0.5})}\}^{0.5}$$

Eqn (19)

where, pr = water pressure, psi

T = water temperature, °C

$\rho(T)$ = water density at p_r and T

(c) For water, $\sum_a \propto N$, number density, which in turn is $\propto \rho(T)$; $\therefore \sum_a \propto \rho(T)$.

As, $\rho(T) = 0.93796 + 0.64448E-3*T - 0.458271E-3 *T^2$ gm/cc

. . . . Eqn. (20)

where, T= water temperature (for 2000psi pressurised water),

So, $\sum_a(T) = \rho(T) * (\frac{T}{T_0})^{0.5} * \sum_a(T_0)$

Next, to evaluate diffusion constant $\bar{D}$ for water, we use the familiar equation

$$\bar{D} = L_{fh}^2 * \sum_a$$ . . . . Eqn (21)

We see that the $\bar{D}$ calculated in the above manner is reasonably accurate.

(ii) Fast group constants:-

(a) The neutron age, τ, in water is not that much affected by temperature as pressure. $\tau \propto \dfrac{1}{\rho^2}$; As temperature & pressure increases, density decreases thus increasing neutron age in water. We arrive at :

$$\tau (T, pr) = \frac{\tau_0 * \rho_0^2}{\rho(T)^2} \qquad \dots\dots\dots\dots \text{Eqn.(22)}$$

where $\tau_0 = 27 \text{ cm}^2$ } at atmospheric pressure
$\rho_0 = 1 \text{ gm/cc}$ } and temperature of 22.1°C

(b) The fast neutron age in core is dependent on temperature in an indirect manner. A temperature increase results in a decrease of ρ, thus increasing the age. This has been elaborated in the subsection that follows.

(iii) Heterogeneous Core constants:

(a) In a heterogeneous lattice, the average absorption cross-section $\overline{\Sigma}_{as}^{*}$ is :-

$$\overline{\Sigma}_{as} = \Sigma_{afu} \cdot V_{fu} + (\Sigma_{am} + \Sigma_{ap}) V_m + \Sigma_{ass} \cdot V_{ss}$$

$$\text{.. Eqn (23)}$$

and

$$\Sigma_{tr} = \Sigma_{trfu} \cdot V_{fu} + \Sigma_{trm}' V_m + \Sigma_{trss} \cdot V_{ss}$$

$$\text{... Eqn. (24)}$$

Σ_{trp} being relatively very small may be neglected.

---

* Hereafter subscript 's' stands for thermal/slow neutron parameters. Subscript 'f' stands for Fast neutron parameters.

(b) The extrapolation distance (E.D.) of the core is then

$$E.D. = \frac{0.71}{\Sigma_{tr}} \qquad \ldots\ldots \text{Eqn(25)}$$

(c) Since average diffusion coefficient, $\overline{D}_s$, of Lattice varies inversely as $\overline{\Sigma}_{tr}$, it follows from Eqn.(24) that :-

$$\frac{1}{\overline{D}_s} = \frac{V_{fu}}{D_{fu}} + \frac{V_M}{D_M} + \frac{V_{ss}}{D_{ss}}$$

$$\text{(Or)} \quad \overline{D}_s = \frac{1}{\frac{V_{fu}}{D_{fu}} + \frac{V_M}{D_M} + \frac{V_{ss}}{D_{ss}}} \qquad \ldots\ldots\ldots \text{Eqn (26)}$$

(d) Now $\overline{L}s$, the thermal diffusion length of core, is determined from Eqn (26) & (23) :-

$$\overline{L}_s = \frac{\overline{D}_s}{\overline{\Sigma}_{as}} \qquad \ldots\ldots\ldots\ldots \text{Eqn (27)}$$

(e) The neutron age in the core is determined from experimental values for age of a U-H_2O mixture (p.206 Ref.(23)). In the above case, a change in temperature (& pressure) has the effect of reducing the atom density of water relative to fuel which is equivalent to increasing the metal-to-water ratio in volume.

As $\S$ is given by Eqn.20, the ratio of U-H_2O mixture, say,

$$X = \frac{\text{Vol. of U}}{\text{Vol. of } H_2O} \times \frac{1}{\S(T)}$$

Using Fig 6.4 of ref[23] , we arrive at the following correlation for age, τ_1 :-

$$\tau_1 = 19.8 + 12.5 * X - 5.0 * X^2 \text{, for } X \leqslant 0.9$$

$$= 27.0 + 6.27 * (X - 0.9) \text{, for } X > 0.9$$

(f) In Eqn (26) D_m is taken from Eqn (21) but D_{ss}, D_p and D_{fu} are still unknown. These are individually calculated as :-

$$\bar{D}_s = \frac{1}{3 \left(\Sigma_2 + \Sigma_s (1 - \mu_0) \right)} \qquad \ldots\ldots \qquad \text{Eqn (28)}$$

(g) Finally, the fast diffusion constant, $\bar{D}_f$ in core since hydrogen scattering cross-section varies significantly with neutron energy, an artifice is used for core transport cross-section. Then, using

$$\Sigma_{af} = \frac{N I_{eff}}{\ln \left(\frac{E_0}{E_m} \right)} \qquad \ldots\ldots\ldots\ldots \text{Eqn (29)}$$

and Eqn.(28), $\bar{D}_f$ is calculated. All the above calculations are shown in Appendix A5-1.

5.2.5 HETEROGENEOUS VERSUS HOMOGENEOUS :-

We are now in a position to comprehend what effects would we have incurred had a homogeneous treatment of the reactor been done. As $\frac{\ell}{\ell_T} > 1$, f (hetero) $<$ f(homo) due to the self-shielding effect of the fuel rods. However, p (hetero) $>$ p(homo) as the above effect reduces the number of neutrons that are parasitically absorbed by fuel resonances. Thus, decrease in f is more than offset by increase in p . So, (f.p) hetero $>$ (fp) nomo.

The fission neutrons pass through a region of pure fuel where they are likely to induce fast fission, before emanating to the moderator. Hence, (ε) hetero $>$ (ε) homo. This effect is not that pronounced as the other factors above. η_T does not, however, change.

In view of the above inequalities, k_{inf} for heterogeneous lattices is greater than its homogeneous equivalent. A homogeneous treatment, though much simpler would consequently give erreneous results.

3. FLUX DISTRIBUTION

The thermal reactor consists of a heterogeneous multiplying core surrounded by a non-multiplying water reflector. Since the core consists of a closely-packed square lattice of fuel rods, it can be considered homogeneous for determining flux distributions in core & reflector. Despite its limitations, 2-group approximation has been used, as it is the simplest that will give reasonably accurate results for multi-region calculations.

The diffusion equations for fast & slow neutrons are is given by :-

$$D_f \nabla^2 \phi_f \; - \; \Sigma_{rf} \cdot \phi_f \; + \; \frac{k_{inf}}{p} \cdot \Sigma_{as} \cdot \phi_s \; = 0 \; \dots\dots \; \text{Eqn (30)}$$

$$D_s \cdot \nabla^2 \phi_s \; - \; \Sigma_{as} \cdot \phi_s \; + \; p \cdot \Sigma_{rf} \cdot \phi_f \; = 0 \; \dots \; \text{Eqn (31)}$$

where, all symbols have their usual meanings ,

$$\Sigma_{as} = \text{thermal absorption cross-section}$$

$$\Sigma_{rf} = \text{slowing-down (fast removal) cross-section.}$$

In core, $k_{inf} > 1$ and in reflector $k_{inf} = 0.0$

The solution of Eqns (30), (31) are solutions of wave equations

$$\nabla^2 \phi_f + B^2 \phi_f = 0$$

$$\nabla^2 \phi_s + B^2 \phi_s = 0$$

This implies the coupling of the solutions by the condition that coupling-coefficient, S , between fast & slow fluxes is

$$S = \frac{\phi_f}{\phi_s} = \frac{\Sigma_{as} + D_s B^2}{p \cdot \Sigma_{rf}} \qquad \dots\dots\dots \text{Eqn(32)}$$

The criticality condition should be satisfied;

i.e. $k_{eff} = 1 = \dfrac{k_{inf}}{\left(1+\dfrac{B^2}{x_s^2}\right)\left(1+\dfrac{B^2}{x_f^2}\right)}$ $\quad \dots\dots$ Eqn. (33)

$$\text{where } x_s = 1/L_s$$

$$x_f = 1/L_f$$

We shall use subscripts '1' for core and '2' for reflector.

Eqn (33) defines 2 values for B$^{(refer fig.5.2)}$ thus :-

$$B_1^2 = \frac{-(x_{1f}^2 + x_{1s}^2) + \sqrt{(x_{1f}^2 + x_{1s}^2)^2 + 4 x_{1f}^2(k_{inf}-1)\cdot x_{1s}^2}}{2}$$

$$\dots\dots \text{Eqn. (34)}$$
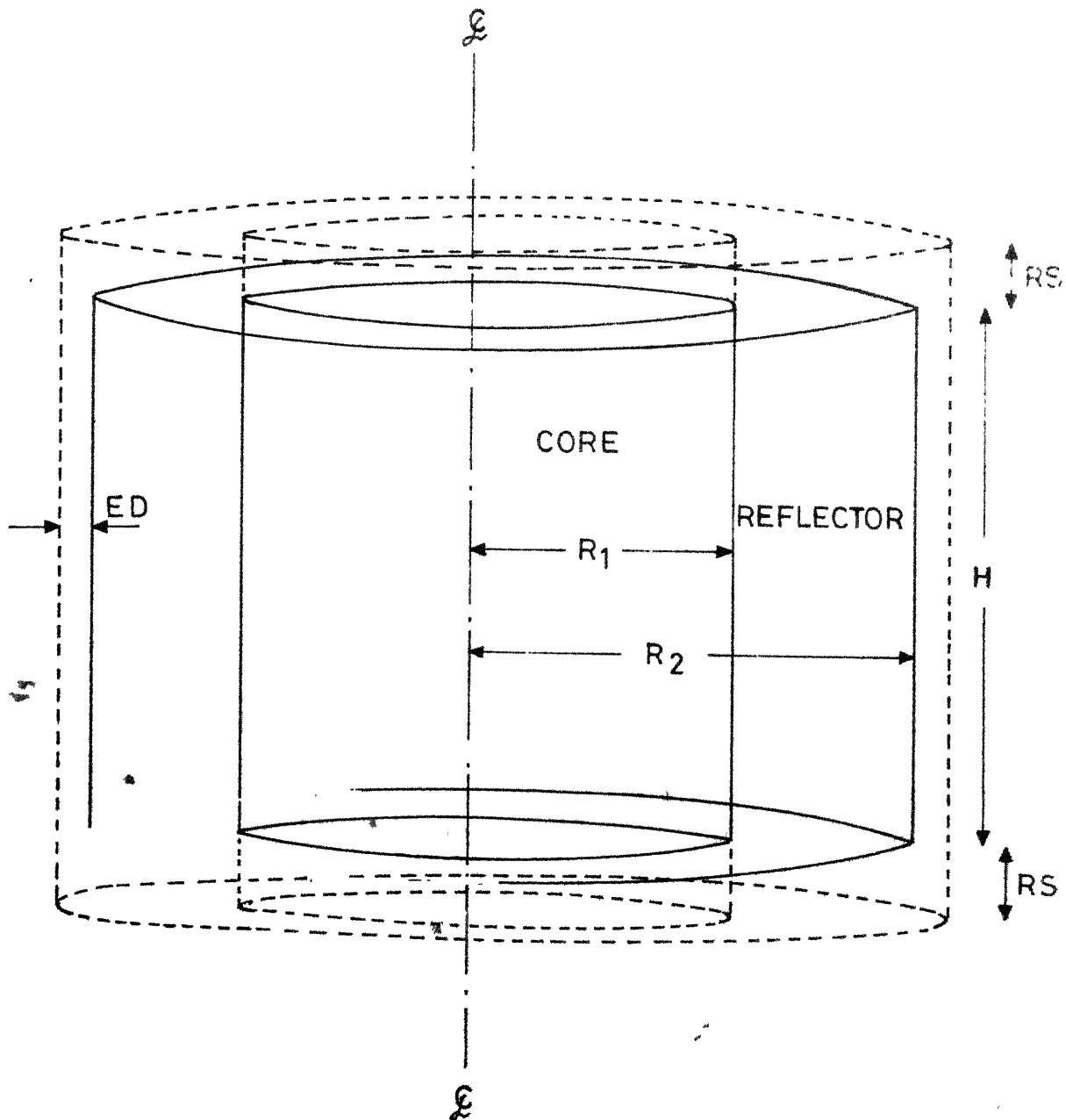
KEY:

ED — Extrapolation distance

RS — Reflector savings

FIG. 5.2 CORE-REFLECTOR CONFIGURATION.

$$B_1'^2 = \frac{-(x_{1f}^2 + x_{1s}^2) - \sqrt{(x_{1f}^2 + x_{1s}^2)^2 + 4 \cdot x_{1s}^2 \cdot x_{1f}^2 \cdot (k_{inf} - 1)}}{2}$$

..... Eqn. (35)

$$B_2^2 = -x_{2s}^2 \qquad \text{.... Eqn. (36)}$$

$$B_2'^2 = -x_{2f}^2 \qquad \text{...... Eqn.(37)}$$

Considering wave-equations are separable in both core & reflector,

$$\emptyset = \cos\left(\frac{\pi}{H + 2RS}\right) * F(r) \qquad \text{..... Eqn. (38)}$$

where, RS = reflector saving* = $\left(\dfrac{D_{1s}}{D_{2s}}\right) \cdot L_{2s} \left(1 - \exp\left(\dfrac{R_2 - R_1}{L_{2s}}\right)\right)$

F(r) is the solution of the equation

$$\frac{d^2F}{dr^2} + \frac{1}{r}\frac{dF}{dr} + \left(B^2 - \left(\frac{\pi}{H+2RS}\right)^2\right) * F = 0$$

since B^2 has 2 values in both core & reflector (given by Eqns(34) to (37)), to define F(r) completely, a total of 4 equations will have to be satisfied :-

$$\frac{d^2F_{1f}}{dr^2} + \frac{1}{r}\frac{dF_{1f}}{dr} + l^2 F_{1f} = 0 \qquad \text{........ Eqn. (39)}$$

$$\frac{d^2F_{1f}}{dr^2} + \frac{1}{r}\frac{dF_{1f}}{dr} - m^2 F_{1f} = 0 \qquad \text{...... Eqn (40)}$$

$$\frac{d^2F_{2f}}{dr^2} + \frac{1}{r}\frac{dF_{2f}}{dr} - \mu_s^2 F_{2f} = 0 \qquad \text{.... Eqn (41)}$$

* From p.69, ref(24) .

$$\frac{d^2 F_{2f}}{dr^2} + \frac{1}{r} \frac{dF_{2f}}{dr} - \mu_s^2 \cdot F_{2f} = 0 \quad \ldots\ldots \text{Eqn (42)}$$

Identical 4 more equations are there for F_{1s} and F_{2s} as well.

1, m, μ_s and μ_f are all +ve constants :-

$$l^2 = B_1'^2 - (\frac{\pi}{H + 2RS})^2 \quad \ldots\ldots\ldots \quad \text{Eqn (43)}$$

$$m^2 = - B_1'^2 - (\frac{\pi}{H + 2PS})^2 \quad \ldots\ldots\ldots \quad \text{Eqn (44)}$$

$$\mu_f^2 = - B_2^2 + (\frac{\pi}{H + 2RS})^2 \quad \ldots\ldots\ldots \quad \text{Eqn (45)}$$

$$\mu_s^2 = - B_2'^2 + (\frac{\pi}{H + 2RS})^2 \quad \ldots\ldots \quad \text{Eqn. (46)}$$

The solutions of Eqns (39) to (42) are Bessel's functions. The complete solutions are as under :-

In core

$$F_{1s}(r) = A \cdot J_0(lr) + C \cdot I_0(mr) \quad \ldots\ldots\ldots \quad \text{Eqn.(47)}$$

$$F_{1f}(r) = A \cdot S_1 \cdot J_0(lr) + CS_1' \cdot I_0(mr) \quad \ldots\ldots \quad \text{Eqn (48)}$$

In reflector

$$F_{2s}(r) = E \cdot I_0(\mu_s r) + G \cdot K_0(\mu_s r) + H \cdot I_0(\mu_f r) + M \cdot K_0(\mu_f r)$$
$$\ldots\ldots\ldots \quad \text{Eqn. (49)}$$

$$F_{2f}(r) = S_2' * (H \cdot I_0(\mu_f r) + M \cdot k_0(\mu_f r)) \quad \ldots\ldots \quad \text{Eqn.(50)}$$

where S_i's given by Eqn. (32) are :-

$$S_1 = \frac{\Sigma_{1as} + D_{1s} B_1^2}{p \cdot \Sigma_{1rf}} \qquad \ldots\ldots \quad \text{Eqn (51)}$$

$$S_1' = \frac{\Sigma_{1as} + D_{1s} B_1'^2}{p \cdot \Sigma_{1rf}} \qquad \ldots\ldots\ldots \quad \text{Eqn (52)}$$

$$S_2 = 0.0 \qquad \ldots\ldots \quad \text{Eqn (53)}$$

$$S_2' = \frac{\Sigma_{2as} + D_{2s} \cdot B_2'^2}{\Sigma_{2rf}} \qquad \ldots\ldots \quad \text{Eqn (54)}$$

Eqns. (47) to (50) contain 6 unknown constants A, C, E, G, H and M. These can be determined by the following boundary conditions :-

$$F_{2f}(R_2) = 0 \qquad \ldots\ldots \quad \text{Eqn (55)}$$

$$F_{2s}(R_2) = 0 \qquad \ldots\ldots \quad \text{Eqn (56)}$$

$$F_{1f}(R_1) = F_{2f}(R_1) \qquad \ldots\ldots\ldots \quad \text{Eqn (57)}$$

$$F_{1s}(R_1) = F_{2s}(R_1) \qquad \ldots\ldots\ldots \quad \text{Eqn (58)}$$

$$D_{1f} \cdot \frac{d F_{1f}(R_1)}{dr} = D_{2f} \frac{d F_{2f}(R_1)}{dr} \qquad \ldots\ldots \quad \text{Eqn(59)}$$

$$D_{1s} \cdot \frac{d F_{1s}(R_1)}{dr} = D_{2s} \frac{d F_{2s}(R_1)}{dr}$$
$$\ldots\ldots\ldots \quad \text{Eqn.(60)}$$

Applying Eqns (55), (56) to (49), (50) gives

$$E = - G \cdot \frac{K_0 (\mu_f R_2)}{I_0 (\mu_s R_2)} \qquad \ldots\ldots\ldots \quad \text{Eqn. (61)}$$

$$H = - M \cdot \frac{K_0 (\mu_f R_2)}{I_0 (\mu_f R_2)} \qquad \ldots\ldots\ldots \quad \text{Eqn. (62)}$$

using Eqns (57) to (62) in (47) to (50), we arrive at the following :-

$$
\begin{array}{cccc}
A & C & G & M
\end{array}
$$

$$
\begin{bmatrix}
Y11 & Y12 & Y13 & Y14 \\
Y21 & Y22 & Y23 & Y24 \\
Y31 & Y32 & Y33 & Y34 \\
Y41 & Y42 & Y43 & Y44
\end{bmatrix}
=
\begin{bmatrix}
0 \\
0 \\
0 \\
0
\end{bmatrix}
\quad ..\text{Eqn.(63)}
$$

where, Y_{ij} 's above are elements of the critical determinent as given in the CODE (line nos 23900 to 25900 of main program). . , the radius is required as it the only unknown

.... The critical determinent given by Eqn(63) = 0 ; only then will A,C,G & M will have non-trivial values as the 4 equations are homogeneous.

Next, the first 3 equations of Eqn(63) are taken and constants C, M and G evaluated with respect to A using Crammer's rule.

Finally, A is determined by the following method. Since the average thermal flux in the core is given by the relation:-

$$\bar{\emptyset}_{sav} = \frac{1}{\pi R^2 H} \int_{-H/2}^{+H/2} \int_{0}^{R_1} \left\{ A \cdot J_0(lr) + C \cdot J_0(mr) \right\} \cdot \cos\left(\frac{z\pi}{H+2RS}\right) \cdot 2\pi \, r \, dr \, dz$$

from A 3.1- 3, this works out as :-

$$\bar{\emptyset}_{sav} = A \cdot \left\{ \frac{2J_1(lR_1)}{lR_1} + 2\left(\frac{C}{A}\right) \frac{I_1(mR_1)}{mR_1} \right\} * \left\{ \frac{2(H+2RS)}{\pi} \frac{1}{H} \cdot \sin\left(\frac{\pi H}{(H+2RS) \cdot 2}\right) \right\}$$

Hence,

$$\frac{A}{\bar{\emptyset}_{sav}} = \frac{1}{\frac{2J_1(lR_1)}{lR_1} + 2\left(\frac{C}{A}\right) \frac{I_1(mR_1)}{mR_1}} * \frac{H}{2(H-2RS)\sin\left(\frac{\pi H}{2(H+2RS)}\right)}$$

$$\ldots\ldots \text{Eqn (64)}$$

It should be recalled that $\left(\frac{C}{A}\right)$ in Eqn.(64) is known and we obtain 'A' as the number of times of $\bar{\emptyset}_{sav}$. From this, the other 5 constants can be evaluated and since all constants in Eqns (47) to (50) are now known the radial flux functions in core & reflector can be easily sketched and is shown in Fig. 5.3
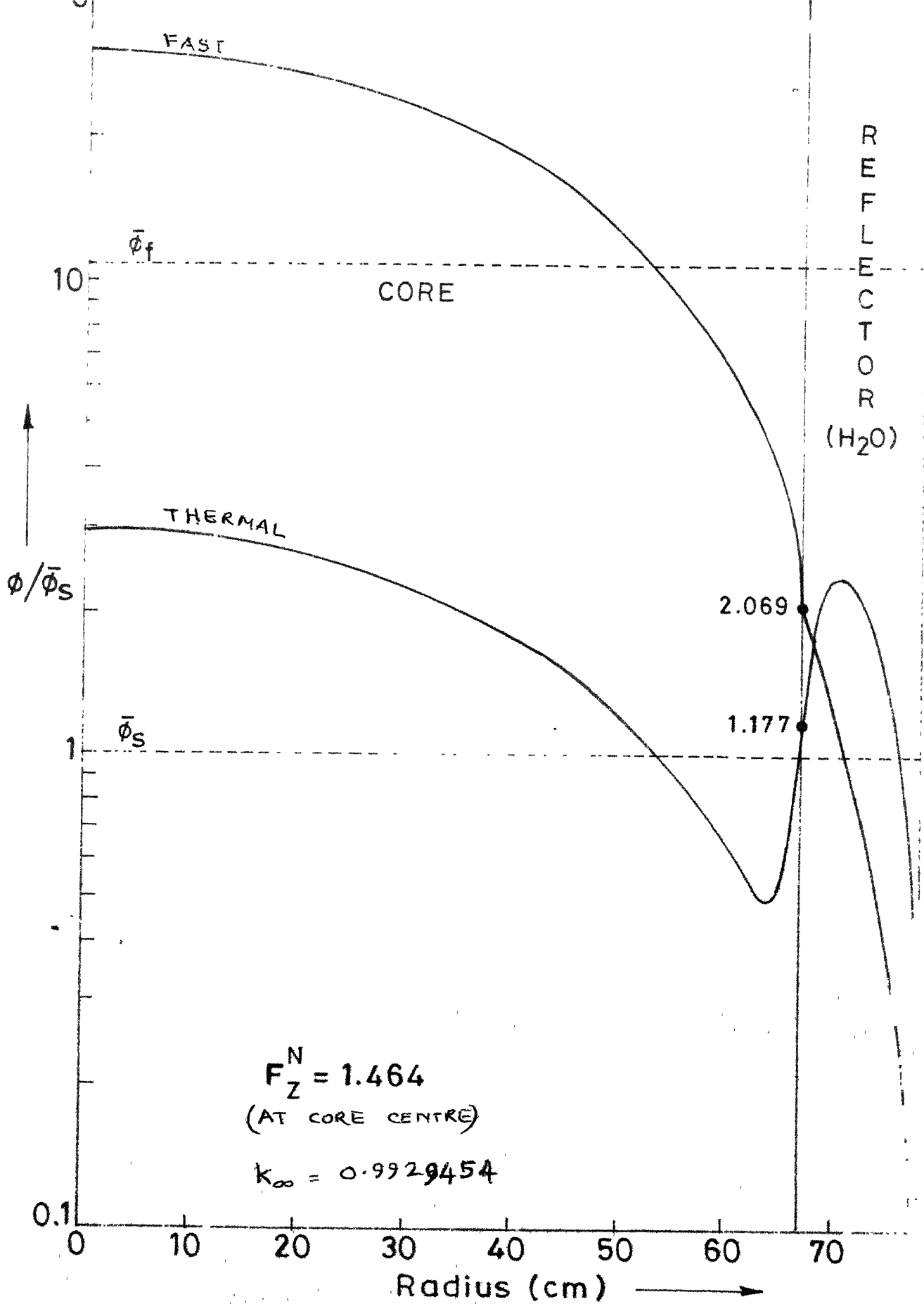
FIG. 5.3 RADIAL FLUX DISTRIBUTION.

5.4 RESULTS

A simple one group calculation of k_{inf} versus number den. ratio of U^{28} & water as per p.306, ref(23), gives a maximum k_{inf} at a ratio of 0.156 for the nuclear parameters chosen; this implies a pitch of 2.12 cm for a fuel rod diameter of 0.858 cm ai a core power density of 24.52 MW/m^3. This is clearly undesirable for the compactness desired. However, a pitch of 1.30cm chosen, though resulting in lesser moderation is a compromise, with the operating point falling only 8% from the k_{inf} peak.

Core criticality has been achieved at k_{eff}=0.992945 with the aid of a 10.99 cm thick water reflector. The various intermediate parameters, criticality determinent & others are shc in file CHECK-OUT(p.39 of computer print-outs). Other nuclear parameters like cross-sections, etc. are displayed in file K.OUT (p.37-38 of Print-outs). Fig 5.3 maps the radial flux variation; a rise in thermal flux at core edge due to moderation by the wate reflector is clearly seen.

Results of reactor control calculations (refer chap 7 evolves a volumetric Poison fraction of 0.92148E-3 for a clean reactor with a maximum of 2.35E-3 (with all rods in) to drive the reactor subcritical by 5% $\Delta k/k$ in the cold condition. File PSN.OUT (p.40 of print-outs) lists some parameters discussed later in Chapter 7.

****

C H A P T E R - 6

REACTOR SHIELDING

R E S U M E

6·1 <u>INTRODUCTION</u>

Shielding of a marine reactor is of far greater importance than its landbased counterparts. Here, the peculiar space, weight and dose rate limitations require an optimization study concerning the shielding materials and the differential shielding thicknesses, on the basis of dose rate mapping. Reactor shielding is essential to :-

(a) Not only protect the personnel working in close proximity to the reactor system but also to

(b) Reduce radiation levels in the vicinity of instrumentation and other equipment that may be damaged by radiation;

(c) Reduce the induced radioactivity of reactor components that may need to be serviced during shutdown (like primary loop components)

(d) Prevent excessive radiation induced heating of the pressure vessel (PV).

(e) Limit the neutron embrittlement of the PV.

The marine reactor shielding design would require a careful study of propagation of radiation through matter (i.e. shield material), system analysis of activity production and release in reactor effluents. It also requires other aspects of the ship & reactor design such as general plant layout & structural studies (not done here). The aim is to

utilize the large amounts of materials needed for shielding also for structural purposes to optimize on weight. For analysis a ⊁MARINE REACTOR SHIELDING CODE has been developed which has been referred to throughout .

6.1.1 TYPES OF SHIELDING

There are 3 Key factors in shielding design- cost, shield volume & shield weight. Any one of these may decide the type of shielding required. There are three types of shielding:-

(i) Unit Shield - that completely surrounds the reactor, like in land-based reactors.

(ii) Compartment Shield - that shields the reactor proper but not all its components like in mobile reactors.

(iii) Shadow Shield- that shields only the crew and important instrumentation, like in aircraft or space reactors.

6.1.2 REACTOR SHIELDING REQUIREMENTS

The control of radiation from a ship-board reactor presents, in particular, the 2 following problems of design:-

-shielding from neutron & gamma sources in a compact geometry layout.

-management of safe release of gaseous activity to satisfy

the requirements of rapid access to the reactor containment after shutdown. Among these, only the former has been studied to some depth.

The scheme of reactor shielding revolves primarily around these 5 considerations:-

(a) Slowing down the fast neutrons ($_0$n').

(b) Capture of slowed down $_0$n'.

(c) Determining the source of the secondary gamma radiations formed as a result of various neutron interactions in shield materials.

(d) Attenuation of all forms of gamma radiation.

(e) Determining the total dose rate of radiation emerging from the shield materials.

Let us examine the above points; for high energy neutrons, use of elements of moderate or high mass number is effective, as they are able to reduce their energies through inelastic scattering. Since elements of low mass numbers are the best moderators, H_2 in the form of water is used as a shield constituent for slowing down intermediate neutrons ($\leqslant$ 1MeV). Hence a combination of a moderately heavy element like steel with water is used.

As a general rule, most of the γ-rays originating from the core get absorbed in the shield region

nearer to the core itself. It is the secondary γ-rays, however, (emitted due to thermal neutron capture within the shield) along with a tiny fraction of the core gammas that control the shield thickness required. The neutron attenuating material to an extent also serve this purpose. However, as γ-ray relaxation lengths are inversely proportional to material density, additional material of higher density (like Lead) is incorporated to attenuate the higher energy γ- rays.

A word about the 'thermal shield'. This is basically to safeguard the PV. High gamma flux from the core leads to very high heat generation rates in any structural elements placed there. If it were the PV, then the resulting large temperatures & thermal stresses when added to the already present high mechanical (pressure) stresses, would bring the total stress on it (PV) to an unacceptably high level. Hence, a thermal shield consisting of layers of stainless steel and water is placed between the core & PV. The arrangement is as shown in Fig. 6.1. The steel has a high melting point & excellent thermal conductivity. Energy is absorbed by attenuating γ-radiation and inelastic scattering of fast neutrons. This heat is immense & is removed by the coolant flowing into the reactor core through these shield layers, thus contributing to the nett available energy from core.
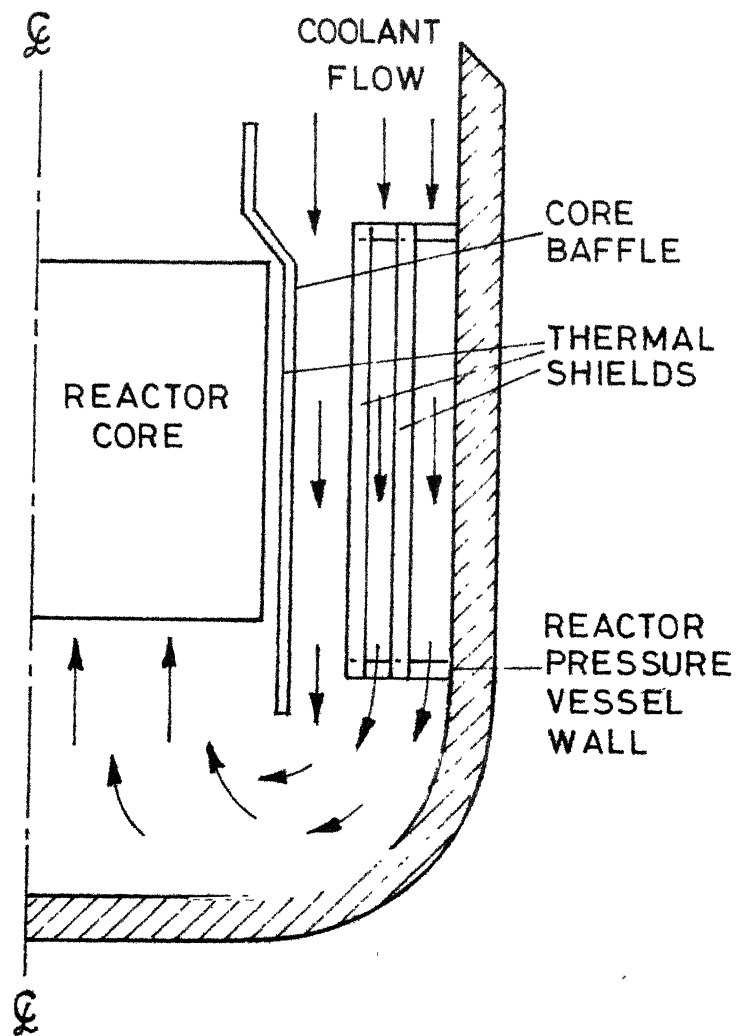
Fig. 6.1

Thermal shield in the PWR.

The core-γ energy is attenuated from $\sim 10^{17}$ MeV/cm^2-s to $\sim 10^{9}$ MeV/cm^2-s and the fast neutron flux from 0.28×10^{14} #/cm^2-s to 0.16×10^{9} # /cm^2-s before impinging onto the PV. Thus high thermal stresses and neutron induced embrittlement (by high-energy neutrons) is effectively reduced.

6.2 SALIENT FEATURES

6.2.1 SHIELDING DESIGN CHARACTERISTICS

The scheme used is as follows:-

(a) Thermal shield: stainless steel (ss 347) and water alternately used.

(b) Pressure Vessel: made of carbon steel, as it is required to withstand high mechanical stresses.

(c) Primary shielding: also called Neutron Shield Tank(NST) surrounds the PV-Made of carbon steel & water alternately, it has important mechanical support functions besides shielding, like supporting the entire PV,CRDM, Cooling ducts, part of primary piping, etc and also to resist shock load acting on the ship. The concentric layers of steel and water makes an optimal shield for both neutrons &γ-rays. Lead is not used here due to its lower melting point & poorer mechanical properties.

(d) Secondary Shielding – It surrounds the containment vessel & the complete primary loop (steam generator, associated piping, primary pump, etc.). It attenuates to the allowed dose, radiations coming from coolant loops (reactor effluents)– mainly γ-rays from O^{16} activation) and those escaping from primary shield. It's made up of one layer each of Lead & Polyethone. Concrete due to its much larger bulk for the same effectiveness has not been used. Study reveals that use of Boron based alloys here do not substantially aid in reducing the shield weight/bulk. Table 6.2 shows the thicknesses of the above shield materials evolved from the shielding CODE.

6.2.2 PERMISSIBLE DOSE RATES

The occupational individual accummulated dose is limited by the well known equation $D = 5 \cdot (N-18)$ rems, where N is age of the person. This implies a maximum dose rate of 2.5 mrem/hr. For personnel working in nuclear sites the limitation however is 1.5 rem/year or 0.75 mrem/hr. This is the design consideration in our shielding calculations. However a total dose of 12 rem[29] under emergency conditions has been allowed with doses in excess of 5 rems being adjusted over the next 5 years.

TABLE 6.2

OPTIMAL SHIELD DESIGNED

SHIELDING TYPE	MATERIAL	THICKNESS (CMS)
REFLECTOR	WATER	10.99
THERMAL SHIELD	Stainless Steel (Core Baffle)	1.27
	Water	13.90
	Stainless Steel	3.00
	Water	3.50
	Stainless Steel	8.00
	Water	10.25
PRESSURE VESSEL	CARBON STEEL	12.00
PRIMARY SHIELDING	Water	32.00
	Carbon Steel	16.00
	Water	10.00
	Carbon Steel	19.00
	Water	31.50
EMPTY SPACE (for housing components of primary loop)	Air	200.00
SECONDARY SHIELDING	Lead	15.10
	Polyethene	13.70

CORE RADIUS   67.145 cms.

TOTAL SHIELDING OUTER DIAMETER   30.67 ft.

6.2.3 OPTIMIZATION TECHNIQUES

The search for the optimum shield consists in evaluating the weight of various possible shield designs giving same dose rates at specified points. B. Chinaglia[28] , has sketched weight variation ΔW for the optimum configuration, as a function of neutron (D_n) to total dose $(D_n + D\gamma)$ i.e. $D_n/(D_n + D\gamma)$. The curve proves that the minimum weight is found for $D_n/(D_n + D\gamma) = 0.10$. This gives the lead & polyethene thicknesses as mentioned.

The optimum primary shield with respect to weight is composed by laminations of heavy metal located at about the middle of NST. No strong difference between the use of iron only or iron and lead is found. Hence only carbon steel is used.

6.3 RADIATION ATTENUATION IN SHIELD

The radiation from core includes α , β and γ-rays, neutrons of various energies, fission fragments, protons & α-particles from (n,p) & (n,α) reactions and neutrines. only neutrons & gamma rays are considered for shielding design as they are most penetrating. The primary and secondary radiations from the core have been briefly summed up in Fig. (6-3). We shall consider neutrons & γ-rays separately.
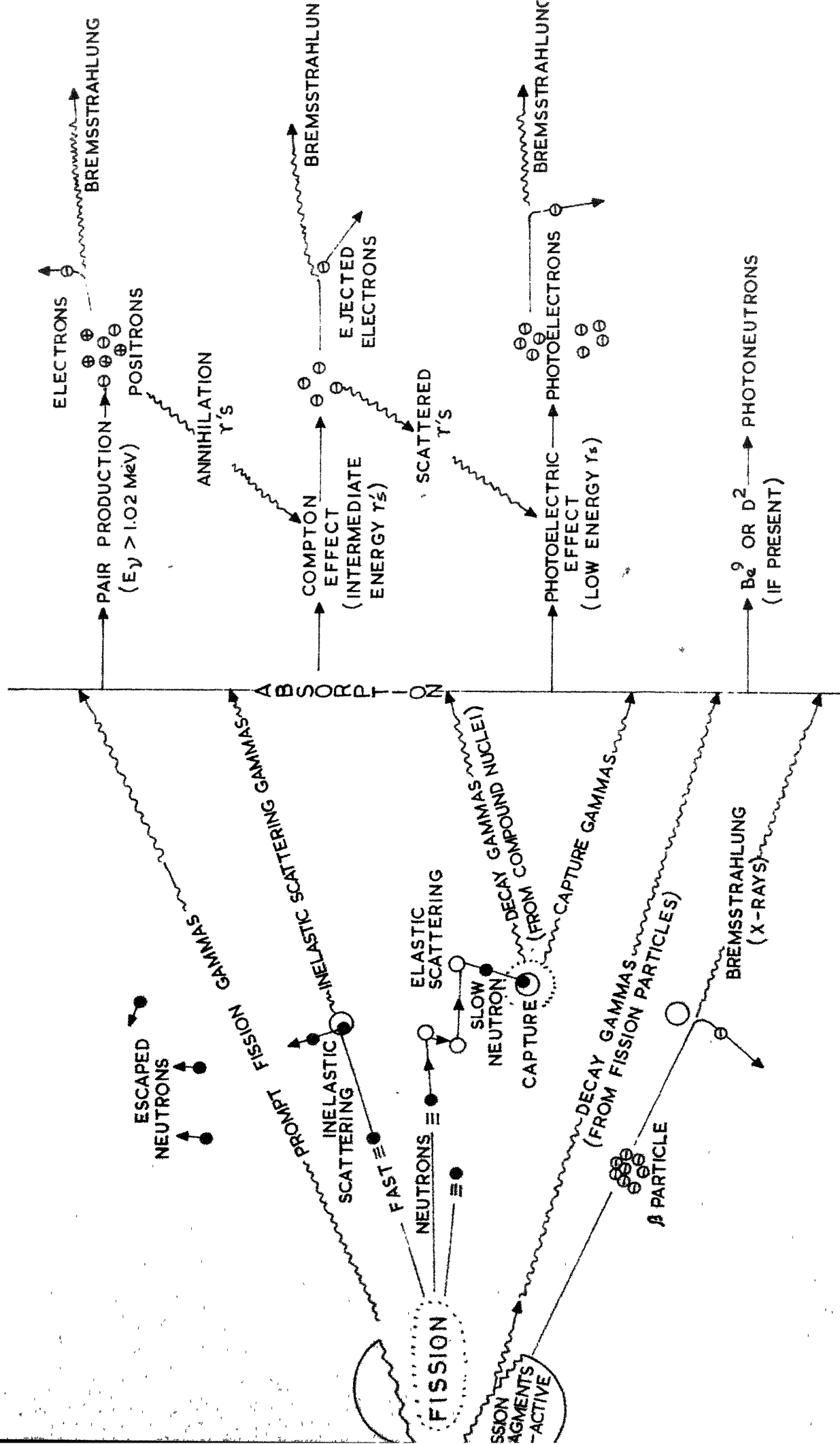
FIG. 6.3 PRIMARY & SECONDARY RADIATIONS 'SCHEMATIC.

6.3.1 <u>NEUTRON ATTENUATION CALCULATIONS</u>

The theory of neutron penetration through thick layers is different from ordinary theories of neutron diffusion used for criticality calculations where the interest is in the behaviour of average particles. But here, the interest is in those exceptional high-energy particles that do not undergo any interaction throughout the shield materials. The average neutrons that do the normal things are not very important as they stand no chance of getting far into the shield.

Neutrons are absorbed in the shield in 2 distinct stages. First, high energy neutrons are slowed down by elastic/ inelastic collisions; these slowed-down neutrons are then captured in shield materials easily as capture cross-secctions are high at low energies. We shall now consider these 2 stages separately.

(i) <u>FAST NEUTRONS</u>

<u>Theory of attenuation</u>

These attenuate as per the following 3 forms:-

(a) Elastic Scattering- Here, neutron K.E. is lost by collision with target nuclei. Dependent on scattering nuclei mass, it is the most important form of energy loss for light nuclei like H_2 where a single collision may result in the removal of the neutron. From 1 eV to 10KeV, this form is dominant.

(b) Shadow Scattering: This occurs at energies greater than 5 to 10 MeV wherein the neutron acts as a wave and is diffracted about the target nucleus. It occures only when neutron wave-length is lesser than nuclear radius. At large neutron energies, its cross section approached πR^2, geometrical nuclear cross-section.

(c) Inelastic Scattering: Its importance is that the incident neutron is strongly degraded since it loses the recoil energy of target nucleus plus energy equivalence of inelastic γ-rays emitted. This is very important for heavy nuclei where allowable energy levels are numerous and smaller are/distances between ground state & first energy level. Its threshold varies from 6 MeV for C_2 to few tenths-of-an MeV for Uranium. At high neutron energies, its cross-section also approaches πR^2.

In marine reactor design, we are interested in minimum weight. Limiting values of both (b) and (c) above approach πR^2 . Hence total cross-section (σ_T) approaches $2\pi R^2$ at high neutron energies. As nuclear radius $R = 1.5 \times 10^{-13} * A^{1/3}$ where A is mass number of the nucleus, the total mass cross-section becomes:

$$\frac{\Sigma_T}{\rho} = \frac{6.022 \times 10^{23}}{A} (2\pi R^2) \qquad = \frac{0.0852}{A^{1/3}} \ cm^2/g$$

which means light elements like H_2 give minimum shielding weights, justifying what was stated previously.

Equations used

Neutron flux follows the exponential attenuation law

$$\phi_f(x) = \phi_0 \cdot \exp\left(-\Sigma \cdot x\right)$$

where x = distance from source

ϕ_0 = source strength

Σ = effective removal macroscopic cross-section

For 2 to 12 MeV neutrons

$$\sigma = 0.35 \times A^{0.42} \quad \text{barns}$$

of material with mass no. A. This is used to evaluate Σ of unlisted materials like steel (refer Appendix A6.1)

Applying inverse square law for spherical attenuation

and considering $\phi_f(R)$ as flux at core edge,

$$\phi_f{}'(x) = \phi_f(R) \cdot \exp\left(-\Sigma \cdot r\right) \cdot R^2/r^2 \quad \text{for } r > R$$

As more than one layer is present, the exponential term for 'n' layers gets modified to

$$\left(\Sigma \cdot r\right) = \sum_{i=1}^{n} \Sigma_i t_i \qquad \text{where } \Sigma_i = \text{cross section},$$
$$t_i = \text{thickness, of layer } i$$

The attenuation prior to the P.V. wall occurs in the water and steel of thermal shield region. Experimental Data (p.153, (26)) for this region show that when build-up is considered,

point kernel can be represented by the sum of 2 exponential terms. For a large planar source of core, flux distribution in x cms of water, $\phi_f^r(x)$, is

$$\phi_f^r(x) = \phi_0 (A*E_1(ax) + (1-A)*E_1(cx))$$

where, ϕ_0 = incident flux

$E_1( )$ = incomplete error functions

(refer App. A6.2)

A = 0.89

a = 0.129 , c=0.091 (constants.)

The attenuation of fast neutrons thro ugh z cms. of steel followed by x cms of water is then well approximated by :-

$$\phi_f(z,x) \stackrel{\sim}{=} \phi_f(x) * E_1(\Sigma_{ss}.z)$$

Where Σ_{ss} = removal cross-sec for steel. Flux thus obtained is multiplied by $\dfrac{R^2}{(R+z+x)^2}$ to account for the spherical geometry.

Method used

The method used in SHIELDING CODE is 'Diffusion Removal Method'. Here, the basic assumptions are :-

(1) The penetrating component of source neutrons consists of high energy neutrons that suffer only a small energy loss and uncollided neutrons.

(2) Neutrons suffering large energy loss are regarded as being

removed from the beam.

(3) The removed neutrons are degraded in energy according to
diffusion theory and don't travel significantly from point
of removal.

The equations explained above have been used in
the code to obtain the fast flux at every layer. The flux
attenuation through the shield material is sketched in Fig.(6.4).

(ii) THERMAL NEUTRONS

The source of thermal neutrons are :-

(a) thermal flux emanating from the core.

(b) neutrons removed from the fast-flux beam. These removed
neutrons, forming local sources can be adequately
described by diffusion theory. This source intensity, is
$\phi_f(r) * \sum$. In any layer a distance L from core
centre,

$$\phi_f(r) = \phi_f(L) * L^2/r^2 * \exp(-\sum(r-L))$$

where $\phi_f(L)$ = fast flux at inner face of the layer
and $r > L$.

These neutrons can then be introduced into the highest energy
group of an appropriate set of multigroup diffusion equations
to calculate the lower energy neutron distributions. Here,

only 2 group ...

theory has been assumed. Hence, all above neutrons are assumed thermalized. (This only results in slightly higher dose rates).

If $\phi_s(r)$ is the slow flux at any radius r,

$$D_s \nabla^2 \phi_s(r) - \Sigma_{as} * \phi_s(r) + \phi_f(r) * \Sigma = 0$$

leakage term   absorption   local source term.
term

$$\text{where} \quad D_s = \text{diffusion constant of layer}$$
$$\Sigma_{as} = \text{thermal absorption cross-section.}$$

$$\text{(or)} \quad \nabla^2 \phi_s(r) - c^2 \phi_s(r) + Q \frac{e^{-\Sigma(r-L)}}{r^2} = 0$$

$$\text{where,} \quad c^2 = \sqrt{\Sigma_{as}/D_s} \qquad Q = \frac{\phi_F(L) \cdot L^2}{D_s}$$

Evaluating for $\nabla^2 = \frac{1}{r^2} \cdot \frac{d}{dr}(r^2 \frac{d}{dr})$ (spherical coordinates, considering only radial variation)

$$\phi_s(r) = -\frac{Ae^{-cr}}{2cr} + \frac{Qe^{\Sigma L}}{2cr} \quad (c-\Sigma) \cdot E_1(y) e^{cr} - E_1(x) \cdot e^{-cr}$$

(refer Appendix A6-3)

where, $x = (c-\Sigma)r$, $y = x/(1+2c/(c-\Sigma))$

As $e^{-cr} << e^{cr}$ we modify as

$$\phi_s(r) = -\frac{Ae^{-cr}}{2cr} + \frac{Qe^L}{2cr}(c-\Sigma) \cdot E_1(y) e^{cr}$$

...eqn (1)

This equation is difficult to evaluate. As the effect of Inverse square law is much lesser than exponential attenuation within a layer, the distance attenuation is neglected within the layer for $\phi_s(r)$ evaluation. This is a resonable approximation if layer thickness $\ll L$.

Now diffusion equation reduses to :-

$$\nabla^2 \phi_s(r) - c^2 \phi_s(r) + Qe^{-\Sigma r} = 0$$

where, $Q = \dfrac{\Sigma}{D_s} \cdot e^{\Sigma L} \cdot \phi_f(L)$

The solution of this equation (refer Appendix A6.3) is :-

$$\phi_s(r) = \frac{Ae^{-cr}}{r} + \frac{Qe^{-r}}{r} \left(\frac{r}{c^2 - \Sigma^2} - \frac{2}{(c^2 - \Sigma^2)^2} - \right)$$

which is easily solvable; flux thus obtained is multiplied by L^2/r^2 for distance attenuation. It must be mentioned that this method gives a slightly higher value for $\phi_s(r)$ than Equation (1).

The thermal flux within every layer is thus obtained & has been mapped in Fig. 6.4 . These flux values will be required later to evaluate the capture gamma-ray sources (local) within the snield material.

6.3.2 GAMMA RAY ATTENUATION CALCULATIONS

THEORY OF ATTENUATION :

Depending on the γ-energy and absorber mass-number, the 3 absorption processes of interest are photoelectric effect, Compton scattering and pair production (in MeV region). Secondary effects such as γ- induced reactions, coherent scattering and Raman scattering have not been considered as their effects are negligible. For illustration, γ-ray cross-section is shown as a function of energy for Iron in Fig. 6.5.

(a) Photoelectric effect : Most important absorption at low

energies ($<$1 MeV) Energy is transferred to orbital electrons

through Einsteins equation:

$$E = h\nu = w + \tfrac{1}{2}mv^2$$

Total energy work K.E of elctron
function

It is a true absorption process as the γ-ray gives up all its

energy in one interaction. The cross-section for this interaction

is proportional to Z^n / E^3 where Z= Atomic number, E=γ-ray energy
in MeV.

& n = 3 to 5 depending on ray energy.

(b) Compton Scattering : Occurs at high energies. Here, γ-rays

undergo billiard-ball type collision with electrons,

according to compton's equation:

$$E = \frac{E_0}{1 + \frac{E_0}{0.511}(1-\cos\theta)}$$

where θ = scattering angle
E_0 = incident γ-energy
E = Scattered γ energy.

FIG. 6·5. GAMMA-RAY CROSS-SECTION FOR
        IRON.*

  *   Fig . 5.3 , ref (26)

It is not a pure absorption process as fractional energy lost depends on incident angle. Its cross-section is proportional to Z/E (nearly constant for all elements (except H_2) where $Z/E = 0.5$).

(c) Pair production : At higher γ - energies, this startling phenomenon occurs wherein under the effect of the coulomb field of the nuclues, a high γ - energy (> 1.022 MeV) can give rise to an electron pair-positron & electron, with any excess energy appearing as particle kinetic energy. Positron always gets annnilated by combination with an electron giving 2, 0.511 MeV γ-rays. Its cross-section is proportional to $Z^2(E-1.022)$. It is a true absorption process as annhilation radiation is soft, emitted isotropically and attenuated easily.

The above 3 process are all added together to give total γ -macroscopic cross-section . For materials like stainless steel containing more than one nuclear species, the individual Σ_i's are added together to give the total. This is shown in Appendix 6.1(b). From the table of mass-absorption cross-sections for γ's (p-762, (21)), it is clear that except H_2, the most efficient γ- absorbers are heavy elements like lead (& iron, to a lesser extent) which have high cross-sections for both photoelectric absorption and pair production.

(i.) <u>CORE GAMMAS</u>

The reactor core exhibits a complex γ ray spectrum. For shielding calculations it can be summed up as follows:-

TABLE 6·3

γ-RAY SOURCE	PHOTON ENERGY - (MeV)				
	1	2	4	6	8
Prompt fission MeV/Fission	3.45	3.09	1.04	0.26	-
Fission product MeV/Fission	5.16	1.74	0.32	-	-
Total	8.61	4.83	1.36	0.26	-

Besides these, capture γ-rays are also being continually emitted through thermal neutron capture in water, cladding material,etc. All this is summed up as in Apprendix A6.4. The core has been considered as a large uniformly distributed source of volumetric density (V_D) dictated by thermal hydraulic design. As 1 watt power is 3.1×10^{10} fissions/cm^3-s considering 200 MeV energy emitted per fission, the volumetric source strength would be

$$S_V^{\gamma} = 3.1 \times 10^{10} \cdot V_D \cdot E_\gamma \quad MeV/cm^2\text{-}s$$

where, γ_i's are chosen energy intervals from

1 to 8 MeV .

since the core absorbs γ-rays emitted by it, this self-absorption phenomenon has been considered. This reduces resultant radiation

level in the core outer surface by F_{pi} times, where F_{pi} is self-absorption function at the γ-energy $E_{\gamma i}$.

$$F_p = \frac{\text{Radiation intensity with self-absorption}}{\text{Radiation intensity without self-absorption}}$$

For a cylindrical source viewed from the side,

$$F_{pi} = \frac{2}{\pi R \Sigma_i}$$ where, R = core radius

$\Sigma_i = \gamma$-absorption cross-section at γ-energy $E_{\gamma i}$.

If dose rates are to be considered at distances $\gg$ R, then the reactor can be considered as a point isotropic source of strength $S_i = S_V^{\gamma i} * V * F_{pi}$ MeV/s , where V = core volume, for γ-energy $E_{\gamma i}$. This is the source strength used in the CODE.

In the CODE, the point kernel method has been employed where the reactor is considered as a source as above. Since γ-rays follow the exponential attenuation law, in spherical coordinates, the γ-flux will be :-

$$\emptyset(r) = \frac{S_i \cdot \exp(-\Sigma r)}{4\pi r^2}$$ where r= distance from source centre.

For attenuation through different layers of thickness t_i and γ-absorption cross sections Σ_i, the exponential term becomes

$$-b = -\sum_{\text{all i}} (\Sigma_i t_i).$$

From the main beam of γ's, the photons being scattered out . of any particular narrow beam are replaced to some extent by particles being scattered- in from.adjucent beams. This results in an increase in particle flux-density depending on γ-energy & material and "b". Hence a factor B_{D_i} , isotropic point-source dose-rate build-up factor (>1) is included in the flux equation.

$$\emptyset (r, E\gamma_i) = S_i \; \frac{B_{DI} \; (\; b(E\gamma_i), E\gamma_i)}{4\pi \; r^2} \quad \exp(-b(E\gamma_i))$$

when the total dose is required to be calculated , the effect of every $E\gamma_i$ is to be summed up. This equation has been used to obtain the effect of various energy fluxes at different layers.

(ii) CAPTURE GAMMAS

These rays emitted throughout the shield, are directly dependent on the thermal neutron fluxes. From this, and a knowledge of material densities & cross-section, the secondary gamma source-rate may be calculated thus:-

Source $(i, r) = \sum_{as}(i) * \emptyset_S \; (r) \quad$ photons/cm^3-s

at layer i. a distance r from core centre. In most cases, a spectrum of γ-rays are emitted. These have to separately be considered thus,

Source $(i, r, E_{\gamma i}) = \sum_{as}(i, E_{\gamma i}) * \emptyset_s(r)$

Here, again, $E_{\gamma i}$ is assumed to vary in discrete steps from 1 to 10 MeV.

Since γ-rays are generated throughout the shield, consideration must be given to the varying shield thickness available to them. So, each layer of the shield has been divided into a series of concentric rings of thickness 1.0 cm and each of these are considered as separate sources. The total radiation outside the shield is obtained by summing the radiation obtained from each of these rings from all layers, plus that obtained from the core itself, following the Point-Kernel technique (described under "Core Gammas") of γ-ray attenuation, for each energy interval, $E_{\gamma i}$. This procedure has been adopted in the CODE.

6.3.3 EMISSIONS FROM REACTOR EFFLUENTS

The use of light water as coolant poses far lesser problem than other liquid coolant in this field. The major reaction of interest is :

O^{16} (n, p) N^{17} activation cross section 2.0E-5 barns ; N^{17} emits gamma rays of everage energy 6.2MeV. The total activation energy (A) evaluates as:-

$$A_\gamma = 8.2925 \text{ E-6} * \emptyset_{fy} * V_{H_2O,eff} * \exp(-0.09367 * \tau) \quad \text{MeV/s}$$

where, $\emptyset_{fv}$ = virgin fission neutron flux

$V_{H_2O, eff}$ = effective water volume to be considered for shielding purposes.

τ = effective time constant for transport.

In the abscence of V_{H_2O}, eff and τ and shape & dimensions of all primary components (extra-core) required to calculate equivalent effective flux for shielding, this emission has not been considered for reactor shielding here. However, since its magnitude is small, it does not introduce great errors in dose calculations.

6.3.4 TOTAL DOSE RATES

Once the neutron and gamma fluxes are known at all interfaces, it is easy to evaluate the total effective dose rates. For this, the flux for unit tissue dose (1 mrem/hr) is used as simple conversion factors (CF). Taken from P.7-66 of Ref(21) they are :-

Table 6.4   Fluxes for unit tissue dose rates :

Particle	flux for 1 mrem/hr dose.
(a) Thermal neutrons	1500 $\#/cm^2$-s
(b) Fast neutrons (1 to 10 MeV)	7.333 $\#/cm^2$-s
(c) γ-rays 1 MeV	577 MeV/cm^2-s
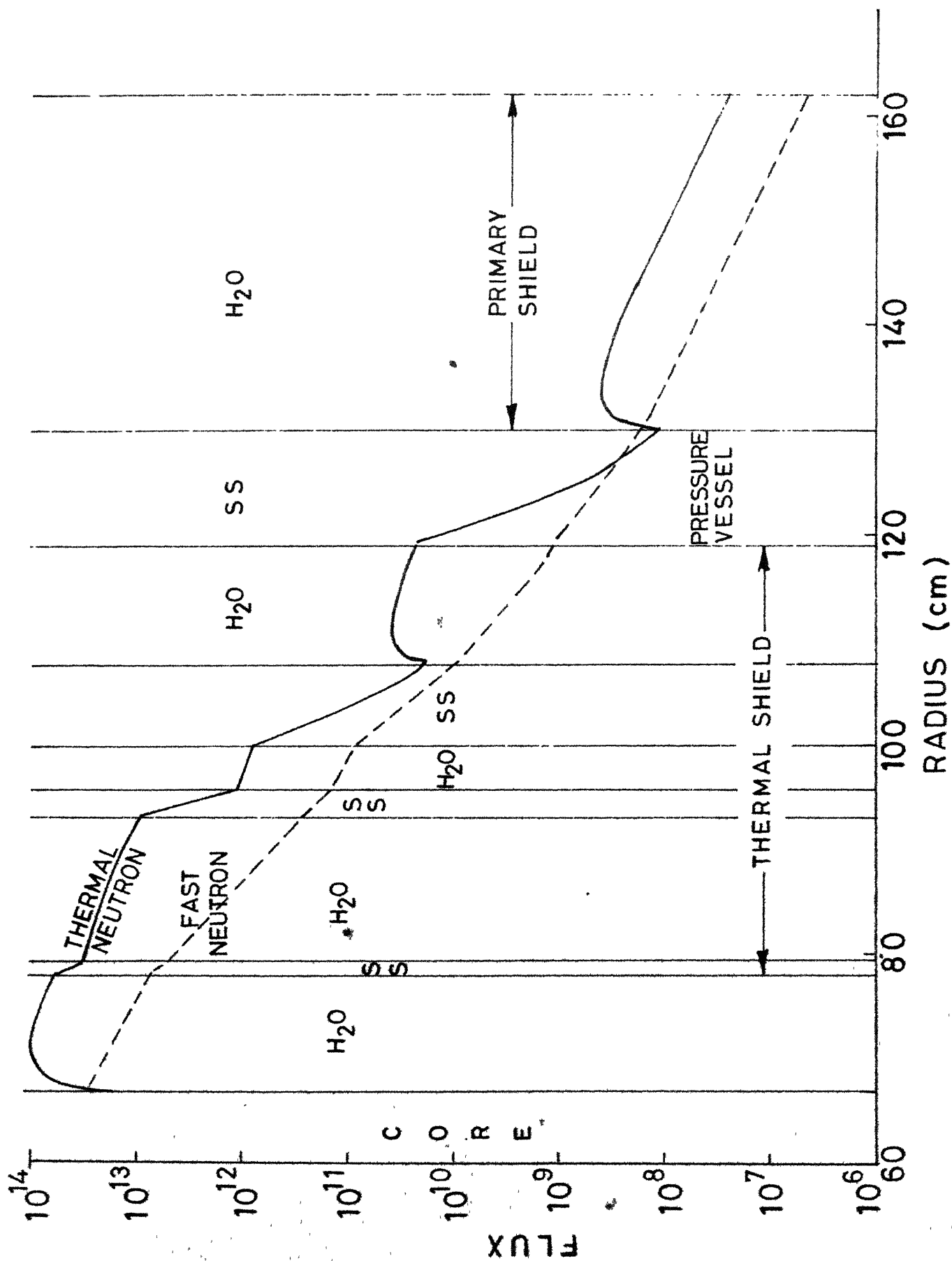
FIG. 6·4 (I) NEUTRON FLUX DISTRIBUTION
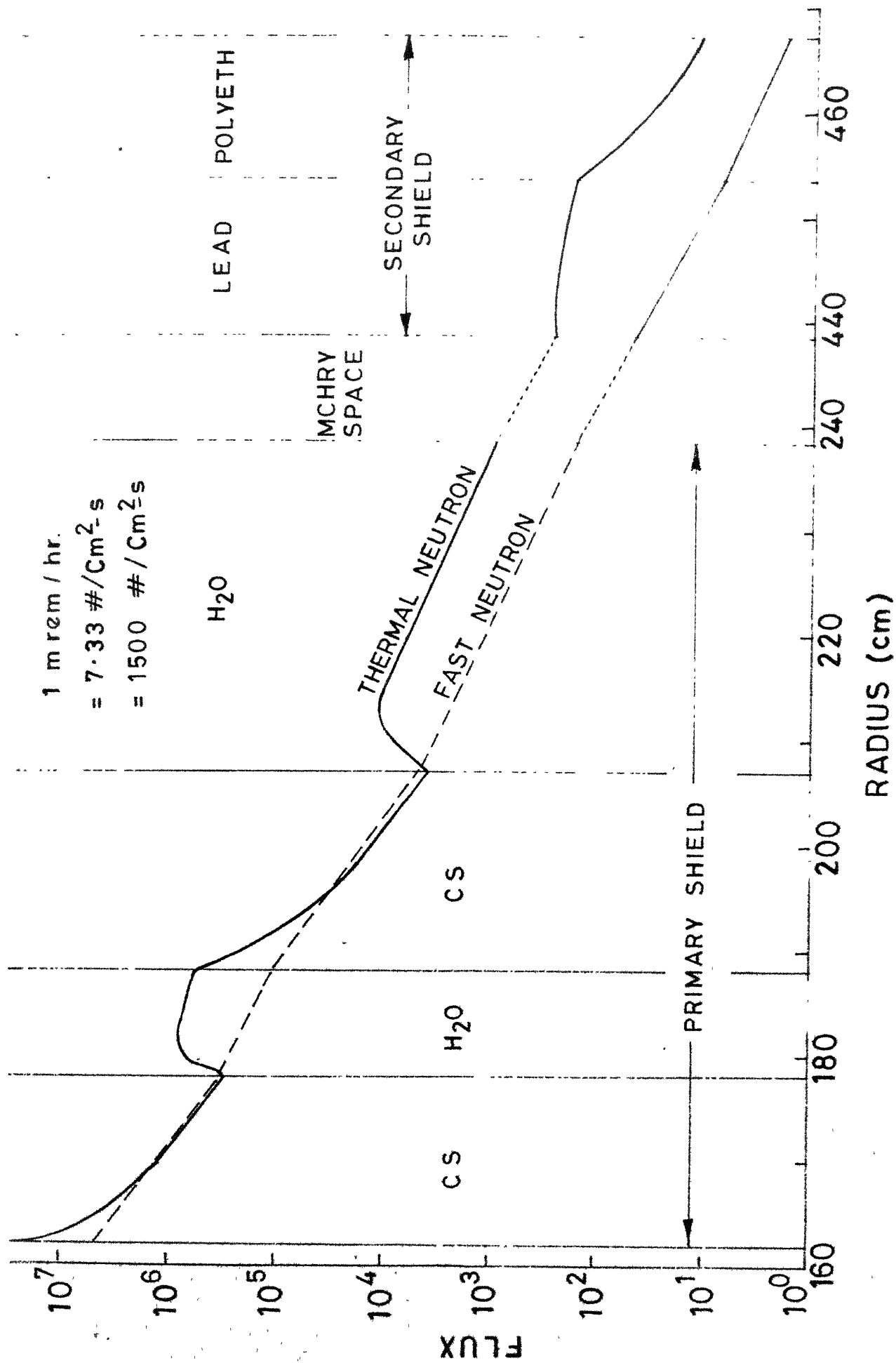
FIG. 6·4 (II) NEUTRON FLUX DISTRIBUTION (contd)

Particle	Flux for 1 mrem/hr dose
2 MeV	681 MeV/cm^2-s
4 MeV	841 MeV/cm^2-s
6 MeV	946 MeV/cm^2-s
8 MeV	1022 MeV/cm^2-s

using these CF_i, the total dose rates at different layers have been calculated & listed in the CODE results.

6.3.5 WEIGHTS OF SHIELDING MATERIALS

In a marine reactor the shielding should weigh minimum possible while still being effective; once the shield dimensions have been arrived at after having analysed many combinations of varying thicknesses in the CODE, the approximate shielding weight has been calculated using simple geometry techniques. For the varying heights of different shield -layers, varying height-scaling factors have been arrived at, after extensive study of a comparative nature done on various marine reactors (information of only those available).

The overall shielding weight (including water-shields) comes to approximately 838.2 tons. The weights of the primary system, Core, Control Rod drive Mechanism (CRDM) and coolant & piping are to be separately considered for the total reactor

weight. An uncertainty error of 10% in the above determined value is anticipated·

6.4 COMMENTS

It has been demonstrated from the CODE output that the maximum dose rate from the secondary shield is 0.735 mrem/hr. and that from the primary shield 4.331×10^{3} mrem/hr. Overall shield outer diameter is 30.62 Ft and weight 838.2 tons; a radial 200 cms space for the primary loop machinery has been assumed. With an increase in this space, the shield weight will increase substantially as the quantity of lead required increases.

The neutron flux at the core edge has been chosen in a conservative manner to ensure proper shield design under all operating conditions. Fluxes obtained from chapter-5 have been incremented by 2.304 times (1.269 Engg. hot-channel factor; 1.178 control-rod peaking factor- $Z \, Sin(Z)$ over $Sin(Z)$; 1.5408 flux increase due to core burnup).

The use of point-kernel technique with build-up factors, however, does not fully account the fact that in-scattered γ-rays is of a lower energy than incident γ-rays, E_{γ}. The scattered component consists of a spectrum of energies from 0 to E_{γ}. This changes with distance traversed through shield. Further, the actual scattering process is anisotropic. So the dose rates obtained by our analysis are/slightly higher than the actual rates. As γ-ray attenuation is correctly described by the Boltzmann's transport equations, improved analysis results when transport codes are used.

****

C H A P T E R - 7

R E A C T O R   C O N T R O L   D E S I G N

In the design of a marine reactor, the control and instrumentation system is a key factor in providing an efficient safe and reliable plant. A warship has stringent manoeuvring requirements which imposes large load variations in relatively shorter times. Consequently, the system should be stable under all conditions of operation with no unallowable overshoots. A knowledge of core reactivity balance and temperatu coefficients is required to assess the above.

The Reactor Physics CODE and subroutine XENON in specific (p.16 of computer print-outs) have been referred to throughout this chapter.

7.1 REACTIVITY COMPUTATIONS

Two important fission products Xenon & Samarium absorb thermal neutrons substantially. In addition the long-lived fission products also absorb thermal neutrons. Thus, if the react were to remain critical it should have sufficient reactivity to override the above deleterious effects. In general, the only significant effects these poisons have on k_{eff} is a reduction of thermal utilization, f to a lower value f' . The poison reactivit ϱ_p , is :-

$$\varrho_p = \frac{f'-f}{f} = -\Sigma_{ap} * f / \Sigma_{afu} \quad \dots \text{ Eqn.}(7.1)$$

The variation of above parameters with temperature should be considered.

7.1.1 Xe^{135} and Sm^{149} Poisoning[⊗] :-
(i) Xe^{135} :-

This is the most important fission product having a neutron absorption cross-section of 2.7 Mb(2200 m/s). The decay chain for this isotope is :-

$$Te^{135} \xrightarrow[\langle 30s]{\beta^-} I^{135} \xrightarrow[6.7hr]{\beta^-} Xe^{135} \xrightarrow[9.2hr]{\beta^-} Cs^{135} \xrightarrow[]{\beta^-} 2.6E6 \text{ yr} \quad Ba^{135}$$

Direct Fission Yield=0.061 (Y_I)   Direct Fission Yield=0.003 (Y_X) Ba^{135} (stable)
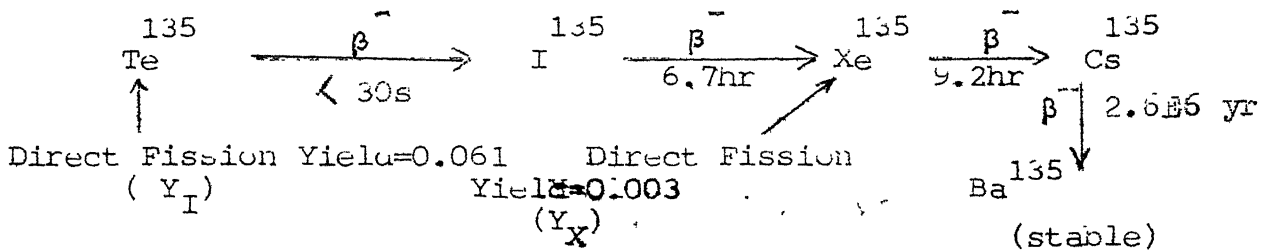
Detailed explanations of differential equations involving the above chain are given in many books & will not be attempted here. The following results, however, ensure:-

$$\overline{\Sigma}_{ax} = \frac{(Y_I + Y_X) * \overline{\Sigma}_f \cdot \overline{\phi}_T}{\phi_x + \overline{\phi}_T} \quad \ldots\ldots\ldots \quad Eqn(7.2)$$

where, $\phi_x = \lambda_x / \overline{\sigma}_{ax}$, a temperature dependent function

$\overline{\Sigma}_f$ = Average fuel fission cross-section

$\overline{\phi}_T$ = Average core thermal flux

$\overline{\Sigma}_{ax}$ = Steady-state Xenon Concentration

⊗ From Ref (23)

Eqn.(7.2) substituted in Eqn.(7.1) (for Σ_{ap}) gives the Xe^{135} activity at steady state. After reactor shutdown, Xe activity rises above this value. The maximum occurs at a time, t_{max}.

$$t_{max} = \frac{1}{\lambda_I - \lambda_x} * \ln\left(\frac{\lambda_I / \lambda_x}{1+(Y_I + Y_x).(\phi_I - \phi_x)/Y_I(\phi_x + \bar{\phi}_T)}\right)$$

$$\ldots\ldots \text{Eqn.(7.3)}$$

where, $\phi_I = \lambda_I / \sigma_{ax}$

The Xe concentration is then given by substituting $t = t_{max}$ in the following Post-shutdown equation:-

$$x(t) = X_0 e^{-\lambda_x t} + \frac{\lambda_I I_0}{\lambda_I - \lambda_x}(e^{-\lambda_x t} - e^{-\lambda_I t}) \quad \text{Eqn. (7.4)}$$

$$\text{where, } X_0 = \frac{(Y_I + Y_X) * \bar{\Sigma}_f \bar{\phi}_T}{\lambda_x + \sigma_{ax} . \bar{\phi}_T} \quad - \text{, Steady-state Xe concn.}$$

$$I_0 = \frac{Y_I \bar{\Sigma}_f . \bar{\phi}_T}{\lambda_I} \quad \text{, Steady-state } I^{135} \text{ concn}$$

obtaining $\bar{\Sigma}_{ax}$ from Eqn.(7.4) and substituting it in Eqn.(7.1), the maximum Xe activity is evaluated.

(ii) Sm^{149} :-

Though a lesser poison, this has a thermal absorption cross-section of 40.8 Kb. It 's decay chain is :-

$$Nd^{149} \xrightarrow[\text{2 hr}]{\beta^-} Pm^{149} \xrightarrow[\text{54 hr}]{\beta^-} Sm^{149} \quad \text{(stable)}$$

direct fission yield = 0.0113
(Y_p)
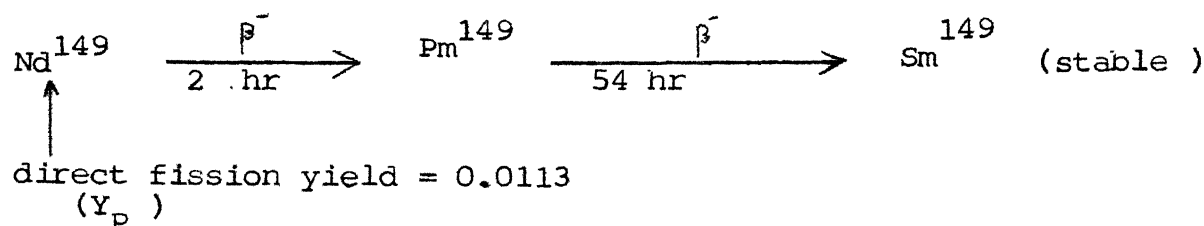
The Steady-state Sm[149] absorption cross-section, Σ_{aS}', is given by :-

$$\Sigma_{aS} = Y_p * \bar{\tilde{\Sigma}}_f \quad \ldots\ldots\ldots\ldots \text{Eqn. (7.5)}$$

Unlike Xe this is independent of neutron flux. The max. Sm[149] concentration after shutdown is given by

$$S_{max} \doteq S_0 + P_0 \quad \ldots\ldots\ldots\ldots \text{Eqn (7.6)}$$

occuring as $t \longrightarrow \inf$, where

$$S_0 = Y_p \bar{\Sigma}_f / \sigma_{aS} \quad \} \quad \text{subscript 'P' stands}$$
$$P_0 = Y_p \bar{\Sigma}_f \bar{\emptyset}_T / \lambda_P \quad \} \quad \text{for Promethium.}$$

Obtaining Σ_{aS} from Eqn.(7.6) and substituting it in Eqn(7.1), the maximum Sm activity is evaluated.

7.1.2 LONG-LIVED FISSION PRODUCTS :-

These also absorb thermal neutrons. Many products having varying cross sections for neutron absorption and decay-times ensue by U^{25} burnup.(Refer Table 9.2,Ref(24)); for computing the long-term effects of the accumulated products, an average cross-section of 45 b per fission is chosen (p.108,Ref(24)). This has been obtained neglecting the rapidly saturating products. Since the concentration of these products is essentially the burnt atoms of U^{25}, it's macroscopic cross-

section, Σ'_{afp}, is given by :-

$$\Sigma'_{afp} = B_{frac} * n^{25} * 43E\text{-}24 \ldots\ldots\ldots \quad \text{Eqn.(7.7)}$$

where, B_{frac} = Fraction of U^{25} burnt at End of core life(see 7.1.4)

n^{25} = number density of U^{25}, $\#/cm^2\text{-}s$

Substituting Eqn (7.7 in Eqn.(7.1), the activity of the above products is obtained.

7.1.3 TEMPERATURE COEFFICIENTS OF REACTIVITY :-

The temperature coefficients of reactivity (α_T) are the basic parameters required for Reactor Stability Analysis. As k_{eff} changes with temperatures of operation, a knowledge of α_T's at various reactor operating levels both for the fuel & moderator is essential. Unlike land-based reactors, the load variations here are from full-load to below 20% for automatic control. Consequently, α_T's at various loads would be different and require separate calculations. For convenience only full load, 3/4, ½ and ¼ loads, as well as full-load at EOL (End of Life) have been considered.

The basic equation for α_T is :-

$$\alpha_T(k_{eff}) = \alpha_T(k_{inf}) + \alpha_T(P_F) + \alpha_T(P_T) \quad \ldots\ldots \text{Eqn. (7.8}$$

where, $\alpha_T(i) = \dfrac{1}{i} * \dfrac{di}{dT}$ \qquad $\ldots\ldots$ Eqn. (7.9)

i = Parameter involved

P_F , P_T = Fast, Thermal Non-leakage probabilities.

Eqn(7.6) can be expanded as below:-

$$\alpha_T(\kappa_{inf}) = \alpha_T(\eta_T) + {}_T(\epsilon) + {}_T(p) + {}_T(f) \quad \ldots. \text{ Eqn.}(7.10)$$

$$\alpha_T(P_T) = \frac{-B^2 L_T^2}{1+B^2 L_T^2} (\alpha_T(L_T^2) + \alpha_T(B^2)) \quad \ldots. \text{ Eqn }(7.11)$$

$$\alpha_T(P_F) = - B^2 \tau_T (\alpha_T(\tau_T) + \alpha_T(B^2)) \quad \ldots.. \text{ Eqn }(7.12)$$

Each of the terms in Eqn. (7.10) to (7.12) can further be expanded but not done here. (Refer Chap.13,Ref(23)).

The basic assumption for computations here is temperatures calculated are uniform for the materials involved, throughout the core. In the Reactor Physics CODE, every parameter is corrected for the operating temperature (except the core dimension variation which is negligibly small). Hence α_T is determined by giving a small perturbation to the operating temperature and determining the consequent variation in k_{eff} and hence α_T using Eqn (7.9). This was done for temperature perturbations of both fuel and moderator operating-temperatures individually, giving α_f and α_m, the respective temperature coefficients. The average fuel and moderator temperatures of different loads were obtained from the Thermal Hydraulics CODE (chap 4) by varying the linear power rating of fuel rod

appropriately. Results obtained are summed up in Table 7.1.

<u>Table 7.1   Reactivity Coefficients of Fuel & Moderator.</u>

LOAD	P_{frac}	k_{eff}	AV.FUEL TEMPR	AV. MOD TEMPR	$-\alpha_f$	$-\alpha_m$
Full	0.9197E-3	0.99294	508.07	287.72	2.7378E-4	6.2327E-4
3/4	1.053E-3	0.99295	442.27	285.84	2.8963E-4	6.0464E-4
1/2	1.1865E-3	0.99296	382.97	283.93	3.0667E-4	5.633E-4
1/4	1.3214E-3	0.99308	329.43	281.98	3.2488E-4	5.3208-4
EOL, FULL	0.0	0.99294	508.07	287.72	2.3940E-4	7.00E-4

<u>7.1.4   Burnup & Reactivity Balance</u>

Knowledge of the fuel fraction burnt is necessary
to obtain the core burnup and reactivity balance. This has been
achieved using a term B_{frac} ('BURNT' in CODE), ie that fraction
of burnt U^{25}, below which the core is unable to override the
Xe-Sm and fission product activities and thus becomes subcritical,
with all control rods removed (P_{frac}= 0.0). This state of core
is termed EOL (End of Life).

The core inbuilt reactivity, reactivities required
to come up from cold to hot-zero-power, and zero to full-power
are all determined by choosing the appropiate temperatures of

fuel & moderator in the CODE and evaluating K_{eff} . At the ECL , core burnup is given by the relation:-

$$\text{Burnup (mwd/ton)} = \frac{(\text{wt. of } U^{25} \text{ per ton of } UO_2 \text{ * } B_{frac})}{\text{wt. of } U^{25} \text{ burnt for producing } 1 \text{ MWd}}$$

$$....Eqn(7.13)$$

and, finally, the core endurance (in days of full power) is:-

$$\text{Endurance} = \frac{\text{Burnup * Total wt. of } UO_2}{\text{operating power level}} \qquad .... Eqn(7.14)$$

(Refer line nos.6900 to 7400 of p.17 of computer printouts for Eqns(7.13) and (7.14)).

Having known the above results, the reactivity balance of the core is made as in Table 7.2. The amount of POISON required in the control rods should be such that the core remains subcritical even in the Cold condition. Hence, a P_{frac}=2.35E-3 was found adequate to drive the core subcritical by over 4% Δk (K_{eff}=0.9582). This means as there are 6 control rods per assembly, by a simple geometric computation, the rod diameter is 0.51 cm (0.494 cm B_4C pellet diameter), assuming a stainless steel cladding of thickness 0.53 mm .

TABLE 7.2 CORE REACTIVITY BALANCE

	$\triangle K \%$
Cold to '0' power	9.6360
'0' to full power	5.4634
Xe, Sm poisoning	2.8563
Xe, Sm override (at EOL)	0.7356
Fission Produce Poisoning	1.8577
Burnup considerations	10.2373
Total inbuilt reactivity	30.7863
Total Control rod worth	34.93
Burn up (Average) - ..... 14697.8 MWd/ton	
Endurance (days of full power) - 84.7 days	

Till now, the basic reactivity requirements, temperature coefficients & core burnup have been computed. Next the control system will be evolved and later certain stability analysis done.

7.2   REACTOR CONTROL SYSTEM

7.2.1   Salient Features:-

The manoeuvring of warships imposes large
load variations on the reactor. A conventional PWR control is
inadequate for this purpose as it is designed for only a small
variation from full load(upto 10%)- the basic signal it uses
is the slow responding average coolant temperature change. In
marine -reactors, however, an additional prompt signal will be
required (Ref(32)) which 'feels' the power transient as soon
as it starts,& disappears gradually at the end of load variation
after which only the slower responding signal would be active.
Care should be taken that the reactivity insertion rates do not
make the reactor prompt critical. For this, the rate is restricted
to 0.03 %Δk (i.e. approx. 0.040β) based on the fact that reactor
should respond by a 2.3%/s power variation to go from 90% to 20%
in 30 secs (Ref(32)).

Thus, in the first part of the operational
transient, the control system should act promptly and efficiently
performing gross regulation and later fine regulation to prevent
it approaching unsafe conditions and oscillations around
equalibrium.

7.2.2 The System :-

A simplified diagram of the system is shown in

REACTOR CONTROL SYSTEM.

Fig. 7.1. It consists of 2 subsystems, viz. 'Power control system' (prompt acting) and 'temperature control system' (slow acting).

(i) Power Control System:-

here the main signal is inbalance between secondary steam flow rate, $\dot{m}_s$, and core generated power (proportional to neutron flux, $\varnothing_T$). 2 additional terms, derivatives of the aforesaid, are added for enhancing prompt cntrol, with scaling factors $\varnothing_1 \propto \varnothing_2$. The resulting power error signal activates either control rod cluster(RCC) A, B or C depending on the signal magnitude. $\frac{\partial \dot{m}}{\partial t}$ is used to sense transient condition; if signal exceeds a certain value, DB(Dead Band) is changed from SP_1 (wide, normally) to SP_2(narrow). Rod speed is controlled by an error signal similar to the above but with a different gain factor $\varnothing_3$. The speed control unit assigns a minimum & maximum insertion rate ($\equiv$ 2.3 %/s power variation) as shown in the figure.

(ii) Temperature Control System:-

Here main signal derives from difference between the primary coolant average tempr. (T_{av}) and a constant reference tempr. Assent for rod-motion is given whenever error signal exceeds the tempr.DB. The characteristics of the various units are as shown in Fig. 7.1.

Signals obtained from the above 2 sub-systems are summed up to obtain the nett error signal. The sequential

control unit decides the RCC that is to be moved, with the speed assigned by the rod-speed control units. The control-rod actuators activate the particular RCC, thus finally varying ϕ_T; this feedback is reflected in the power control system resulting in a reduction of the original error signal; this effect continues ensuing automatic control.

7.2.3 Control Scheme

Here, a brief concept of the rod-control strategy over the core operating life time is elucidated.

(i) Control group is constituted of 3 RCC's A, B and C as in Fig. 3.3; each cluster moves as a bundle, independent of each other.

(ii) A constitutes the 'Scram' rod, capable of shutting down the reactor and is kept fully retracted under normal operation.

(iii) B constitutes 'coarse' and C, 'fine' control clusters.

(iv) Initially, B is kept fully inserted and C moved till it reaches the top limit.

(v) Then C is fully inserted and B half extracted; C is moved up till it reaches the top limit.

(vi) Finally, C is fully inserted & B fully extracted; C is moved till it reaches the top limit(This would then signify the end of core-life).

The above scheme is only a concept & should be supported by extensive calculations which is beyond the scope

of the present work.

7.3 STABILITY ANALYSIS

7.3.1 Computation of some parameters:-

(a) The average neutron life-time, l^* is

$$l^* = \frac{1 + L_{th}^2 B^2}{\bar{v} \cdot \bar{\Sigma}_a} \qquad \dots\dots\dots\dots \text{ Eqn (7.15)}$$

where, $\bar{v}$ = neutron speed (average)

$\bar{\Sigma}_a$ = Fuel absorption cross-sec (average)

l^* changes with load as Σ_a changes with operating fuel temperatures. Table 2.3 gives l^* for different loads.

(b) For neutronics calculations, one-precurs-or group-model has been chosen. The transfer function, $G_n(s)$, is given by :-

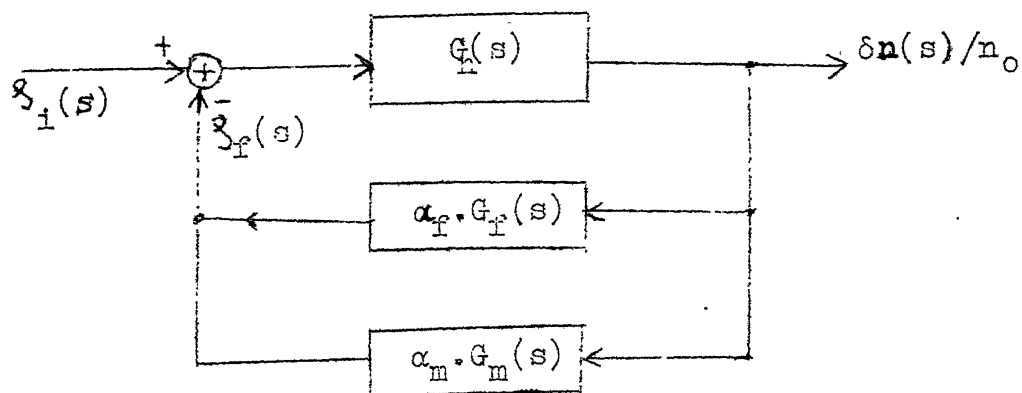$$G_n(s) = \frac{\delta n(s)/n_0}{\delta(s)} = \frac{s + \lambda}{l^* s \cdot (s + \lambda + \beta/l^*)} \qquad \text{Eqn.(7.16)}$$

where, $\lambda = 0.08 \ s^{-1}$ $\left.\right\}$ one-group

$\beta = 0.0065$ $\left.\right.$ values.

Rest of the symbols have their usual meaning.

7.3.2 Two-temperature Feedback :-

The control loop for temperature feedback effects of fuel and moderator is :-

We require to evaluate the moderator & fuel transfer functions, G_m and G_f.

Taking an elementary heat balance for a fuel rod in the reactor and applying a small perturbation to the fuel temperature, T_f. We arrive at the following relation (from p.92, ref(34)).

$$G_f = \frac{\Delta T_f^*}{1+s\tau_f} \qquad \dots\dots\dots \text{Eqn (7.17)}$$

For the moderator a similar equation as above is obtained:-

$$G_m = \frac{\Delta T_m^*}{1+s\tau_m} \qquad \dots\dots\dots \text{Eqn. (7.18)}$$

where, $\Delta T_f^* = (T_f - T_c)$ at steady-state

$\Delta T_m^* = (T_m - T_c)$ at steady state

τ_f = fuel time constant = $m_f \cdot C_{pf}/h_f$

$h_f = \dfrac{\text{Power produced per fuel rod}}{\Delta T_f^*}$

τ_m = moderator time constant.

Refer Appendix A7.1 for evaluation of τ_f and τ_m.

The 2 feedback paths can be combined to one as follows:-

$$H(s) = A . \frac{s + \gamma}{(s + \frac{1}{\tau_m})(s + \frac{1}{\tau_f})}$$
 ...... Eqn (7.19)

$$\text{where} \quad A = \frac{\alpha_f . \Delta T_f^*}{\tau_f} + \frac{\alpha_m . \Delta T_m^*}{\tau_m}$$

$$\gamma = \frac{H(0)}{A \tau_m \tau_f} \quad , \quad H(0) = \alpha_f . \Delta T_f^* + \alpha_m . \Delta T_m^*$$

Hence the open loop transfer function is :-

$$G_n(s) * H(s) = \frac{A/1^* * (s + \gamma)(s + \lambda)}{(s + 1/\tau_m)(s + 1/\tau_f)(s + \lambda + \beta/1^*)} \quad \text{Eqn}(7.20)$$

All functions calculated above are functions of operating temperatures and require individual consideration at part-loads. Results thus computed are presented in Table 7.3. The points of intersection of Eqn. (7.20) for different loads are evaluated by the normal rationalizing technique. Calculations are quite involved and hence not shown. The Nyquist Plots consequently obtained for Eqns. (7.19) and (7.20) are sketched in Fig. 7.2

Table 7.3   Two Temperature Feedback Parameters

Parameter	Full Load	75%	50%	25%	EOL, FULL-LOAD
τ_f (sec)	3.693	3.409	3.162	2.963	3.693
ΔT_f^* ($^\circ$C)	220.19	156.44	99.05	47.46	220.19
τ_m (sec)	0.483	0.482	0.481	0.480	0.483
ΔT_m^* (sec)	7.72	5.84	3.93	1.98	7.72
H (O)	0.0651	0.0488	0.0326	0.0165	0.0581
A	0.0263	0.0206	0.0142	0.0074	0.0255
γ	1.3882	1.4421	1.5088	1.5664	1.2788
l^* (μs)	11.31	10.55	9.82	9.11	17.43
Points of Intersection on Imaginary axis of G(s).H(s):-					
w (H_z)	$\pm$ 27.74	$\pm$ 28-02	$\pm$28.31	$\pm$ 28.56	$\pm$ 22.33
GH ($\times 10^{-5}$)	$\mp$ 6.252	$\mp$ 6.169	$\mp$ 6.126	$\mp$ 6.073	$\mp$ 11.956

Open-load transfer function G(jw)·H(jw)

Imag AXIS

Real axis

W = -0

R → ∞

—— 6.075 (w = 28.6), $\frac{1}{4}$ P
– – 6.125 (w = 28.3), $\frac{1}{2}$ P
—— 6.17 (w = 28), $\frac{3}{4}$ P
—— 6.25 (w = 27.7) full load P
– – 11.96 (w = 22.3)

W = 0

FULL LOAD P

EOL P

W = ∞

-1.0

Feed back function H(jw)

Real axis

Imag AXIS

0   0.016   0.032   0.048 0.058 0.065   W = 0

$\frac{1}{4}$ P

$\frac{1}{2}$ P

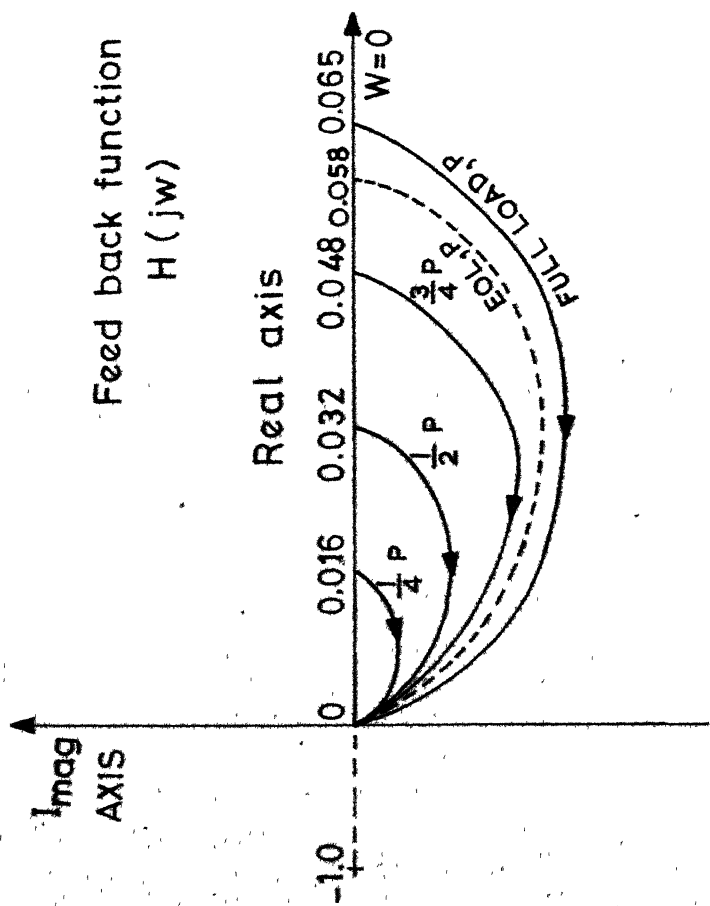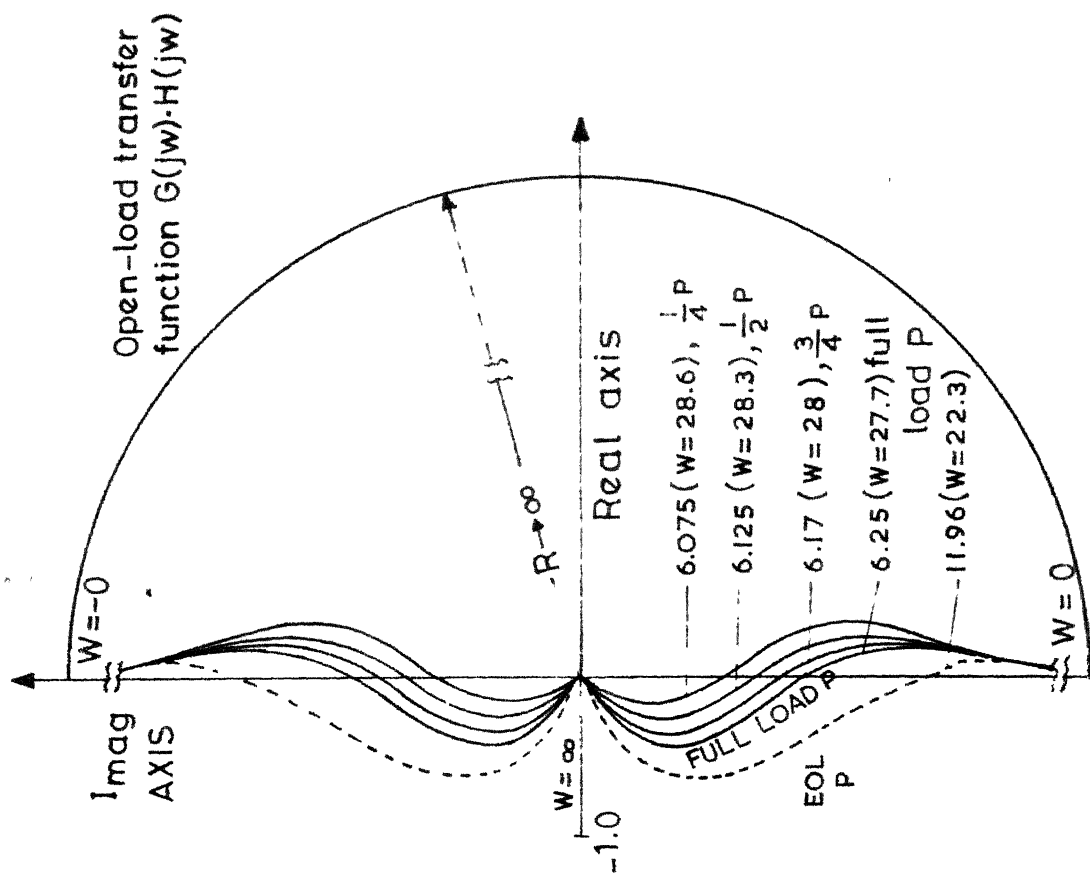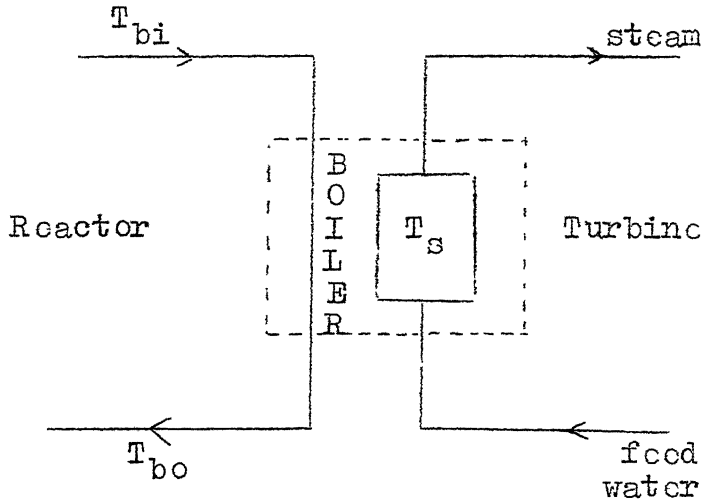$\frac{3}{4}$ P

EOL, P

FULL LOAD, P

-1.0

FIG. 7.2   NYQUIST PLOT OF 2-TEMPERATURE FEEDBACK SYSTEM

7.3.3 Boiler Transfer Function

This figure shows the lumped model used.

Assumptions made in this study are :-

(i) Primary Temperature $T_p = \frac{1}{2}(T_{bi} + T_{bo})$

(ii) Secondary Temperature is that of saturated steam, T_s which is a function of pressure.

(iii) Steam-water mass in secondary side is constant.

(iv) Throttle is kept constant; power output of boiler is proportional to secondary pressure, P_s.

using basic heat balance for Boiler Power (BP) the following result ensues (from p.99, ref(34)) for Boiler Transfer Function

$$G_b(s) = K. \frac{1 + \tau^- s}{1 + \tau^+ s} \qquad \ldots\ldots \text{Eqn(7.21)}$$

Where $K = \frac{X-1}{X+1}$

$$X = 2 \frac{(T_p - T_s)}{(T_{bi} - T_{bo})} * \left(1 + \frac{P_s / P_s'}{(T_p - T_s)}\right)$$

$$\tau^+ = \frac{(m\ C_p)\,\text{secondary}\ /BP}{1/(T_{bi}-T_s) + p_s'/p_s}$$

$$\tau^- = \frac{(mC_p)\ \text{secondary}\ /\ BP}{1/(T_{bo}-T_s) + p_s'/p_s}$$

In the above equation p_s' is the slope of saturation curve

($\text{d}\ p_s/\text{d}T$) at the appropriate pressure of operation; it is got

by purturbing the following equation :- (p in p.s.i.)

$$T_s(p) = 235.7 + 0.061294*p - 0.5661E\text{-}5*p^2.$$

The secondary side pressure has been chosen as

500 psi at full load & proportionally lesser for part loads thereof

(by virtue of assumption (IV) above). As before boiler transfer

functions have to be evolved at various loads and results are

in Table 7.4. τ^+ and τ^- are still unknown (as secondary side

design has not been done). The Bode plots, however, for Eqn.(7.21)

may be plotted, but break frequencies cannot be determined.

As w $\longrightarrow$ inf, the plots tend to $K \cdot \tau^-/\tau^+$ which is a design

parameter, and at low frequencies, the plots tend to K.

Fig. 7.3 gives the plots obtained.

Table 7.4   Boiler Tranfer function parameters.

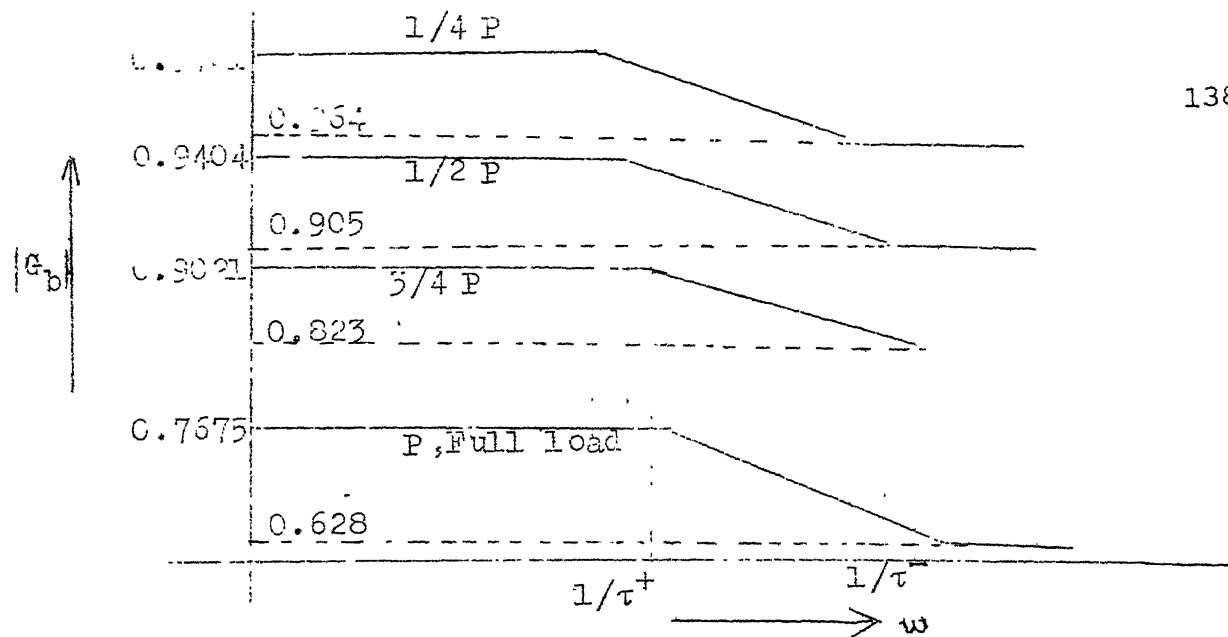| Parameter	Full load	75%	50%	25%
T_s	240.688	255.732	204.977	173.524
p_s'/p_s (°C)	71.256	53.255	48.829	42.109
K	0.7675	0.9021	0.9404	0.9741
$K.\dfrac{\tau^-}{\tau^+}$	0.628	0.823	0.905	0.964

Fig.7.3 Boiler Transfer Function- Bode Plot

7.3 RESULTS AND COMMENTS

The Core Reactivity Balance is displayed in Table 7.2. From figs. 7.2 & 7.3, the reactor is stable under all conditions of operation. Many parameters are however still, unknown & require extensive calculations to be determined- In the reactor control system $\emptyset_1$, $\emptyset_2$, $\emptyset_3$ and all dead-bands are yet to be evaluated & hence an overall study of the system would not be possible. Transient Analysis & reactor dynamics have not been done in the present study but do require careful consideration for check of unallowable overshoots. Throttle variations as described in Chap.4, ref(34), were studied to an extent; but further progress was not possible due to many unknown parameters beyond the scope of the present design.

****

C H A P T E R -8

REACTOR   ON   SHIP

RESUME

8.1   SHIP'S   MOTION   EFFECTS

8.2   COLLISION   BARRIER   &   GROUNDING   PROTECTION

8.3   MISCELLANEOUS   FEATURES

Integration of the reactor with the ship
includes certain specific design considerations hitherto not
discussed like ship's motion effects, induced vibrations, collision
& grounding protection for reactor, etc.

6.1 SHIP'S MOTION EFFECTS ON STEAM GENERATOR PERFORMANCE:-

Location of the reactor on board should be such
as to minimize ship's roll & pitch on the steam generator-
location at about the ship's CG(Centre of Gravity) would be ideal.

In the U-tube steam generator, feed water gains
heat by a 2-phase natural circulation system-firstly, feed water
absorbs thermal energy from primary coolant becoming partly steam;
next, this steam-water mixture from the tube bundle passes through
a steam swirl vane located in the riser which separates water
from steam certifugally and subsequently through additional
dr yers to decrease the moisture content. This 2 phase system,
under the effect of ships 3-dimensional motion could present
flow oscillations causing loss of heat transfer efficiency,
large level fluctuations in the down comer, pulsation in Steam
Supply, etc., thus forcing a barely stable reactor control
unit into a region of instability. Special simulation computer
CODES have to be developed to study the effects of ship motion
on steam generator circulation; this is not attempted here but
a brief sketch of the associated problem given.

The recirculation loop is divided into a number of small equal portions of, say, Δz. The normal heat balance is done for each element. Additionally, the rolling & pitching effects subject Δz to tangential & centrifugal forces, modifying the momentum equation. The dipping effect results in a modification of 'g' (accln. due to gravity) by an oscillatory motion. Consequently, the thermodynamic stability of the recirculation loop in presence of the above effects is done. Finally comes the secondary water level control system. Power level, feed water flow & secondary pressure dynamically alter this level; this necessitates the development of an auto level control loop to ensure system stability.

Extensive studies in the ship motion effects have been done by N.Secolo, G.Selvaggi et al (Ref (37)) using 3 main computer CODES- Sabre-3M, F-111 MO and DCR-2. The study evaluates dynamic behaviour for following perturbations:-

Roll — $30°$ (max) ; period = 12 s.

Pitch — $10°$ (max) ; period = 7 s.

Dip — 0.3g ; period = 7 s.

Results obtained reflect the overall performance of a marine steam generator as summed up below:-

(i) System presents an oscillatory performance for an impressed step perturbation.

(ii) Insertion of an orificed plate suitably positioned in the downcomer region increases stability margin & damps the

oscillations induced by ship's motion effects.

(iii) Steam quality increases with decreasing water level in the downcomer.

(iv) System stability decreases with increasing steam generator inclination or lower system operating pressures.

(v) System stability increases with lower pressure drops in heated zone or lower feed water temperatures.

8.2 COLLISION AND GROUNDING PROTECTION

To minimize collision effects for reactor, protection is required to avoid reactor damage consequenting in uncontrolled release of fission products (approx. 6 curies/W generated !). This is done by a grid structure of about 80 cm x 90 cm arranged between longitudnal bulkheads & outerhull, supported by decks behind the longitudnal bulkheads (ref(36)). This structure transfers the collision load into the transverse bulkheads of the reactor compartment, thus destroying the striking blow. As per a test program conducted (p.422, ref ibid), no mechanical damage will occur for components behind the collision structure; in addition, the protection is adequate against penetration of a jet aircraft at nominal speed.

For the grounding protection, a grid type support structure 140 cm high is located above a 200 cm high double-bottom (DB). If DB is damaged, the grid is capable of witnstanding the weight of reactor containment. Consequently,

during severe loads, the DB being more easily deformable, acts as an elastic spring.

8.2.3 MISCELLANEOUS FEATURES:-

Vibrations are excited by sea-motions, oscillatory propeller forces & auxiliaries; frequency range varies from < 1 Hz to 80 Hz. High energy vibrations from propellers are specially significant & require detailed analysis. As compared to conventional ships of equal power, the machinery weight as well as the normal cruising load on machinery is higher by 1.7 & 3.5 times respectively (approximate figures). The Power consumed by the primary coolant pump is substantial.

The ship's speed depends on the SHP(Shaft Horse Power) developed by the engine. The speed versus SHP characteristics of a ship is dependent on the displacement, profile at the water line & certain other factors; it however follows an approximate cubic law with linear speed increments requiring cubic SHP increments. Consequently, at 50% of power developed, the ship achieves nearly 75% of its maximum speed. A rough estimate of 22 knots may be expected as the maximum speed of the ship presently under consideration, with a 30,000 SHP maximum power output(assuming 70% of steam to be used for propulsion only, and a plant efficiency of 22%).

An important aspect hitherto ignored is requirement of a secondary propulsion system. Coupled to the main gear box, a compact gas turbine of approximately 15000 SHP may be included so that, in the event of a main engine breakdown, the ship is still capable of making way at 65% of its maximum speed which, now, would correspond to that of 45000 SHP ($\approx$ 25 knots).

C H A P T E R -9

C O N C L U S I O N

RESUME

9.1   SUMMARY

9.2   SUGGESTIONS   FOR   FURTHER   STUDY

By now, the salient aspects of marine reactor design have been covered. In conclusion, the destroyer class ship is about the smallest to which nuclear propulsion can be reasonably applied – a preliminary study of containment weight reveal this (chap 6), as a propulsion machinery weight of $\approx$ 2500 tons is bound to accrue (& a displacement of the ship of $\approx$ 8000 tons).

9.1   SUMMARY

Some of the design parameters evolved are briefly summed up in Table 9.1. Since the various design processes are inherently interactive, change of a parameter may have a retrospective effect in other processes. In the shielding design a machinery space of 300 cms (instead of the 200cms assumed) would have resulted in a dose rate of 0.4982 mrem/hr outside the containment with a weight increase of 262.0 tons and diameter of 6.6 ft. This space can be fixed only after all components of primary/secondary loop are designed. Core burnup obtained has been low for a 5% enrichment. This immolation is due to the compact, close-latticed core configuration chosen that is so vital in reducing overall containment weight in marine reactors.

Table 9.1   Design Characteristics

I   GENERAL REACTOR DATA

    A. Reactor Thermal Power   .... 120 MW
       No. of Primary coolant loops   ... 2

B. Primary Coolant

- System pressure ...... 2000 psi
- Total flow rate ...... 5553 tons/hr
- Inlet tempr. ...... 280 °C
- Average rise in core ...... 15.42 °C

C. Fuel (UO_2)

- No. of core regions ----- 1
- No. of fuel asslys. ---- 29
- No. of fuel rods per assly.--- 282
- Enrichment --- 5 w %
- Core Power density .... 63.51 MW/m^3
- Eqbm. core average burnup ... 14,697.8 MWd/t
- Wt. of UO_2 in core .... 6.919 tons

D. Control rods

- Type/Number RCC/29
- Absorbing Material ..... B_4C
- Rods outer dia/pellet dia ... 0.51/0.494 cm

E. Secondary System
- Steam pressure (at full load) ... 500 psi
- Steam quality 0.9975

F. Plant Physical Parameters

- Overall Wt. of shielding ...... 838.2 tons
- Containment outer dia ...... 30.67 ft.

II. NUCLEAR DESIGN DATA

A. Structural characteristics
- Core dia/height 134.29 cm/133.4cm
- Fuel rod & control rod cladding ss347
- Fuel cell type/pitch ... square/1.30cm
- Fuel rod dia/pellet dia ... 0.99/0.858 cm

-Volume fraction H_2O/UO_2 in core 1.592

B. Physical & performance characteristics

- Fuel type/density ...... sintered UO_2/10.97gm/cc

- Fuel Enrichment -...... 5 w%

- Hot channel factors

  F_Q^N / F_Q^e /total F_Q 3.44/1.04/3.58

  F_R^N / F_H^e / total F_H 1.994/1.22/2.105

- Flux functions analysed BOL/Normal/EOL ...... $z Sin(z)/Sin(z)/(\pi-z)*Sin(\pi-z)$

C. Control characteristics

- Type ..... mechanical, RCC

- Absorbing material .... B_4C(den 0.7 gm/cc)

- Rods per assembly/No.of. asslys. ... 6/29

D. Kinetic characteristics

- Moderator tempr. coeff. (full load) ...-6.233E-4 $\Delta k/k$

-Fuel tempr. coeff.(full load) ....-2.738E-4 $\Delta k/k$

III. Core Reactivity Balance
    Refer Table 7.2.

9.2 Suggestions for further study

Some important aspects of marine reactor design not done in the present work are:-

(a) Materials design - The performance of only a few materials has been studied; optimization study of different reactor materials is suggested to evolve better design parameters.

(b) Ship-motion effects on the steam generator require a study in far greater depth than mentioned in chapter 8. This problem

is peculiar of marine reactors and has a direct effect on overall system stability.

(c) In-core instrumentation design requires careful consideration as it conveys core fluxes and temperatures at various points in the core; these signals structure the basic inputs for the reactor auto-control loop. Control rod worth evaluation is also suggested.

(d) In the Shielding Design the radiation from reactor effluents requires evaluation after steam-generator and piping design is done; its magnitude is, however, small & the shielding thicknesses may require marginal modification to counteract this additional dos

(e) The pressure-vessel & piping design for mechanical, thermal and other stresses necessitates careful checking out; in the present design a vessel thickness of 12 cm has been assumed based on available literature and not on calculations.

(f) Design of pressurizer, steam generator, components of secondary loop & subsequent heat balance is also proposed.

(g) Reactor start-up & shutdown procedures are suggested for the present design.

Study of an extensive topic as a reactor design in a limited time frame effects in simplifications & exclusions. The core flux functions for thermal hydraulic study do not precisely represent actual flux variations. Other flux functions as considered adequate may be assumed to evolve more

realistic performances. The core nuclear design(Reactor Physics & Shielding) has been done using a heterogeneous 2-group theory with constant core temperatures for fuel & moderator-multigroup theory using local temperature variations and development of transport theory computer CODES is suggested; this evolves a more precise design, closer to a practical reactor unit. The reactor automatic control loop may be studied in detail, both for system stability & transient characteristics, once the loop constants (of Fig.7.1) are evaluated. Study of reactor transient for an ahead-astern simulation consisting of a load variation from 90% to 20% in 30 secs and immediate return to 90% in another 30 secs would be of significance in ascertaining the system performance.

An earnest attempt has been made to describe the complex, varied & multi-dimensional problem that a warship reactor design is. Both strategically and tactically, nuclear propulsion is the ultimate form of propulsion for warships today; it is obvious to all who pause to ponder this matter. It will remain so until a superior form of ocean propulsion for supporting modern weapon systems is architectured.

****

BIBLIOGRAPHY

1. W.J.Gallagh, G.H.Kaiz, J.N. Sorensen and Y.S. Kim,
   NUS Corp.USA - 'Analysis of the core performance and
   the first refuelling, of N.S. SAVANNAH' - Paper presented
   in Symposium on Nuclear Ships, Hamburg, Vol.I (1971).

2. L. Chinaglia, G. Cesoni, L. Criscuolo and G. Previti,
   Fiat-division, Italy - 'P.W.R. Development for Nuclear
   Ship propulsion' - ibid.

3. A.M. Petrosy'ants- 'Problems of Nuclear Science and Technology',
   fourth edition, Pergamon Press (1981).

4. 'Hearing and subsequent enquiry of the sub-committee on
   military applications of the joint committee on Atomic
   Energy Congress of the United States on Nuclear propulsion
   for Naval Warships - US Govt. printing office, Washington
   D.C. (1972)

5. 'Reactors on the line No.11- N.S. SAVANNAH' -
   Nucleonics, Vol.20, No.7, Jul 1962.

6. S. Sasaki, 'The Japanese Nuclear Ship MUTSU' - paper
   presented in Conference on peaceful uses of atomic energy,
   Geneva (1971).

7. HNE Whitside, 'Nuclear-powered Merchant Ships' -
   paper presented in symposium on Nuclear Ships,
   (1960).

8. A Saiz--de-Bustamante, 'Nuclear propulsion for merchant ships'- paper presented in symposium on Nuclear ships, Madrid (1972).

9. Hiroshi Murata, 'Nuclear Floating Island' - JAERI-M-8559, INIS 844815 (1979).

10. B. Hildrew and J. McCallum of Lloyd's Register of Shipping, 'Classification standards for Nuclear-powered Ships'- paper presented in symposium on Nuclear ships, (1960).

11. Capt J.E. Moore, RN (Editor), 'Jane's Fighting Ships', Jane's Yearbooks, London (1982-83).

12. S. Glasstone and A. Sesonske, 'Nuclear Reactor Engineering', third edition, Van Nostrand Reinhold Co., NY (1981).

13. RA Knief (3-mile Island, Pennsylvania), 'Nuclear Energy Technology', Mc Graw Hill Book Co., NY (1981).

14. World Directory of Reactors, Nuclear Science and Engineering, April 1983 supplement.

15. CD Gregg King, 'Nuclear Power Systems' Mac Millan Co., NY (1964).

16. JR Lamarsh, , 'Introduction to Nuclear Engineering', Addison Wesley Publishing Co. (1975).

17. MM El Vakil, 'Nuclear Energy Conversion', International Text book Co., NY (1971).

18. MM El Vakil, 'Nuclear Heat Transport', International Textbook Co., NY (1971).

19. TC Reihman, 'Nuclear Engineering Modules' - Thermal Hydraulics for PWRs', Virginia Polytechnic Institute and State University Press.

20. LS Tong and J. Weisman, 'Thermal Analysis of PWR', American Nuclear Society (1970).

21. H. Etherington, 'Nuclear Engineering Handbook', Mc Graw Hill Book Co., NY (1958).

22. J.L. Meem, 'Two-Group Reactor Theory', Gardon and Breach, NY (1964)

23. JR Lamarsh, 'Nuclear Reactor Theory', Addison Wesley Co., Ontario (1966).

24. K. Sri Ram, 'Basic Nuclear Engineering', Wiley Eastern Ltd., New Delhi (1977).

25. I.I. Bonarenko, 'Group Constants for Reactor Calculations', Consultants Bureau, NY(1964).

26. J. Weisman, 'Elements of Nuclear Reactor Design', El-Sevier Publishing Co., NY (1977).

27. 'Reactor Shielding'- IAEA Panel Report, Vienna (1964).

28. B. Chinaglia and Sorin Saluggia, Fiat, Italy, 'PWR Development for Nuclear Ship Propulsion: Shielding Studies and control of the gaseous activity release'- paper presented in Symposium on Nuclear ships, Hamburg (1971).

29. F. Brown and A. Jackson, 'Shielding of Marine Reactor Installations' - paper presented in Symposium on Nuclear Ships ' (1960).

30. S.J. Thunell,'Neutron fluxes in a metal-water shield:
A Comparitive study ' - ibid.

31 H. Goldstein, 'Fundamental Aspects of Reactor Shielding',
Addison Wesley Company, Mass.(1959).

32. F. Basile, R. Merino and G. Selvaggi (Fiat, Italy),
'PWR Development for Nuclear Ship Propulsion: Reactor
Control and in-core instrumentation Design'- paper
presented in Symposium on Nuclear Ships, Hamburg (1971).

33. MA Schultz, 'Control of Nuclear Reactors and Power Plants',
Second Edition, Mc Graw Hill Book Co., NY (1961).

34. J. Lewins, 'Nuclear Reactor Kinetics and Control',
Pergamon Press, Oxford (1978).

35. B.C. Kuo, 'Automatic Control Systems', Third Edition,
Prentice Hall of India (1982).

36. D.L. Hetrick, 'Dynamics of Nuclear Reactors', University
of Chicago Press (1971).

37. N. Secolo Etal, 'PWR Development for Nuclear Ship Propulsion:
Ship Motion effects on Nuclear Steam Generator Performance'-
Paper presented in Symposium on Nuclear Ships, Hamburg(1971).

38. W.Jager, H. Lettnin etal,'Nuclear Ships: Engineering a
future Transport System'- paper presented at ASME-ANS Int.
Conference on 'Advanced Nuclear Engineering Systems (1976).

39. L. Chingalia and P. Rucci, 'Some safety problems in the
Fiat Ansaldo Nuclear Ship Study'- Paper presented at
Symposium on Nuclear Ships,   (1960).

40. Jahnke-Emde and Losch, 'Tables of Higher Mathematical
Functions', Sixth Edition, Mc Graw Hill Book Co.,NY (1960).

41. E. Kreyszig, 'Advanced Engineering Mathematics', Wiley
Eastern Ltd., New Delhi (1972).

****

A 4.1 CALCULATION OF HOT-CHANNEL FACTORS
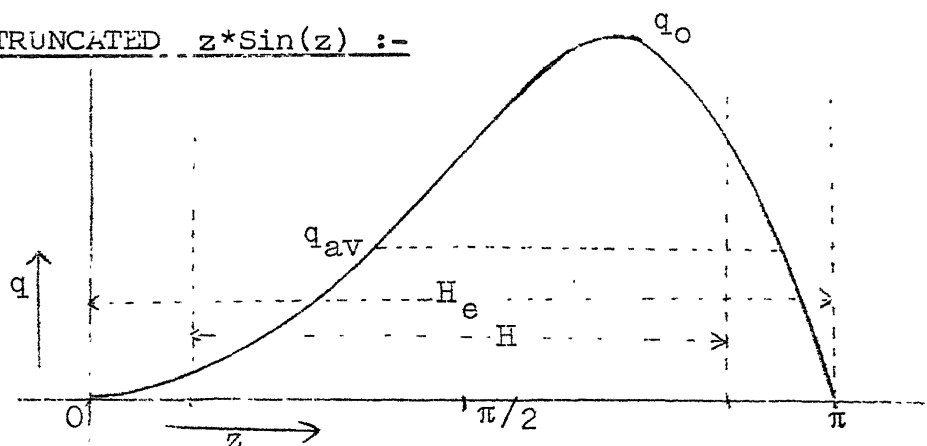
1. TRUNCATED COSINE
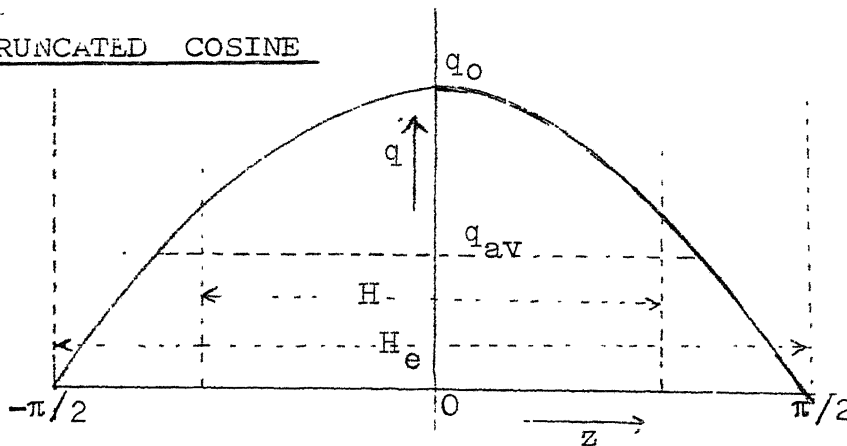
$$q(z) = q_0 * \cos\left(\frac{\pi}{H_e} z\right)$$

$$q_{av} \quad = \quad \frac{2q_0}{H} \int_0^{H/2} \cos\left(\frac{\pi}{H_e} z\right) \cdot dz$$

$$= \frac{2}{\pi} \left(\frac{H_e}{H}\right) * q_0 * \sin\left(\frac{\pi H}{2H_e}\right)$$

$$\therefore \quad F_z^N = \frac{q_0}{q_{av}} = \frac{\pi}{2} * \frac{H}{H_e} * \frac{1}{\sin\left(\frac{\pi H}{2H_e}\right)}$$

2. TRUNCATED z*Sin(z) :-

Let us find the normalizing factor for z.Sin(z).

$$\frac{d}{dz}(zSinz) = 0 \quad \text{at maximum ;}$$

$$\Rightarrow Tan(z) = -z$$

The above eqn. is satisfied when z=2.02877

So, maximum = 2.02877*Sin (2.02877) = <u>1.8197</u>

We shall choose the axis as above in diagram.

$$q_{av} = \frac{q_0}{H} \star \int_{e}^{H} \frac{z.Sin.z.dz}{1.8197} \qquad \text{where, } e = \frac{H_e - H}{2}$$

As z is distance in cms we will have to convert it to radians :-

$$q_{av} = \frac{q_0}{H} \star \int_{e}^{H} \frac{\pi}{H_e} z \star Sin(\frac{\pi}{H_e} z) \star dz \star \frac{1}{1.8197}$$

Let $x = \frac{\pi}{H_e} z \Rightarrow dx = \frac{\pi}{H_e} .dz$

$$q_{av} = \frac{q_0}{1.8197} \cdot \frac{1}{H} \cdot \frac{H_e}{\pi} \int_{\frac{e\pi}{H_e}}^{\frac{H\pi}{H_e}} x \cdot \operatorname{Sin} x \cdot dx$$

$$= \frac{q_0}{1.8197} \cdot \left(\frac{H_e}{H}\right) \cdot \frac{1}{\pi} \left\{ -\frac{H\pi}{H_e} \operatorname{Cos}\left(\frac{H\pi}{H_e}\right) + \right.$$

$$\frac{e\pi}{H_e} \cdot \operatorname{Cos}\left(\frac{e\pi}{H_e}\right) + \operatorname{Sin}\left(\frac{H\pi}{H_e}\right) - $$

$$\left. \operatorname{Sin}\left(\frac{e\pi}{H_e}\right) \right\} \cdot $$

Putting $A = \frac{H\pi}{H_e}$, $B = \frac{e\pi}{H_e} = \frac{(H_e - H)\pi}{2H_e}$

$$\therefore \quad F_Z = \frac{q_0}{q_{av}} = \frac{1.8197 * \pi * H}{H_e(-A\operatorname{Cos}(A) + B\operatorname{Cos}(B) + \operatorname{Sin}(A) - \operatorname{Sin}(B))}$$

3. TRUNCATED BESSEL'S FUNCTION :
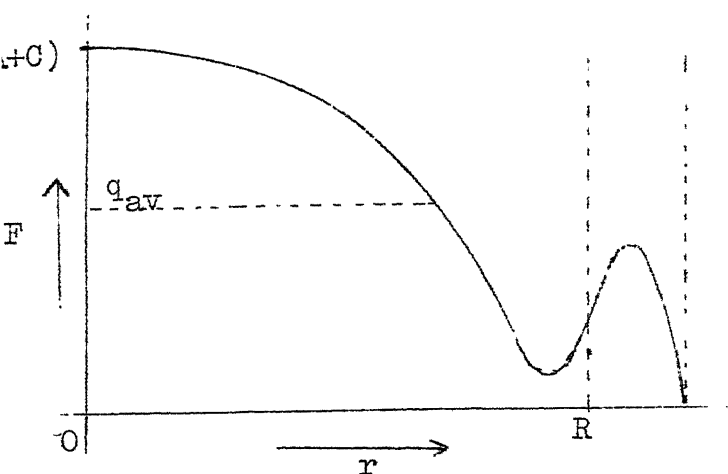
Function

$$F(r) = AJ_0(1r) + CI_0(mr)$$

R = core radius

A, C, 1 & m are all constants determined

from the Reactor Physics CODE and hence known. By definition:-

$$\overline{q}_{av} = \frac{1}{\pi R^2 H} \int_0^H \int_0^R F(r) \quad * \text{(Axial function)} * 2 \, r dr dz$$

The axial function integration is done in (1) and

(2) above.

The radial integration is:-

$$q_{av} = \frac{1}{R^2} \int_0^R (A \cdot J_0(1r) + C \cdot J_0(mr)) * 2 \cdot r \cdot dr$$

Since , $\int 1r \cdot J_0(1r) \cdot dr = 1r \cdot J_1(1r)$

and $\int mr * I_0(mr) dr = mr * I_1(mr)$,

$$q_{av} = \frac{2}{R^2} (\frac{A}{1} \cdot R \cdot J_1(1R) + \frac{C}{m} \cdot R \cdot I_1(mR))$$

At $r = 0$, the peak flux occurs; its value is $(A + C)$

$$\therefore \quad \frac{q_0}{q_{av}} = \frac{A + C}{2 \cdot A \cdot \dfrac{J_1(lR)}{lR} + 2C \cdot \dfrac{I_1(mR)}{mR}}$$

$$= \frac{1 + \dfrac{C}{A}}{2 \cdot \dfrac{J_1(lR)}{lR} + 2\left(\dfrac{C}{A}\right) \cdot \dfrac{I_1(mR)}{mR}}$$

As $\dfrac{C}{A} \lll 1$,

$$\therefore \quad F_R^N = \frac{1}{2\, \dfrac{J_1(lR)}{lR} + 2 \cdot \left(\dfrac{C}{A}\right) \cdot \dfrac{J_1(mR)}{mR}}$$

A 3.2 <u>DETERMINING</u> K_{fu}:

Let $K_{fu}(T) = a + bT$, be a linear function of temperature.

<u>AIM</u> :- To determine what value of $K_{fu}(T)$ is to be used in the heat conduction equation, Eqn. (4.3).

<u>Solution</u>

We shall develop an equation relating T_0 and T_s using $K_{fu}(T) = a+bT$ then compare this with Eqn. (4.3).

In the steady-state condition

$$q''' . \pi r^2 \Delta l = - K_{fu}(T).2\pi r.\Delta l.\frac{dT}{dr}$$, in any fuel ring

of thickness dr at radius r. Integrating from $r=0$ to $r=r_{fu}$:-

$$\therefore q''' \left(\frac{r^2}{2}\right)_0^{r_{fu}} = -2\left(aT + \frac{bT^2}{2}\right)_{T_0}^{T_f}$$

(or) $$T_f = T_0 - \frac{q''' . r_{fu}^2}{4\left(a+b\left(\frac{T_0+T_f}{2}\right)\right)}$$

This means $K_{fu}(T)$ in Eqn (4.3) is evaluated at the arithmetic mean fuel temperature for determining T_f i.e. at $T = \dfrac{T_0 + T_f}{2}$

A 5.1 CALCULATION OF $\bar{D}_{ss}$:-

Element	NUM DEN* ($\#/cm^3$)	$\sum_a$*	σ_s (b)	$\sum_s$	$(1-\bar{\mu}_0)$	$\sum_{tr}$
F_e	6.044 E22	0.093180	11.4	0.68902	0.9880	0.68075
C_r	1.6719E22	0.030758	4.2	0.07022	0.9871	0.06931
N_i	8.2291E21	0.025058	17.0	0.139895	0.9885	0.13829
S_i	1.7536 E21	0.000178	2.2	0.003858	0.976	0.00376
N_b	4.1611 E20	0.000290	6.5	0.002705	0.9928	0.00269
M_n	1.7541 E20	0.001401	1.9	0.000333	0.9878	0.00033
C	3.2091 E20	0.0000009	4.7	0.001500	0.9440	0.00142
	Total	0.150867		0.90754		0.896555

* Taken from Table A6.1

$$\bar{D}_{ss} = \frac{1}{3 \cdot (\sum_a + \sum_{tr})} = \underline{\underline{0.318241 \text{ cm}}}$$

A 5.2 <u>CALCULATION OF</u> D_{1f}

The fast diffusion constant for core, D_{1f} is given by the expression :-

$$D_{1f} = \frac{1}{3(\bar{\Sigma}_{1a} + \tilde{\Sigma}_s(1-\bar{\mu}_0))} \quad \cdots\cdots\cdots \text{ Eqn.(1)}$$

where, $\bar{\Sigma}_{1a}$ = av-fast absorption cross section.

$\bar{\Sigma}_s$ = averaged scattering cross section.

since, the scattering cross section of Hydrogen varies strongly with neutron energy, we use an artifice to calculate its scattering cross-section. Let us make an initial guess of $\varsigma_{(H)} = 10$ barns -

The parameters are :-

#	H.	O(total)	S.S.	Total
n (#/cm^3)	0.3641E23	0.3622E23	0.8407E22	
δ_s (b)	10	4.2	11.4	
ξ	1.0	0.12	0.353	
$(1-\bar{\mu}_0)$	0.333	0.258	0.988	
$\bar{\Sigma}_s$	0.5094	0.15212	0.09584	0.7577

For the above parameters,

$$\xi_{reac} = \frac{\sum_{i=1}^{3} \xi_i \bar{\Sigma}_{si}}{\bar{\Sigma}_s (TOT)} \quad = 0.6862$$

$$(1-\bar{\mu}_o)_{reac} = \frac{\sum_{i=1}^{3}(1-\bar{\mu}_o)_i \cdot \bar{\Sigma}_{si}}{\bar{\Sigma}_s \text{(TOT)}} = 0.55205$$

$$\bar{\Sigma}_s = \left[\frac{\ln(\frac{E_o}{E_{th}})}{3\xi(1-\bar{\mu}_o)} \cdot \frac{1}{\tau}\right]^{\frac{1}{2}} = 0.7475$$

We see $\bar{\Sigma}_s$ above & one from tabulation do not agree.
So we guess higher values of $\sigma_s(H_2)$ and continue calculations.
We obtain convergence when $\sigma_s(H_2) = 13.7$

$$\xi_{reac} = 0.69693$$

$$(1-\bar{\mu}_o)_{reac} = 0.54459$$

$$\bar{\Sigma}_{s\,reac} = 0.7488 \text{ cm}^{-1} \dots\dots\dots \text{Eqn.(2)}$$

Next we have to determine $\bar{\Sigma}_{1a}$.

$$\bar{\Sigma}_{1a} = \frac{N \cdot I_{eff}}{\ln(\frac{E_O}{E_{th}})}$$

we know from calculation for 'p', that

$$I_{eff} = A + \frac{C}{\sqrt{a\rho}} = 21.254 \text{ barns for } UO_2.$$

$$\therefore \bar{\Sigma}_{1a} = 2.6323E22 * 21.254E-24 = 0.03858 \text{ cm}^{-1} \dots\dots\dots \text{Eqn (3)}$$

From Eqns. (2) & (3), we can evolve D_{1f} through Eqn (1):-

$$\bar{D}_{1f} = \frac{1}{3*(0.03858 + 0.54459*0.7488)}$$

$$= \underline{0.74674 \text{ cm}^{-1}}$$

A6.1(a)

MACROSCOPIC CROSS-SECTIONS FOR STAINLESS STEEL[@]
-THERMAL CAPTURE & FAST REMOVAL CROSS-SECTIONS-

CONSTITUENT	WEIGHT %	WEIGHT PER CM³	MOL. W.T.	NUMBER DENSITY (n/cm^3)	THERMAL CAPTURE σ_{as}^{+} (barns)	NEUTRON CROSS-SECTIONS Σ_{as} (cm⁻¹)	FAST REMOVAL σ^{*} (barns)	NEUTRON CROSS-SECTIONS Σ (cm⁻¹)
Fe_{26}	69.9	5.606	55.85	6.0446E22	2.1535	0.13017	1.89591	0.114600
Cr_{24}	18.0	1.444	52.01	1.6719E22	2.573	0.042968	1.84003	0.030763
Ni_{28}	10.0	0.802	58.69	8.2291E21	4.254	0.035006	1.93582	0.015930
Si_{14}	1.02	0.0818	28.09	1.7536E21	0.1418	0.000249	1.41992	0.002490
Nb_{41}	0.80	0.0642	92.91	4.1611E20	0.9748	0.000486	2.34776	0.000977
Mn_{25}	0.20	0.0160	54.93	1.7541E20	11.1664	0.001959	1.88273	0.000330
C_{6}	0.08	0.0064	12.01	3.2091E20	0.00398	0.000001	0.9942	0.000319
TOTAL -	100.0	8.02	-	-	-	0.210759	-	0.165409

* Using $\sigma = 0.35 * A^{0.42}$ for consituents unlisted in table 5.3, ref(26)

+ $\phi(th) = \sqrt{\pi}/2 * \sigma(2200)$; At tempr.T, $\Sigma_a(T) = \Sigma_a(th) * \sqrt{295.1/(273.1+T)}$

@ For carbon steel parameters are taken as that for F_e

A.6.1(b). Linear Absorption Coefficient* for gamma rays for stainless steel[@]

CONSTI-TUENT.	WEIGHT PER (cm³) (%)	Eγ =1 MeV		Eγ = 2 MeV		Eγ = 4 MeV		Eγ = 6 MeV		Eγ = 8 MeV	
		Σ/ρ	Σ	Σ/ρ	Σ	Σ/ρ	Σ	Σ/ρ	Σ	Σ/ρ	Σ
Fe 26	5.606	0.0595	0.3356	0.0424	0.2377	.0330	.163	.0314	.172	0.0255	0.165
Si 14	0.0818	0.0635	5.194E-3	0.0447	3.656E-3	.0323	2.6244-3	.0277	2.266-3	0.0254	2.07-3
C 6	.0064	0.0636	4.0701E-4	0.04444	2.842E-4	0.0324	1.546E-4	0.0245	1.506E-4	.0215	1.363E-4
Cr . Ni 24 28 Np . Mn 41 25	2.3256		0.138385		0.0966		0.0767		.0707		0.0686
TOTAL	8.02		0.4775		0.3402		0.2046		.2435		0.2362

* from ref(21), pp.762

[⊛] taken as for Fe, since not listed.
^{26}

[@] for carbon steel, Σ/ρ is taken same as Fe.
^{26}

A6.2   INCOMPLETE   ERROR   FUNCTIONS*

$$E_n = \int_1^\infty \frac{e^{-tx}}{t^n} dt = x^{n-1} \int_x^\infty \frac{e^{-t}}{t^n} dt$$

are called incomplete error functions.

They have series solutions.

$$E_0(x) = e^{-x}/x$$

$$E_n{}'(x) = -E_{n-1}(x)$$

In general,

$$E_n(x) = \sum_{\substack{m=o \\ m \neq n-1}}^{\infty} \frac{(-x)^m}{(n-1-m)m!} + (-1)^n \frac{x^{n-1}}{(n-1)!}(\gamma + \ln(x) - A_n)$$

$$\forall n \geq o$$

where, $\gamma = 0.577216 \ldots \ldots$, $A_1 = 0$, $A_n = \sum_{m=1}^{n-1}\left(\frac{1}{m}\right)$

In particular ,

$$E_1(x) = -(\gamma + \ln x) + x - \frac{x^2}{4} + \frac{x^3}{8} - \text{------}$$

$$E_2(x) = 1 + x(\gamma + \ln x) - \frac{x^2}{2} + \frac{x^3}{12} - \frac{x^4}{32} + \text{------}$$

The following integral has been used :-

$$\int e^{kx} . E_n(ax+b).dx = \sum_{i=0}^{n-1} \frac{a^i}{k^{i+1}}.e^{kx} . E_{n-i}(ax+b) -$$

$$\frac{a^{n-1}}{k^n}.e^{-\frac{bk}{a}} . E_1\left(\frac{ax+b}{1-\frac{k}{a}}\right)$$

---

* Ref(31), page 355

In particular,

$$\int e^{kx} . E_1(ax+b) . dx = \frac{e^{kx}}{k} E_1(ax+b) - \frac{e^{-bk/a}}{k} * E_1\left(\frac{ax+b}{1-k/a}\right)$$

If $\quad x \gg 10,$ $\qquad\qquad E_r(x)$ is well approximated by:-

$$E_n(x) \cong e^{-x} Q_n(x)$$

$$\text{where, } Q_n(x) = \frac{1}{x+n} + \frac{n}{(x+n)^3} \cdots$$

A6.3

(a) Solution $\quad \nabla^2 \phi_s(r) - c^2 * \phi_s(r) + \frac{Qe^{-\Sigma(r-L)}}{r^2} = 0$.
of

$$\nabla^2 \phi_s(r) - c^2 * \phi_s(r) + P \frac{e^{-\Sigma r}}{r^2} = 0$$

$$\text{where } P = Qe^{+ L \Sigma}$$

In spherical coordinates

$$\nabla^2 = \frac{1}{r^2} * \frac{d}{dr}\left(r^2 . \frac{d}{dr} \right)$$

$$\frac{1}{r}\left(r\frac{d^2\phi_s}{dr^2} + 2.\frac{d\phi_s}{dr} \right) - c^2 \phi_s(r) + \frac{Pe^{-r\Sigma}}{r^2} = 0$$

Substituting $\quad r.\phi_s(r) = X$, equation reduces to

$$(D^2-c^2) X = - \frac{P e^{-r\Sigma}}{r}$$

By using the simple integrating factor method by first

considering $(D+c) X=Y$, solving for Y and later,

solving for X, we get the equation :-

$$X = \frac{Ae^{-2cr}}{-2c} + Be^{cr} - P.e^{cr}\int dr.e^{-2cr}\int \frac{e^{(c-\Sigma)r}}{r}.dr$$

From appendix A6.2, $\int e^{\frac{(c-\Sigma)r}{r}}.dr = -E_1((c-\Sigma).r)$

As $x = \phi_s * r$

$$\phi_s * r = -\frac{Ae^{-2cr}}{2c} + \frac{Be^{cr}}{} + Pe^{cr}\int dr.\, e^{-2cr}.\, E_1(r.(c+\Sigma))$$

Again using the integral identity of A6.2,

$$\phi_s(r) = -\frac{Ae^{-2cr}}{2cr} + \frac{Be^{cr}}{r} + \frac{Pe^{cr}}{r}\left\{ \frac{(c-\Sigma)}{2c}.E_1\left(\frac{(c-\Sigma)r}{1+\frac{2c}{c-\Sigma}}\right) - \frac{e^{-2cr}}{2c}*E_1((c-\Sigma)r)\right\}$$

As $\phi_s(r) \to 0$ as $r \to inf$, $B = 0$ is essential.

Thus, substituting back for P, we obtain:-

$$\phi_s(r) = -\frac{Ae^{-2cr}}{2cr} + \frac{Qe^{L\Sigma}}{2cr}\left\{(c-\Sigma)*E_1(Y)e^{cr} - E_1(X)*e^{-cr}\right\}$$

where, $X = (c-\Sigma).r$

$Y = X/(1+\frac{2c}{c-\Sigma})$

(b) <u>Solution of $\nabla^2 \phi_s(r) - c^2.\phi_s(r) + Qe^{-\Sigma r} = 0$.</u>

Here the approach is similar. Substituting for

$r * \phi_s(r) = X$, we obtain:-

$(D^2-c^2) X = -Pr.e^{-r\Sigma}$.   .... Eqn (1)

The complementary Function of this differential Eqn. is

$$X = Ae^{-cr} + Be^{cr} \; ;$$

The particular Integral is obtained by choosing a particular solution for $X = (Dr + E)e^{-\Sigma r} \; ;$

Putting this is eqn.(1), we obtain the coefficients

$$D = \frac{1}{c^2-\Sigma^2} \quad ; \quad E = - \frac{2}{(c^2-\Sigma^2)^2} \quad ,$$

Hence, $\phi_s(r) = \frac{Ae^{-cr}}{r} + \frac{Be^{cr}}{r} + Q\frac{e^{-\Sigma r}}{r}(\frac{r}{c^2-\Sigma^2} - \frac{2}{(c^2-\Sigma^2)^2})$

as $\phi_s(\inf) = 0$, $B=0$

$$\therefore \phi_s(r) = \frac{Ae^{-cr}}{r} + \frac{Qe^{-\Sigma r}}{r}\{\frac{r}{c^2-\Sigma^2} - \frac{2}{(c^2-\Sigma^2)^2}\} \; .$$

****

A 6.4 TOTAL GAMMA EMISSIONS FROM COKE

SOURCE	Σ_{as}^*	$E_\gamma = 1\,MeV$		$E_\gamma = 2\,MeV$		$E_\gamma = 4\,MeV$		$E_\gamma = 6\,MeV$		$E_\gamma = 8\,MeV$	
		Photons	Nett Energy MeV	Photons	Nett Energy MeV	Photons	Nett Energy MeV	Photons	Nett Energy MeV	Photons	Nett energy MeV
Prompt Fission	–	–	3.45	–	3.09	–	1.04	–	0.26	–	–
Fission Product	–	–	5.16	–	1.74	–	0.32	–	–	–	–
CAPTURE GAMMAS:–											
H_2 (in water)	0.01099	–	–	1.115	0.11732	–	–	–	–	–	–
In stainless steel											
Fe	0.09318	–	–	0.1	0.01597	0.24	0.07645	0.22	0.10512	0.5	0.31854
Cr	0.03076	0.37	9.726 E-3	0.16	8.4117E-3	0.12	0.01262	0.8	0.28369	0.69	0.14510
Ni	0.02506	–	–	–	–	0.14	0.01199	0.30	0.03846	0.72	0.12378
Nb	0.00029	–	–	–	–	0.54	5.155E-4	0.1	2.082E-4	–	–
Si	0.00018	–	–	1.0	3.042E-4	2.29	1.3934E-4	0.4	3.742E-4	0.16	1.947E-4
TOTAL(MeV)	–	–	8.61973	–	4.97196	–	1.46297	–	0.68614	–	0.58761

* Taken at T=300°C applying 1/v correction. Ⓧ Nett Energy $= \left(\dfrac{V_x}{V_{fuel}}\right)*\left(\dfrac{\Sigma_{ax}}{\Sigma_{fuel}}\right)*\left(\dfrac{E_x}{\ast\,\text{photons}}\right)*\text{photons}$ per fission;

(x=material) (from p.116, ref(26)).

A 7.1 EVALUATION OF MOLERATOR TIME CONSTANT (τ_m)

Heat balance for a fuel rod channel gives :-

eat added) = (heat supplied to coolant) - (heat carried away

flowing coolant).

r) $mC_p \dfrac{d\,T_{ac}}{dt} = A\,h_c(T_{cl}-T_{ac}) + \dot{m}\,C_p\,(T_i-T_{ac})$ .... Eqn(1)

where, T_i , T_{ac} = coolant inlet/average temprs. in core

T_{cl} = ^{C}ladding outer tempr.

$\dot{m}$ = coolant flow rate

minating T_{cl} in Eqn(1) by substituting

$$T_{cl} = \frac{h_f\,T_{af} + h_c\,T_{ac}}{h_f + h_c}$$ got by Steady-state

t transfer between fuel & coolant, where h_f, T_{af} are fuel

: transfer coefficient and average tempr. given by Eqn(7.17);

obtain:-

$$\frac{d\,T_{ac}}{dt} = \frac{A\,h_c^2}{(h_e+h_f)mC_p}\,(\,T_{af}-T_{ac}) - \frac{\dot{m}}{m}(T_{ac}-T_i)$$ .. Eqn(2)

e moderator time constant is the coefficient of its differential

,

$_m = (Ah_c^2\,/(h_c+h_f)mC_p + \dot{m}/m\,)^{-1}$ .... Eqn(3)

; evaluated from Eqn(2) by putting $\dfrac{dT_{ac}}{dt} = 0$

r Steady State condition). We obtain :-

$$h_c = \frac{1 + \sqrt{1+4DH_f}}{D} \qquad \ldots\ldots\ldots \text{Eqn (4)}$$

where, $D = A \cdot (T_{af} - T_{ac}) / \dot{m} C_p (T_{ac} - T_i)$;

since all terms in Eqn(3) are known, τ_m is evaluated. As temperatures change with load variations, τ_m varies with load variations as well .

*   *   *   *   *